



**Michigan  
Technological  
University**

Michigan Technological University  
**Digital Commons @ Michigan Tech**

---

Dissertations, Master's Theses and Master's Reports

---

2021

## **COMPARATIVE STUDY OF BIOCIDES AND NANOPARTICLES ON BACTERIAL MICROORGANISMS**

Rehab Alhajjar

*Michigan Technological University, ralhajja@mtu.edu*

Copyright 2021 Rehab Alhajjar

---

### **Recommended Citation**

Alhajjar, Rehab, "COMPARATIVE STUDY OF BIOCIDES AND NANOPARTICLES ON BACTERIAL MICROORGANISMS", Open Access Dissertation, Michigan Technological University, 2021.  
<https://doi.org/10.37099/mtu.dc.etr/1274>

Follow this and additional works at: <https://digitalcommons.mtu.edu/etr>

COMPARATIVE STUDY OF BIOCIDES AND NANOPARTICLES ON BACTERIAL  
MICROORGANISMS

By

Rehab Khalid Alhajjar

A DISSERTATION

Submitted in partial fulfillment of the requirements for the degree of

DOCTOR OF PHILOSOPHY

In Biological Sciences

MICHIGAN TECHNOLOGICAL UNIVERSITY

2021

© 2021 Rehab Khalid Alhajjar

This dissertation has been approved in partial fulfillment of the requirements for the Degree of DOCTOR OF PHILOSOPHY in Biological Sciences.

Department of Biological Sciences

Dissertation Advisor: *Dr. Stephen M. Techtmann*

Committee Member: *Dr. Ebenezer Tumban*

Committee Member: *Dr. Gordon Paterson*

Committee Member: *Dr. Daisuke Minakata*

Department Chair: *Dr. Chandrashekhhar P. Joshi*

# Contents

List of Figures .....	v
List of Tables .....	ix
Author Contribution Statement.....	x
Acknowledgments.....	xi
Abstract.....	xiii
1 Chapter 1 .....	1
Introduction and Background .....	1
1.1 Background.....	1
1.2 Biocides and nanoparticles .....	2
1.2.1 Biocides.....	2
1.2.2 Nanoparticles .....	4
1.3 Antimicrobial vs antibacterial.....	5
1.4 Modes of action of biocides and nanoparticles.....	5
1.4.1 The mechanisms for action to biocides.....	5
1.4.2 The mechanisms for action to nanoparticles.....	8
1.5 The effects of biocides and nanoparticles on the aquatic environment of microbial communities.....	10
1.6 Mechanism of resistance to biocides and nanoparticles .....	18
1.6.1 The mechanisms for resistance to biocides.....	18
1.6.2 The mechanisms for resistance to nanoparticle .....	22
1.7 The influence of natural organic matter (NOM) on the efficiency of biocides and nanoparticles.....	25
1.8 Goals of this study .....	27
2 Chapter 2 .....	30
Biocides More Strongly Alter Microbial Communities in Hydraulic Fracturing Impacted Stream than Metal Oxide Nanoparticles .....	30
2.1 Abstract.....	30
2.2 Introduction.....	31
2.3 Materials and methods .....	35
2.3.1 Microcosm set up.....	36
2.3.2 Nanoparticle characterization .....	40
2.3.3 pH measurements.....	41
2.3.4 Membrane permeability assessment - lactate dehydrogenase assay (LDH).....	41
2.3.5 DNA extraction.....	42
2.3.6 Bacterial abundance analysis (qPCR).....	43

	2.3.7	Microbial community composition analysis (16S rRNA) gene sequencing.....	44
2.4		Results.....	47
	2.4.1	Metal oxide nanoparticles size and stability .....	47
	2.4.2	Change in pH over time and treatment .....	49
	2.4.3	Cytotoxicity effects of biocides and nanoparticles on bacterial membrane permeability (LDH).....	50
	2.4.4	Effect of NPs and biocides on 16S rRNA gene copies...51	
	2.4.5	Microbial community structure.....	53
	2.4.6	Differentially enriched taxa between NPs and biocides microcosm:.....	59
2.5		Discussion.....	62
	2.5.1	Stability of NPs in stream water .....	62
	2.5.2	The change in pH of microcosms as a result of treatment	63
	2.5.3	The cytotoxicity of NPs & biocides.....	63
	2.5.4	The effects of NPs & biocides on bacterial community composition and diversity.....	65
3		Chapter 3 .....	68

		Experimental evolution to investigate the mechanism of biocide and nanoparticle resistance.....	68
	3.1	Abstract.....	68
	3.2	Introduction.....	69
	3.2.1	Mechanisms of resistance to biocides and nanoparticles.....	71
	3.3	Materials and methods .....	73
	3.3.1	Chemicals.....	73
	3.3.2	Bacterial strains and growth conditions. ....	73
	3.3.3	Stability of nanoparticles in growth medium.....	73
	3.3.4	Experimental evolution study to adapt <i>E. coli</i> to biocides and NPs- minimal inhibitory concentrations MIC.....	74
	3.3.5	Morphology and interaction with bacterial cells with nanoparticles. ....	75
	3.3.6	Study the mechanism of the resistant bacteria to biocide and NPs	76
	3.3.7	Cytotoxicity effects of biocides and nanoparticles -lactate dehydrogenase assay (LDH).....	78
	3.3.8	Cytotoxicity effects of biocides and nanoparticles - reactive oxidative species (ROS).....	78
	3.3.9	Study the mechanism of the resistance - The impact of efflux pumps on conferring antimicrobial resistance .....	79
	3.3.10	Study the mechanism of the resistance - Genome-wide analysis of the adapted strains .....	80
3.4		Results.....	82
	3.4.1	Silver nanoparticles size and stability.....	82

3.4.2	Experimental evolution study to adapt <i>E. coli</i> to DBNPA and Ag-NPs.....	84
3.4.3	Effects of DBNPA and Ag-NPs to <i>E. coli</i> cells morphology.....	88
3.4.4	Impact of adaptation on the growth of <i>E. coli</i> in the absence of antimicrobials.....	90
3.4.5	Cytotoxicity effects of DBNPA and Ag-NPs on bacterial membrane permeability (LDH) and reactive oxidative species (ROS) 91	
3.4.6	Role of efflux pumps in acquired resistance to DBNPA and Ag-NPs.....	95
3.4.7	Study the mechanism of the resistant bacteria to DBNPA and Ag-NPs- Genome-wide analysis of the adapted strains.....	97
3.5	Discussion.....	103
4	Chapter 4.....	109

Impact of different natural organic matter (NOM) on antimicrobial activity of Silver Nanoparticles (Ag-NPs) and 2, 2-dibromo-3-nitrilopropionamide (DBNPA) Against *E. coli* 109

4.1	Abstract.....	109
4.2	Introduction.....	110
4.3	Materials and methods.....	113
4.3.1	Chemicals.....	113
4.3.2	Organic matter description.....	114
4.3.3	Bacterial strains and growth conditions.....	115
4.3.4	Treatments used for the study.....	115
4.3.5	Bacterial growth in the presence of antimicrobials in the liquid medium.....	118
4.3.6	Bacterial count in the presence of antimicrobials.....	118
4.3.7	Stability of nanoparticles in growth medium.....	119
4.4	Results.....	120
4.4.1	The impact of NOM on bacterial growth in the presence of antimicrobials.....	120
4.4.2	Effect of NOM on the antimicrobial activity of Silver nanoparticles.....	120
4.4.3	Effect of NOM on DBNPA antimicrobial activity.....	123
4.4.4	Effect of NOM on the combination of Ag-NP and DBNPA antimicrobial activity.....	125
4.4.5	The impact of NOM on bacterial viability count in the presence of antimicrobials.....	127
4.4.6	Effect of NOM on bacterial viability count in the presence of Silver nanoparticles.....	127
4.4.7	Effect of NOM on bacterial viability count in the presence of DBNPA.....	129

4.4.8	Effect of NOM on bacterial viability count in the presence of the combination of Ag-NP and DBNPA .....	131
4.4.9	The effect of different NOM on the size and stability of the Silver nanoparticles.....	133
4.5	Discussion .....	136
5	Chapter 5 .....	143
	Conclusions, Implications, & Recommendations for Future Work.....	143
5.1	Conclusions.....	143
5.2	Implications.....	147
5.3	Recommendations for Future Work.....	147
	Reference List .....	149

# List of Figures

Figure 1.1 The electrostatic double-layer repulsions and Van der Waals forces inspired by (Buschow, 2001). .....	14
Figure 1.2 (A) Showing Comparative between two types of antimicrobial Biocides (2, 2-dibromo-3-nitrilopropionamide (DBNPA)) and Nanoparticles (silver nanoparticles (Ag-NPs)) industrial applications. (B) Showing comparative mechanisms of microbial resistance to DBNPA and Ag-NPs inspired by (Merchel Piovesan Pereira and Tagkopoulos, 2019).....	24
Figure 2.1 Microcosm set up of nanoparticles and biocides stock solution with the Lower Greys Run, PA surface water.....	39
Figure 2.2 Transmission electron microscopy photomicrograph of (A) TiO <sub>2</sub> NPs stock solution, (B) ZnO NPs stock solution, (C) SiO <sub>2</sub> NPs. stock solution scale bars = 50 nm. ....	49
Figure. 2.3 pH measurements of NPs and Biocides in Lower Grays Run, PA. Showing change in pH over time and treatment. ....	50
Figure 2.4 Showing relative LDH and the standard error for 16.7 mg/L concentration of biocides and NPs (n=3).....	51
Figure 2.5 Showing the plots of the mean $\pm$ standard deviation of microbial abundance changes over time to compare the effect of nanoparticles and biocides in Lower Grays Run, PA samples. ....	53
Figure 2.6 Three different richness and evenness alpha diversity estimates, (A) Inverse Simpsons, (B)Shannon, and (C)richness (observed ASVs). Represent the differences in alpha diversity on day 0 and day 14 to compare the effect of NPs and biocides in Lower Grays Run, PA samples.....	55
Figure 2.7 Principal coordinate analysis (PCoA) of Bray Curtis Dissimilarity of the rarified ASV table of microcosms from Lower Grays Run, PA samples with 16.7 mg/L concentration of three metal oxides NPs and biocides. This is showing the dissimilarity of the microbial community on day 0 (open symbols) and day 14 (closed symbols). Treatments are shown in different colors .....	58
Figure 2.8 Bar graph of taxonomic diversity shows the relative abundance of bacterial order with those classes represented with different colors. This figure shows the relative abundance of bacterial orders on day 0 and day 14 for Lower Grays Run, PA samples incubated with three metal oxide nanoparticles, and biocides at 16.7 mg/L concentration for all treatments.....	61
Figure 3.1 Transmission electron microscopy photomicrograph of Ag-NPs stock solution (A) Scale bars= 500 nm, (B) Scale bars = 200 nm, (C) Scale bars = 10 nm. ....	83

- Figure 3.2 Minimum inhibitory concentrations of silver NPs & DBNPA as determined for *E. coli* after each of 10 consequent culture steps. The DBNPA MIC is shown in red and the Ag-NP MIC is shown in blue.....85
- Figure 3.3 Example of a MIC plate from the experimental evolution study to adapt and parent *E. coli* and to different concentrations of DBNPA and Ag-NPs. (A) Showing the MIC of parent *E. coli* (P) with Ag-NPs, (B) Showing the MIC of Adapt *E. coli* (A-NP) with Ag-NPs, (C) Showing the MIC of parent *E. coli* (P) with DBNPA, (D) Showing the MIC of Adapt *E. coli* (A-NP) with DBNPA. ....86
- Figure 3.4 The images demonstrate the aggregation and precipitation of silver NPs after 48 hours of incubation with silver NPs. (a, left) The tube on the left side of the picture contains ‘adapt *E. coli* without silver NPs (A-NP). (b, right) The first tube on the right side of the picture contains ‘adapt *E. coli* without silver NPs (A-NP). The second tube on the right side of the picture contains parent *E. coli* and to below the maximum MIC (5 mg/L) of silver NPs (P-L-NP). The third tube on the right side of the picture contains adapt *E. coli* cultivated to below the maximum MIC (150 mg/L) of silver NPs (A-L-NP). .....87
- Figure 3.5 Scanning electron microscopy (SEM) showing interactions of Ag-NPs and DBNPA with (A) Parent *E. coli*, (B) Adapt *E. coli* with 5mg/L of Ag-NPs (C) Adapt *E. coli* with 150mg/L DBNPA.....89
- Figure 3.6 Growth curves for the parent *E. coli* (blue) and DBNPA-adapted (red) and Ag-NP adapted *E. coli* (green) after 24h incubation (n=3) and the data showed as mean and error bars represent standard error.....91
- Figure 3.7 Showing relative LDH of Ag-NPs and DBNPA on the tested bacteria for the conditions illustrated in Table.3.1 after 24h incubation (n=3). Colors represent the different treatments. Error bars are standard errors. The same parental strain without antimicrobials (P) as measured from the same triplicate conditions are shown in both groups of data for sake of comparison. ....93
- Figure 3.8 Showing relative ROS of Ag-NPs and DBNPA on the tested bacteria for the conditions illustrated in Table.3.1 after 24h incubation (n=3). Colors represent the different treatments. Error bars are standard errors. The same parental strain without antimicrobials (P) from the same triplicate conditions are shown in both groups of data for sake of comparison. ....94
- Figure 3.9 Showing the effect of efflux pump inhibitors (EPLs) 1-(1Naphthylmethyl)-piperazine (NMP) on the tested bacteria for the conditions illustrated in Table.3.1 after 24h incubation (n=3). Showing the effect of different concentrations of (NMP) against adapted and parent *E. coli* treated with Ag-NPs. Showing the effect of efflux pump inhibitors (EPLs) 1-(1Naphthylmethyl)-piperazine (NMP) on the tested bacteria for the conditions illustrated in Table.3.1 after 24h incubation (n=3). Showing the effect of different concentrations of (NMP) against adapt and parent *E. coli* treated with DBNPA.....97
- Figure 3.10 A Venn diagram summary of identified gene mutations that were considered the high and moderate impact of the *E. coli* adapted to Ag-NPs and DBNPA from

the genome sequenced in this study. The underlined genes indicate genes with high impact and the rest had moderate impacts. ....99

Figure 4.1 Showing silver nanoparticles antimicrobial activity on the bacterial abundance of *E. coli* with different NOM after 24 h incubation (n=3) (average  $\pm$  standard deviation). and the data shown as mean and error bars represent standard deviation. The control (blue) shows *E. coli* abundance only. The NOM treatments show different NOM with three concentrations incubated with (2 mg/L) silver nanoparticles (Table 4.1). The 0 mg/l (red) without NOM from the same triplicate conditions is shown in the groups of data for sake of comparison. The NOM treatments abbreviations are the following: (HA-NP)-Humic Acid with Ag-NPs, (FA -NP)-Fulvic Acid with Ag-NPs, (NOM1-NP)-Suwannee River NOM with Ag-NPs, (NOM2-NP)- Upper Mississippi NOM with Ag-NPs. ....122

Figure 4.2 Showing DBNPA antimicrobial activity on the bacterial abundance of *E. coli* with different NOM after 24 h incubation (n=3) and the data shown as mean and error bars represent standard deviation. The control (blue) shows *E. coli* abundance only and the 0 mg/l (red) without NOM. The NOM treatments show different NOM with three concentrations incubated with (50 mg/L) DBNPA (Table 4.1). The NOM treatments abbreviations are the following: (HA-Bio)-Humic Acid with DBNPA, (FA -Bio)-Fulvic Acid with DBNPA, (NOM1- Bio)-Suwannee River NOM with DBNPA, (NOM2- Bio)- Upper Mississippi NOM with DBNPA. ....124

Figure 4.3 Showing the plots of bacterial abundance changes with different NOM. Compared the effect of NOM on a mix of Ag-NPs and DBNPA antimicrobial activity (n=3) (average  $\pm$  standard deviation). The control (blue) shows *E. coli* abundance only. The same 0 mg/l (red) without NOM from the same triplicate conditions are shown in the groups of data for sake of comparison. The NOM treatments show different NOM with three concentrations incubated with (2 mg/L) silver nanoparticles & (50 mg/L) DBNPA (v/v) (Table 4.1). The NOM treatments abbreviations are the following: (HA-Bio-NP)-Humic Acid with Ag-NPs & DBNPA, (FA-Bio-NP)-Fulvic Acid with Ag-NPs & DBNPA, (NOM1-Bio-NP)-Suwannee River NOM with Ag-NPs & DBNPA, (NOM2-Bio-NP)- Upper Mississippi NOM with Ag-NPs & DBNPA, (HA-FA-NOM1-NOM2-Bio-NP)- Humic Acid & Fulvic Acid & Suwannee River NOM& Upper Mississippi NOM with Ag-NPs & DBNPA. ....126

Figure 4.4 Showing silver nanoparticles antimicrobial activity on the bacterial cell viability of *E. coli* with different NOM after 24hrs incubation (n=3) and the data shown as mean and error bars represent standard deviation. The control (blue) shows *E. coli* abundance only. The NOM treatments show different NOM with three concentrations incubated with (2 mg/L) silver nanoparticles. The 0 mg/l (red) without NOM from the same triplicate conditions is shown in the groups of data for sake of comparison. The NOM treatments show different NOM with three concentrations incubated with (2 mg/L) silver nanoparticles (Table 4.1). The NOM treatments abbreviations are the following: (HA-NP)-Humic Acid with Ag-

NPs, (FA-NP)-Fulvic Acid with Ag-NPs, (NOM1-NP)-Suwannee River NOM with Ag-NPs, (NOM2-NP)- Upper Mississippi NOM with Ag-NPs. ....128

Figure 4.5 Showing DBNPA antimicrobial activity on the bacterial cell viability of *E. coli* with different NOM after 24h incubation (n=3) and the data shown as mean and error bars represent standard deviation. The control (blue) shows *E. coli* abundance only. The NOM treatments show different NOM with three concentrations incubated with (50 mg/L) DBNPA (Table 4.1). The same 0 mg/l without NOM from the same triplicate conditions is shown in the groups of data for sake of comparison. The NOM treatments abbreviations are the following: (HA-Bio)-Humic Acid with DBNPA, (FA-Bio)-Fulvic Acid with DBNPA, (NOM1-Bio)-Suwannee River NOM with DBNPA, (NOM2-Bio)- Upper Mississippi NOM with DBNPA. ....130

Figure 4.6 Showing the plots of bacterial cell viability changes with different NOM. Compared the effect of NOM on a mix of Ag-nanoparticles and biocides antimicrobial activity (n=3) (average  $\pm$  standard deviation). The NOM treatments abbreviation is illustrated in (Table 4.1). The control (blue) shows *E. coli* abundance only and 0 mg/l (red) without NOM. The NOM treatments show different NOM with three concentrations incubated with (2 mg/L) silver nanoparticles & (50 mg/L) DBNPA (v/v) (Table 4.1). The NOM treatments abbreviations are the following: (HA-Bio-NP)-Humic Acid with Ag-NPs & DBNPA, (FA-Bio-NP)-Fulvic Acid with Ag-NPs & DBNPA, (NOM1-Bio-NP)-Suwannee River NOM with Ag-NPs & DBNPA, (NOM2-Bio-NP)- Upper Mississippi NOM with Ag-NPs & DBNPA, (HA-FA-NOM1-NOM2-Bio-NP)- Humic Acid & Fulvic Acid & Suwannee River NOM & Upper Mississippi NOM with Ag-NPs & DBNPA. ....132

Figure 4.7 Showing relative NPs size distribution was determined based on intensity for each replicate with different NOM in MH media (n=3) (average  $\pm$  standard deviation). Compared the effect of NOM on NPs size. The control is 0 mg/l without NOM and the NOM concentrations show different NOM with three concentrations incubated with (2 mg/L) silver nanoparticles (Table 4.1). **A.** showing the size of Ag-NPs with different NOM under different NOM concentrations without any biocides (DBNPA). The NOM treatments abbreviations are the following: (HA-NP)-Humic Acid with Ag-NPs, (FA-NP)-Fulvic Acid with Ag-NPs, (NOM1-NP)-Suwannee River NOM with Ag-NPs, (NOM2-NP)- Upper Mississippi NOM with Ag-NPs. **B.** showing the size of Ag-NPs with different NOM and with DBNPA. The NOM treatments abbreviations are the following: (HA-Bio-NP)-Humic Acid with Ag-NPs & DBNPA, (FA-Bio-NP)-Fulvic Acid with Ag-NPs & DBNPA, (NOM1-Bio-NP)-Suwannee River NOM with Ag-NPs & DBNPA, (NOM2-Bio-NP)- Upper Mississippi NOM with Ag-NPs & DBNPA, (HA-FA-NOM1-NOM2-Bio-NP)- Humic Acid & Fulvic Acid & Suwannee River NOM & Upper Mississippi NOM with Ag-NPs & DBNPA. ....135

# List of Tables

Table 2.1 The biocides or NPs used in this study. ....	36
Table 2.2 Showing the average of three measurements of the mean NPs size, zeta potential, and their standard error in Lower Grays water treated samples over time (n=3) (average $\pm$ standard error). ....	48
Table 2.3 Permutational multivariate analysis of variance (PERMANOVA) of Bray Curtis dissimilarity of Lower Grays Run, PA samples comparing nanoparticle and biocide treatments days 0 and 14. ....	57
Table 3.1 Conditions tested to investigate the physiological response to antimicrobials. ....	77
Table 3.2 Relative Ag-NPs size, zeta potential, and their standard error over time (n=3) (average $\pm$ standard error). ....	83
Table 3.3 Summary comparison between mutations found near efflux pumps and flagellin genes on adapted E. coli to Ag-NPs and DBNPA to E. coli Parent genome sequenced in this study. The predicted strength of the mutation is shown next to the gene name. Modifier indicates mutations that occurred near a gene or a mutation with a minimal effect on the gene sequence. Low effect impact indicates one or many codons are changed. ....	101
Table 4.1 Conditions tested to investigate the physiological response to antimicrobials. ....	117

# Author Contribution Statement

Chapter 2 is in revision at Chemosphere. Coauthors are this manuscript are Rehab K. Alhajjar, Ryan B. Ghannam, Jeremy R. Chen See, Olivia G. Wright, Maria Fernanda Campa, Terry C. Hazen, Regina Lamendella, and Stephen M. Techtmann.

For chapter 2, RKA performed experiments, analyzed data, and wrote the manuscript, RBG analyzed data and edited the manuscript, JRCS collected samples and edited the manuscript, OGW collected samples, MFC assisted manuscript preparation and edited the manuscript, TCH oversaw part of the analysis, RL oversaw sample collection, SMT assisted in experimental design, analyzed data and wrote the manuscript.

Chapter 3 and Chapter 4 are the work of Rehab K. Alhajjar and Stephen M. Techtmann. RKA performed experiments, analyzed data, and wrote the manuscript. SMT assisted in experimental design, analyzed data, and reviewed the manuscript.

# Acknowledgments

I am thankful to almighty Allah, who bless, helped, and give me the courage to complete this work. Without my faith would not go through all the challenges or success in my life.

I would like to express my deepest appreciation and give special thanks to my advisor Dr. Stephen Techtmann who made the completion of this Ph.D. possible. I am very grateful for his kind support. I also thank all my committee members Dr. Ebenezer Tumban, Dr. Gordon Paterson, and Dr. Daisuke Minakata for all their suggestions and support.

I would like to thank all my friends and family, my mother, father, sisters, and brothers. I love you all and I thank you. I want to give special thanks to my mom Sarah for her prayers and love for all my life. I also want to thank my best friend and sister Nouf for her support, encouragement, generosity, and helping me to achieve my goals. I would like to thank Chad and his family for their love and support during the COVID pandemic.

I would like to extend my deepest gratitude to my King, Salman bin Abdelaziz Al Saud for always being supportive and always having confidence in the Saudi citizen's ability. I would like to thank my government Saudi Arabia and The Saudi Arabian Cultural Mission (SACM) for funding all my living expenses, full support, and supervision as a

student during my stay in the United States. This work also, was funded by the National Science Foundation CBET awards 1804685 (Michigan Technological University), 1805152 (University of Tennessee), and 1805549 (Juniata College).

Finally, I would like to recognize the opportunities of sharing the education that I received from the United States to make my dream to study abroad come true and thanks to Michigan Technological University and its employees for their assistance at the time of my need and the opportunity to use all their resources to accomplish my study.

# Abstract

The increase in antimicrobial-resistant bacteria has posed challenges to treating resistant diseases. Antimicrobials such as nanoparticles (NPs) and biocides are commonly used to control microbial growth in household and industrial settings. Several studies have shown that bacteria that become resistant to biocides can also resist antibiotics. There are fewer reports of resistance to nanoparticles. Our study goals were to compare the environmental effects of biocides and nanoparticles by investigating their impacts on stream microbial community structure, the mechanism of bacterial resistance, and their interactions with natural organic matter (NOM). Our results showed that biocides dramatically altered microbial community composition and diversity in comparison to NPs. We used an experimental evolution approach to demonstrate that *E. coli* quickly acquired resistance to both biocides and NPs. We demonstrated that efflux pumps play an important role in resistance to DBNPA and Ag-NPs. Resistance to both Ag-NPs and DBNPA resulted from mutations in multiple genes such as flagellar genes and efflux pumps. We also demonstrated that NOM can interrupt the antimicrobial activity of Ag-NPs and DBNPA. Before this work, there were very few studies directly comparing the impacts of both NPs and biocides on microbial communities and how the microorganisms develop resistance to biocides and NPs on a molecular level. This work provides a comparison of the environmental effects of these antimicrobials as well as a comparison of the mechanisms of acquired resistance. Our findings support the importance of considering the environmental risk of Ag-NPs and DBNPA. This work shows that while nanoparticles resulted in fewer alterations to microbial community composition in

microcosms from stream water, bacteria can rapidly develop resistance to nanoparticles.

Novel technologies and comparative studies such as the one performed here are important for identifying strategies for microbial control that do not contribute to the spread of antimicrobial-resistant bacteria.

# Chapter 1

## Introduction and Background

### 1.1 Background

Microorganisms are incredibly diverse and ubiquitous in natural and engineered settings. They are important for controlling biogeochemical cycles such as the carbon and nitrogen cycle (Gougoulas et al., 2014). The processes that microorganisms catalyze are essential for human and ecosystem health. While most microbes are beneficial, certain microbes can cause disease and, in some settings, microbial growth can interfere with industrial processes (Moënne-Loccoz et al., 2014). There is therefore a need to control microbial growth. Diverse methods have been used for the disinfection of water and surfaces to control pathogens and other microorganisms (Cozad and Jones, 2003). Physical methods such as high temperature or filtration are used for the inactivation of unwanted microorganisms. Alternatively, there are many chemicals used to control microbial growth. Antimicrobials are a broad class of chemicals used for controlling microbial growth and include classes of chemicals such as antibiotics, biocides, and nanoparticles.

In this study, we sought to understand the environmental impacts of two common classes of antimicrobials biocides, and nanoparticles. In order to accomplish this, we performed

comparative studies evaluating the impact of these antimicrobials on natural microbial communities. We performed a comparative experimental evolution study to investigate the potential for the development of resistance. We also investigated the relative effects of natural organic matter on antimicrobial efficacy.

## **1.2 Biocides and nanoparticles**

### **1.2.1 Biocides**

Antimicrobials include several different chemicals aimed at controlling microbial growth. Antibiotics are chemotherapeutic chemicals that are prescribed to deal with microbial infections and control microbial growth in humans and animals (Russell, 2003). Biocides are chemical substances used as antiseptics, disinfectants, and preservatives, which are aimed at controlling microbial growth in industrial and household applications (Fink, 2013). Biocidal products are made by mixing one or more active substances and additives in a range of formulations (Coors et al., 2018). Biocides have been used as food preservatives as well as to control microbial growth on surfaces and in water treatment. The need for microbial control in various settings such as health care, industrial, and residential settings along with the low cost and effectiveness of biocides has led to the common use of biocides in diverse settings (Guardiola et al., 2012b, Levy, 2002a). There are more than 23 kinds of biocides used in different industrial applications (Guardiola et al., 2012b). Some examples include quaternary ammonium compounds (QACs),

glutaraldehyde (GA), triclosan (TCS), triclocarban (TCC), chlorine dioxide, etc. (Levy, 2002a).

Many household biocides are used on large scales; for example, TCS and TCC were pervasively used in household products in particular in antibacterial soaps and other health care products (Heidler and Halden, 2009, Chattopadhyay et al., 2004). Despite the widespread use of TCS and TCC, concern about their safety and efficacy and the potential environmental effects of their release to the environment led to the FDA banning the use of TCS and TCC in household products in 2017 (federalregister, 2016). Other examples of household biocide are QACs such as Benzalkonium Chlorides (BACs), which are broad-spectrum antimicrobials with activity against bacteria, fungi, and viruses and as such are commonly used in consumer products such as fabric softeners, cosmetics, and other personal care products (Merchel Piovesan Pereira and Tagkopoulos, 2019). Conversely, biocides such as 2, 2-dibromo-3-nitrilopropionamide (DBNPA) is a potent biocide used in industrial settings for disinfection of water systems, paper production facilities, and oil, and gas extraction equipment (Chattopadhyay et al., 2004, Siddiqui et al., 2017a).

The pervasive use of biocides has led to some concerns about the ability of bacteria to develop resistance to these compounds in response to exposure at sub-minimum inhibitory concentrations (Merchel Piovesan Pereira and Tagkopoulos, 2019). The

minimum inhibitory concentration is the lowest concentration of an antimicrobial needed to completely inhibit growth. Biocides are often inadvertently released into the environment in wastewater effluent from household and industrial sites. During wastewater treatment and upon release, biocides are diluted to sub-Minimum Inhibitory Concentrations (sub-MIC). At sub-MIC levels, the biocides are not able to inactivate microorganisms but could select for the growth of microorganisms that are resistant to these biocides.

### **1.2.2 Nanoparticles**

Another important class of antimicrobials is nanoparticles (NPs). Interest in the applications of nanoparticles has increased since 1959 when Richard P. Feynman gave his famous lecture “There’s Plenty of Room at the Bottom” (Khan et al., 2017).

Nanotechnology is the science of the behavior and use of particles with diameters of 1 – 100 nm (Whatmore, 2005, Pal et al., 2011). Nanotechnology has benefitted many areas such as pharmaceuticals, drug delivery, and other industries such as the development of catalytic materials as well as microbial control (Pal et al., 2011, Mende, 2015).

Engineered nanoparticle materials such as silver, titanium dioxide, zinc dioxide have shown strong antimicrobial properties (Paterson et al., 2011). Furthermore, metal oxide NPs and other metals such as silver and copper are the ones are commonly used to control microbial activity (Wang et al., 2017b). NPs have different designs and shapes

which give them unique properties; For example, spherical NPs often have different antimicrobial activity than the same material as a rod or crystalline.

### **1.3 Antimicrobial vs antibacterial**

Antimicrobials and antibacterial are different due to the different kinds of microorganisms they affect. Antimicrobial agents are more generic and can inhibit the growing presence of bacteria, mold, and fungi and that makes them useful in controlling break classes of microbes. Conversely, antibacterial agents are targeted for controlling the growth of bacteria and are effective against a broad spectrum of pathogen bacteria such as *E. coli*. Most biocides inhibit the growth of microbes in an untargeted manner and thus are more accurately considered antimicrobials (McDonnell and Russell, 1999). Additionally, it has been reported that nanoparticles such as zinc and silver nanoparticles (Ag-NPs) have broad-spectrum of Gram-positive and Gram-negative bacteria antibacterial properties against both and that can provide a safer alternative to the old antimicrobial and antibacterial agents (Lanje et al., 2010)

### **1.4 Modes of action of biocides and nanoparticles**

#### **1.4.1 The mechanisms for action to biocides**

Antibiotics used to treat infections in humans and animals require that they act in a specific manner to selectively inhibit cellular functions that are specific to bacterial cells, while not affecting the animal. Therefore, functions such as peptidoglycan synthesis, bacterial transcription, and translation are often targeted. The need to target processes that are essential for bacterial growth while not affecting the animal cells, often requires that antibiotics function by inhibiting bacterial-specific enzymes (bacterial ribosome) or processes (enzymes involved in peptidoglycan synthesis). Alternatively, biocides have more generic modes of action to increase their efficacy and spectrum. Biocides can act by inhibiting growth while the biocide is present (bacteriostatic) or by completely inactivating that microorganism (bactericidal) depending on the extent of their damage to the bacterial cell (Denyer, 1995). Despite the more generic nature of biocide action, different classes of biocides have different mechanisms of action and therefore may differentially affect bacteria depending on different factors.

In general, the mechanism(s) of action of a biocide may be defined as an interaction between biocides and bacterial cell components including the cell wall, the cell membrane, and cytoplasmic constituents (Maillard, 2002). The mode of action for biocides can be divided into three broad classes electrophilic, lytic, and oxidizing. Glutaraldehyde and DBNPA are both electrophilic biocides. QACs such as BAC are considered lytic biocides as they destabilize the cell membrane. Oxidizing biocides include chemicals such as chlorine dioxide and sodium hydroxide (Kahrilas et al., 2015b,

Geueke, 2014). In our study, we focus on glutaraldehyde, DBNPA, and triclosan as examples of biocides.

Glutaraldehyde inhibits microbial growth by reaction of the aldehyde groups on glutaraldehyde with proteins and cell wall components (Bajpai, 2015). It has been reported that glutaraldehyde interacts mainly with Gram-negative outer components, especially lipoproteins (McDonnell and Russell, 1999). Glutaraldehyde primarily acts by reaction of the aldehyde group with free amines in proteins. Glutaraldehyde is a well-known cross-linker that can be used to cross-link proteins to each other in the cell membrane or cell wall. As these proteins are crosslinked they lose their activity, which causes inactivation of the cell. The electrophilic nature of glutaraldehyde makes it a very broad spectrum biocide (McDonnell and Russell, 1999). DBNPA is another example of an electrophilic biocide which inactivates cells through interaction between biocides and bacterial cellular components. DBNPA is considered a fast-acting biocide that reacts with thiol groups (-SH) in sulfur-containing organic molecules such as glutathione or cysteine which leads to irreversible damage of proteins and inhibition of compounds transport processes (Siddiqui et al., 2017b). In contrast to the electrophilic biocides discussed above, Triclosan has a more specific mode of action. Triclosan works by inhibiting the enoyl-acyl carrier protein reductase (FabI). FabI is an essential enzyme in bacterial fatty acid synthesis. Inhibition of FabI results in the inhibition of cell growth as fatty acids are essential for bacterial cell growth (Heath et al., 1999). Therefore, the action of triclosan is more similar to antibiotics in that it targets a specific protein whose

function is involved in bacterial cell growth. More recently, TCS has been shown to also disrupt the membrane potential which can disrupt the proton motive force, which is essential for ATP synthesis (Maiden and Waters, 2020).

#### **1.4.2 The mechanisms for action to nanoparticles**

Nanoparticles, like biocides, have a more generic mechanism of action than targeting specific enzymes like antibiotics. Many factors can affect the antibacterial properties of NPs such as the metal core material, size, shape, and concentration of NPs. The type of NPs plays an important role in antimicrobial activity; for example, metal NPs have high toxicity against microbes compared to carbon NPs (Simonin and Richaume, 2015).

Nanoparticles have mechanisms of action that range from increasing reactive oxygen species to disruption of essential proteins involved in the key process in the cell, or general destabilization of the cytoplasmic membrane. Much work has been invested in studying the mechanism of silver nanoparticles (Ag-NP). Our study focuses on Ag-NP as well as metal oxide nanoparticles such as ZnO, TiO<sub>2</sub>, and SiO<sub>2</sub>. Previous reviews such as (Nisar et al., 2019) have reviewed the mechanism of many commonly NPs. Below we summarize the mechanism of some of the NPs used in this study.

**Mechanism of Ag-NP antimicrobial activity:** The release of silver ions and/or the particle-specific functions considering the most common mode of toxicity of Ag-NPs. Silver nanoparticle ions are formed when they are attached to the cell membrane surface

which causes a distribution of pores in the membrane and leads to damage to the cell membrane structure by the Ag-NPs penetration.

Ag-NP can generate highly reactive molecules or Reactive Oxygen Species (ROS). These ROS products could disturb the cell membrane by penetrating and damaging respiratory enzymes and DNA inside the cell and lead to cell death. Ag-NP can damage the bacterial DNA due to the acid/base interaction between Ag-NP and phosphorous / sulfur in the DNA. Another antimicrobial mechanism of Ag-NP is through the release of silver ions that can inhibit many enzymes through interactions with the thiol groups (-SH) (Prabhu and Poulouse, 2012).

**Mechanism of ZnO antimicrobial activity:** the most common mechanism of ZnO NPs has increased levels of oxidative stress exerted on the cell. This increase oxidative stress causes a negative effect on bacterial DNA or the virulence of bacterial genes. ZnO NPs also have been shown to alter membrane integrity. For example in *Campylobacteri jejuni*, treatment with ZnO NPs causes increased expression of oxidative stress genes as well as membrane leakage (Nisar et al., 2019).

**Mechanism of TiO<sub>2</sub> antimicrobial activity:** TiO<sub>2</sub> has photocatalytic characteristics such that under UV-A light (at 385 nm) results in the production of high levels of ROS. However, TiO<sub>2</sub> causes redox reactions that cannot be compensated by common

antioxidant defense systems such as catalases and superoxide dismutase which inhibit  $\text{OH}_2^{\cdot-}$  and  $\text{OH}^{\cdot}$  radicals and lead to the death of the cell by damaging important cells structures (López de Dicastillo, 2021).

**Mechanism  $\text{SiO}_2$  antimicrobial activity:**  $\text{SiO}_2$  has been used as a control nanoparticle because it was believed to have limited toxicity to bacteria. However, some studies have shown that  $\text{SiO}_2$  in fact can inhibit the growth of both gram-positive and gram-negative bacteria (Adams et al., 2006). The mechanism for antimicrobial activity of  $\text{SiO}_2$  is believed to be due to production of ROS.

## **1.5 The effects of biocides and nanoparticles on the aquatic environment of microbial communities**

**Effect of biocides on aquatic microbial communities:** The extensive use of biocides and nanoparticles and their release to the environment has risen many concerns regarding the potential for their release to cause ecological problems (Taghavi et al., 2013, Kahrilas et al., 2015a). Even though there is regulatory guidance regarding the active substances of biocide products and their formulation additives, the environmental risk assessment and the interaction effects should be in consideration (Coors et al., 2018). Many of these antimicrobials are not removed during wastewater treatment and eventually find their way into receiving waters (J.Y.Maillard, 2007). When biocides and other antimicrobial chemicals remain in the water they may affect aquatic life (Gehrke et al., 2015, Kahrilas et al., 2015a). Part of the rationale for the FDA's decision to remove TCS from

antibacterial hand soaps was due to TCS being an endocrine disruptor in humans and fish (Wang and Tian, 2015, Wang et al., 2017a). Furthermore, when these biocides are released into the environment, they are diluted during the transmission from point of use to the environment, and thus are present at sub-minimum inhibitory concentrations (MIC) (J.Y.Maillard, 2007). Currently, many studies report a change in bacterial genomes at low concentrations of biocides (Gilbert and McBain, 2003, Maillard, 2005). . Since the dose is a key factor in determining the activity of antimicrobials, the concentration is important for determining the ecological effect of released biocides (Grant and Bott, 2005). In water researches, concentration can often be measured as milligrams per liter (mg/l). This gravimetric concentration can be useful in identifying the amount of a particular compound in the water. However, on a molecular level, the dose is often determined as the number of molecules of a compound that an organism is exposed to. Therefore, the concentration of a compound in molarity may be a more informative measure of exposure.

One study had shown that microbes exposed to biocides at sub-lethal doses can develop resistance to antimicrobials (Gilbert and McBain, 2003). Glutaraldehyde or other biocides in the aldehyde class, for example, are commonly used biocides in the healthcare industry (Takigawa and Endo, 2006, Chattopadhyay et al., 2004). Low concentrations of glutaraldehyde can be released into the environment and have harmful effects. This kind of interaction between biocides and the environment raises many concerns (Kahrilas et al., 2015a). As discussed previously, different antimicrobials have distinct modes of

action, thus the release of different classes of antimicrobials could selectively alter the biological community in an environment. For example, the presence of glutaraldehyde could lead to certain taxa being inhibited in environments with biocide contamination, which may alter the bacterial community composition changing the balance in the food chain, and biogeochemical cycling in certain environments (Hernandez-Moreno et al., 2019). Previous studies have shown that in microcosms from stream water, the addition of glutaraldehyde can select for a particular set of microorganisms that can persist and even grow in the presence of glutaraldehyde (Campa et al., 2018). The release of biocides into the environment can strongly affect natural bacteria that play an important role in environments and may cause an ecological issue in the future (Kahrilas et al., 2015a).

**Factors that could affect antimicrobial activity of nanoparticles in the environment:**

With the increased production of nanoparticles (Taghavi et al., 2013), there is growing concern about the influence of nanoparticles on environments (Ray et al., 2009, Paterson et al., 2011). In particular, the antimicrobial activity of some NPs may have adverse effects on the biological communities (Wang et al., 2017b). In the aquatic system, NPs create a concern due to their small size and the large surface-to-volume ratios enhance their ability to interact with organic and inorganic materials (Klaine et al., 2008).

Previous studies have shown that nanomaterials have toxic effects on humans health by affecting the respiratory tract, skin penetration, and gastrointestinal tract (Borm et al., 2006). Moreover, Metal oxide, such as iron oxide at concentrations around 30 mg/l can

inhibit human cell's metabolic activity compared to nontoxic NPs such as silica (Brunner et al., 2006). Due to this potential toxic effect, there is a growing concern over the environmental impact of nanoparticles.

Many factors may affect the interactions between nanoparticles (NPs) and microorganisms in the environment. The nature of the particles if organic or inorganic can control the stability of the nanoparticles in the environments and also control their aggregation (Bhatt and Tripathi, 2011). Aggregation increases the particle size and may prevent microbial cells from taking them up or altering how NPs interact with bacteria (Bhatt and Tripathi, 2011). One study showed that aggregation of Ag NPs caused by increased expression of flagellar proteins alters the antibacterial properties of Ag-NP (Panacek et al., 2018).

In general, the smaller and more stable the nanoparticle, the higher the antimicrobial activity. Many forces such as electrostatic and Van der Waals forces affect the stability of particles in water environments. DLVO theory has been used to explain the stability of colloids. DLVO is named after Derjaguin, Landau, Verwey, and Overbeek who established this theory (Derjaguin 1987). DLVO theory is defined as the bulk of the stability energy that originates from the total of the electrostatic double-layer repulsion and Van der Waals forces (Fig.1.1) (Buschow 2001). The van der Waals forces and electrostatic double-layer repulsion are the two forces that modulate the stability of the

particles or molecules in aquatic environments (Jiang, Oberdörster et al. 2009). To understand NP stability, it is important to understand these two forces.

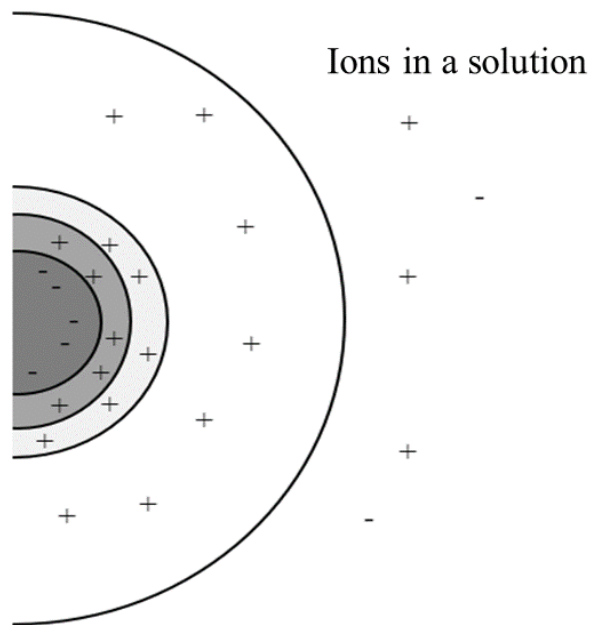


Figure 1.1 The electrostatic double-layer repulsions and Van der Waals forces inspired by (Buschow, 2001).

First, Van der Waals forces are attractive forces between two neighbor dipole-dipole atoms or molecules in the environment (Song et al., 2019). These forces are distance-dependent. However, the distance between the two particles is not long and the equation is represented by the sixth power of the radius between the two particles or London dispersion (Tadros, 2007).

The other force that is part of DLVO is electrostatic, which is the force between similarly charged particles. This causes the two particles to disperse from each other and prevents them from aggregating if they are similarly charged. Examples of electrostatic forces are Surface charge, electrical double-layer, and zeta potential (Tadros 2007). Electrostatic force can come from the surface charge of the particles which are sourced by ionization of acidic/basic groups, or from absorption from different smaller ions, such as amine groups, controlling the charges of the proteins (Alias 2012). The electrostatic double layer can be defined as the method of organizing the charges surrounding the particles (Park 2016). For example, if the particle has a negative charge then the layer that surrounds it will have a positive charge and vice versa. That a positive charge layer also will surround with negative charge layer and by technique, the double electrical layer covered liquid particles (Alias, 2012). Moreover, the outer layer will contain a single particle called zeta potential, or the hydrodynamic plane of shear (Alias, 2012, Ohshima, 2014). However, the two layers are affected by two factors; electrolytes and temperature. These influence the stability of the liquid and the zeta potential accordingly (Alias 2012).

We can determine the stability of the nanoparticle in suspension by using the zeta potential to measure the charge of the surface particles and how it repulses other particles in the solution, hindering aggregation (Hunter, 1981). The  $P_i$  or the isoelectric point is the stable point that determines the stability of the solution and is used as a measurement point (Alias 2012). The range between -30 mV to + 30 mV reflects stable solutions and

indicates whether a solution is strongly anionic or cationic (Jeffrey Clogston 2010, Ohshima 2014). However, high zeta potential refers to high stability for the solution and low zeta potential value means low stability (Alias 2012). In this context, the pH can affect Zeta potential if it is strongly acid or basic (Ohshima 2014, Alias 2012). In addition, the range of zeta potential can be used as measurements for particles such as nanoparticles (NPs), which have ranged from -10 mV to +10 mV (Jeffrey Clogston 2010).

Zeta potential is a useful quality to measure in the study the cytotoxicity of NPs and the tendency of NPs to interact with the negatively charged microbial cell membrane (Jeffrey Clogston, 2010). Hydrodynamic and electrostatic forces are other properties that have a marked effect on bacterial interactions with NPs due to the chemical structure of the bacterial cell membrane and NPs (Fernando et al., 2018a). For example, the hydrophobic nature of bacterial cell walls that contain phospholipids, lipopolysaccharide, or lipoprotein substances attracts hydrophobic NPs to the cell surface and allows more interactions between the cell and hydrophobic NP than hydrophilic NPs (Fernando et al., 2018a). Also, the charge of the particles as measured by zeta potential can affect the adhesion of NPs to the bacteria. The different charges between NPs and the bacterial cell membrane can increase the bacterial membrane permeability (Wang et al., 2017b). This accumulation of cationic NPs on the bacterial membrane also reduce the bacterial attachment and inhibit their growth; Also, it has been reported that the adhesion of NPs on *staphylococcus aureus* outer regions led to penetration of NPs into the cell and effect

the ion exchange inside the bacterial structures (Wang et al., 2017b). In addition to stability in suspension and resistance to agglomeration, other factors can affect the antimicrobial activity of nanoparticles (NPs).

**Effect of nanoparticles on aquatic microbial communities:** While some studies have investigated the impact of nanoparticles in wastewater treatment settings, recent work is beginning to investigate the impact of NP on microbial communities in natural environments. The fate of these nanoparticles in the environment and the environmental impacts of nanoparticles require more investigation. While many studies have examined the antimicrobial properties of NPs in controlled lab environments, previous studies have also shown that NPs, such as TiO<sub>2</sub> NPs, caused a shift in microbial community structure and diversity in soil and stream environments (Battin et al., 2009, Moll et al., 2017). In addition, some NPs such as TiO<sub>2</sub> NPs affect the removal of nitrogen and phosphorus from the environment and cause an essential decrease in aquatic microbial diversity and composition of microbial species (Zheng et al., 2011, Liu et al., 2018, Ward et al., 2019, Londono et al., 2017). One study showed that the addition of silver nanoparticles changed microbial diversity and community composition compared to the control (Ward et al., 2019). In Ward et al Ag NP was added to a wetland environment. They found that *Flectobacillus* and *Oxalobacteriaceae* microbial genus increased in abundance while Betaproteobacteria class decreased in abundance. These changes in diversity suggest that the addition of Ag-NP can differentially affect bacterial classes and result in altered community composition.

## 1.6 Mechanism of resistance to biocides and nanoparticles

### 1.6.1 The mechanisms for resistance to biocides

Bacteria that are resistant to antimicrobials have been known since 1940 when Penicillin-resistant *Staphylococcus* was described as the first antibiotic resistance bacteria. In 2014 the World Health Organization identified antibiotic-resistant bacteria as a major problem that must be addressed (Ventola, 2015, WHO, 2014). The widespread use of biocides and their persistence in the environment may lead to increased antimicrobial resistance (Campa et al., 2019c, Mannan, 2013, Fahimipour et al., 2018). Also, it has been reported that overuse of biocides in hospitals can increase the number of antibiotic-resistant bacteria (Russell, 1999). We previously discussed the mode of action of various classes of biocide and nanoparticles. Due to the implications for healthcare, much work has been done to understand the mechanisms by which bacteria become resistant to antibiotics. Additionally, many studies have sought to understand the mechanisms of resistance to commonly used household biocides such as TCS and TCC. Biocide resistance can be catalyzed by various mechanisms including mutations of the biocide target, degradation of the biocide, increased cell wall thickness, increased expression of efflux pumps, and biofilm formation among others (Poole, 2002).

**Mutations in the target of the biocide:** As described above, most biocides act on many sites in a non-specific manner. However, some biocides such as TCS act on a particular target protein (enoyl-acyl carrier protein reductase enzyme (ENR)) (Carey and

McNamara, 2014). Mutations in the ENR protein can lead to resistance to TCS (Carey and McNamara, 2014). The mutated genes that may be carried on plasmids can be spread through microbial communities and confer resistance to antibiotics via Horizontal Gene Transfer (HGT) mechanisms (Munita and Arias, 2016).

**Degrade the biocide:** Some microbes contain genes that allow for biocide degradation (Maillard, 2005). Possessing these genes allows for the bacteria to break down the biocide allowing for resistance; for example, *E.coli* changes the alkyl hydroxypoxidase structure to resist some biocides (Maillard, 2005). Resistance to Quaternary ammonium compounds (QACs) is one example where biodegradation is a key mechanism for resistance. QACs are used as cationic biocides and have been shown to be released into the environment (Oh et al., 2013). One study found that during adaptation to QACs there was a horizontal transfer of particular genes involved in QAC degradation, which conferred resistance (Oh et al., 2013).

**Increased cell wall thickness:** Another set of mechanisms for resistance to biocides involve limiting the ability of the biocide to enter the cell. Increasing the thickness of the cell wall prevents the entry of the biocide into the cell and therefore protects the cell from the effects of the biocide (Munita and Arias, 2016). For example, the change in the amount of porin protein (a class of protein that responsible for passing small molecules or ions through the cell wall) of *Pseudomonas aeruginosa* can be responsible for resistance

to biocides such as QACs (J.Y.Maillard, 2007). Changes in cell wall thickness will affect the hydrophobicity of the bacterial cell surface and prevent the biocides from entering the cell (J.Y.Maillard, 2007). Another example of this is how *Pseudomonas stutzeri* modifies the proteins and lipopolysaccharides of its outer membrane which increases its resistance to chlorhexidine (Tattawasart et al., 2000).

**Increased expression of efflux pumps:** A primary mechanism for resistance to biocides is the increased expression of efflux pumps (Poole, 2002). These efflux pumps are proteins that can pump out toxic compounds like biocides before they can act upon the cell (Soto, 2013). In general efflux pumps are used in bacteria as a model for cellular transport and can be used to remove toxic substances from the cell (Munita and Arias, 2016). Efflux pumps require energy such as ATP or the proton motive force for the transfer of the substrate outside the cells (Webber, 2002). Many prokaryotic species use efflux systems to resist biocides and antibiotics (Webber, 2002, J.Y.Maillard, 2007, Levy, 2002a). Previous work has shown that efflux pumps are important for resistance to diverse biocides including chlorhexidine, QACs, phenolics, triclosan, and glutaraldehyde (J.Y.Maillard, 2007, Levy, 2002a, Vikram et al., 2015c) (Figure 1.2).

**Biofilm formation:** Biofilm formation is another way to keep the biocides from entering the cell. Many bacteria exist in a biofilm where the cells are attached to a surface and often are surrounded by a layer of exopolysaccharides, which limit the ability of

antimicrobials to reach the cells. The exopolysaccharides produced in biofilms act as physical protection from the biocides (Vikram et al., 2015c).

Some of the mechanisms for biocide resistance are shared with antibiotic resistance. Mechanisms such as thickening of the cell wall, efflux pumps, and biofilm formation are not specific to a particular class of antimicrobials and may serve as a more generic mechanism for resistance to antimicrobials. Some of these mechanisms may be a genetic stress response to toxic chemicals and not specific to biocides. Many of these mechanisms involve changes of phenotypes that are native to the bacteria or may be acquired mutations (Reygaert, 2018). Antibiotic resistance, however, is often conferred by particular proteins which break down the antibiotic (Munita and Arias, 2016). These antibiotic resistance genes can be transferred on plasmids and spread via conjugation, transformation, or transduction (Munita and Arias, 2016). However, there have been few genes that have been specifically identified as catalyzing the breakdown of biocides. Therefore, thickening of cell walls, efflux, and biofilm formation are more often considered mechanisms for biocide resistance. The shared mechanisms between biocide and antibiotic resistance make the development of biocide resistance even more concerning as co-resistance may develop to commonly used antibiotics in response to biocide resistance.

### 1.6.2 The mechanisms for resistance to nanoparticle

Nanoparticle resistance is less well understood. One recent study demonstrated that bacteria can become resistant to NPs by increasing the aggregation of NPs and thus decreasing their ability to interact with the cell (Panacek et al., 2018). In this study, it was shown that overexpression of flagella increased the aggregation of Ag-NP and thus decreased the toxicity and increased the MIC of Ag-NP (Panacek et al., 2018). However, in this study, there was no genetic mechanism identified for this change in expression of the flagellin protein as well as a genome-wide study on the mutations that resulted in increased NPs resistance found that resistance to silver nanoparticles proceeds without any genetic changes (Figure 1.2). Further work is needed to understand the mechanisms of bacterial resistance to NP in a more generalizable manner. Some bacteria have a mechanism to avoid interaction with NPs. For example, the ionic form and the release of NPs can be toxic to bacteria. For example, reducing nitrate and nitrous oxide production is one resistant mechanism used by some bacteria. This reduction will affect the nitrate and nitrous oxide production catalytic pathway of the bacteria and not inhibited them (Zheng et al., 2018).

In general, bacteria have a negative charge, which makes NPs such as  $\text{Ag}^+$  ions have an attraction to the bacterial cell membrane (Richter, Brown et al. 2015). In addition, some bacterial resistance mechanisms can involve altering the interactions between NPs and bacteria. Some bacteria can reduce ionic silver  $\text{Ag}^+$  which is limits the effect of the silver and changes the ionic form (Panacek et al., 2018).

Other bacteria use an efflux system to pump the  $\text{Ag}^+$  out of the cell, and can prevent the interaction between bacteria and the  $\text{Ag}^+$  ion (Panacek et al., 2018).

Another common mode of action for the antimicrobial activity of NPs is often a disruption of the bacterial membranes and the production of reactive oxygen species (ROS). This increase in ROS caused by NPs can inactivate microbes and alter membranes causing proteins oxidation of the membrane (Richter et al., 2015). Many bacteria have mechanisms for coping with oxidative stress and detoxifying reactive oxygen species. Therefore, the native systems for coping with oxidative stress could be a mechanism of resistance to NPs that act through increasing ROS levels.

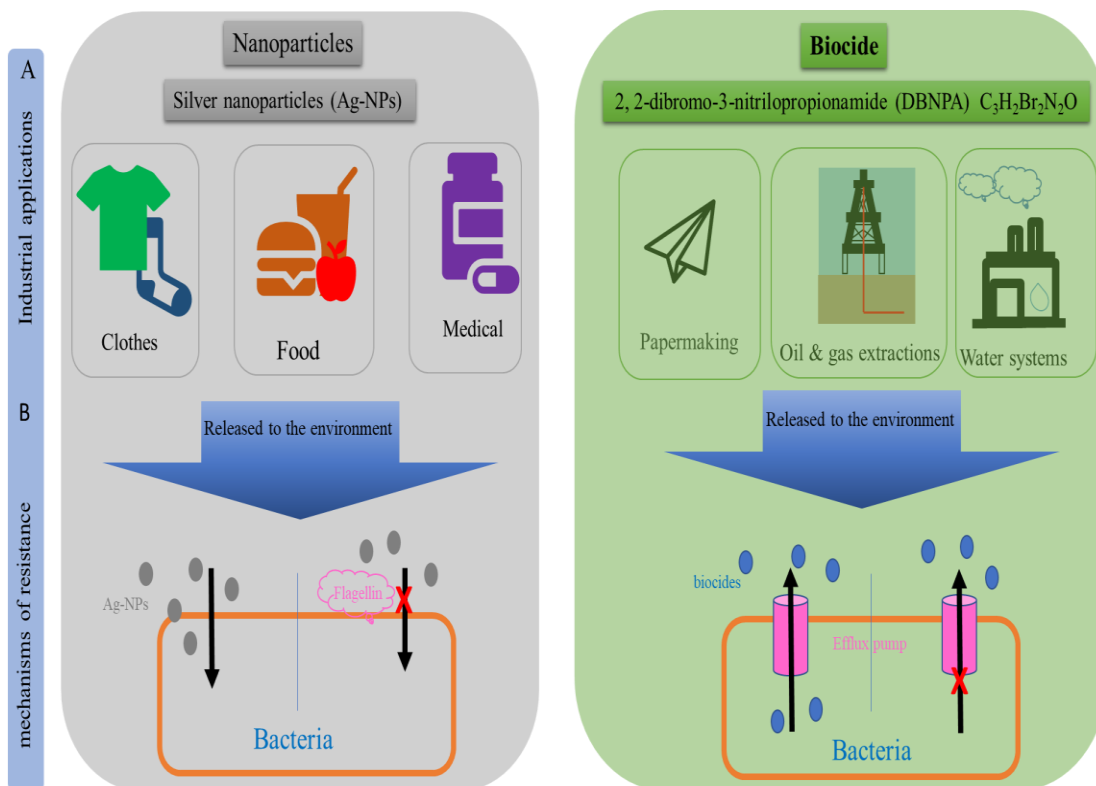


Figure 1.2 (A) Showing Comparative between two types of antimicrobial Biocides (2, 2-dibromo-3-nitropropionamide (DBNPA)) and Nanoparticles (silver nanoparticles (Ag-NPs)) industrial applications. (B) Showing comparative mechanisms of microbial resistance to DBNPA and Ag-NPs inspired by (Merchel Piovesan Pereira and Tagkopoulos, 2019).

## **1.7 The influence of natural organic matter (NOM) on the efficiency of biocides and nanoparticles**

The ecological impacts of biocides and nanoparticles released into natural waters in part depend on their stability and activity under natural conditions. To better understand the fate of these two classes of antimicrobials in the environment, it is important to understand the interactions between these antimicrobials and natural organic matter (NOM) (Taghavi et al., 2013). NOM is a complex chemical mixture of different compounds with ranges of molecular weights, Natural organic matter is derived either from primary production or decomposition of organisms such as plants or animals (Hyung and Kim, 2008). Most NOM in the environment has a negative charge due to carboxylic and phenolic groups. This chemical property has been taken advantage of in drinking water treatment using activated carbon to encourage the adsorption of NOM onto the activated carbon surface (Hyung and Kim, 2008). Previous work has shown that NOM can interact with nanoparticles (Bo et al., 2017). These interactions between NOM and NP can alter the stability of the NP and potentially alter their antimicrobial activity. The van der Waals forces and the electrostatic double-layer repulsion are the two forces that control the stability of the particles or molecular in aquatic environments due to DLVO theory (Jiang et al., 2009).

It has been proposed that NP may be useful as a tool for clean-up in both drinking water and wastewater treatment (Alvarez et al., 2018). However, if the interaction of NOM with

nanoparticles affects their stability or antimicrobial activity, this may limit the utility of NPs in water treatment. It is especially important to understand the influence of NOM on the efficiency of NPs in water and wastewater (Fan et al., 2018). Previous studies have shown that NP aggregate in the presence of NOM (Sikder et al., 2020). Previous studies have shown that NP size is a major factor affecting antimicrobial activity, with small NPs (size < 100 nm) being more effective antimicrobial agents (Wang et al., 2017b, Wu et al., 2021). Therefore, this increased aggregation of nanoparticles in the presence of organic matter may inhibit antimicrobial activity. In order for NP to be of use in water treatment processes, they must be stable and maintain antimicrobial activity in conditions expected to be encountered during the treatment process. However, some studies have shown that interactions between gold (Au) nanoparticles and NOM increased the stability and provided a stabilizing effect under low ionic strength conditions (Stankus et al., 2011b).

Additionally, many biocides used in water treatment are highly reactive and may react with functionalities in NOM. For example, the biocide DBNPA will react with sulfhydryl groups. It is possible that biocide efficacy may be limited in organic matter (OM)-rich environments due to the inactivation of biocides via OM rather than reaction with viable cells. Furthermore, NOM contains many free amine groups, which are the sites of glutaraldehyde reactivity. Therefore, excess NOM in a system may decrease the activity of biocides due to unproductive reactions. Since NOM is a major factor affecting water treatment processes such as coagulation and filtration processes, it is essential to understand the impact of NOM on the antimicrobial properties of NPs.

## 1.8 Goals of this study

Most of the previous studies on the impact of biocides and nanoparticles on microbial communities have focused on either biocides or nanoparticles and very few studies have sought to directly compare their activity. Since many of the modes of action are shared between these two types of antimicrobials, it's possible that they would have similar effects on microbial community composition. Furthermore, while there are many reports of cross-resistance between biocides and antibiotics, there are fewer reports of resistance to antimicrobial nanoparticles. With the growing concern over antibiotic resistance, there is a need to select novel methods for control microbes. Therefore, nanoparticles have been proposed as an appealing alternative to biocides as they are believed to be less likely to select for antimicrobial resistance. As such, we sought to perform a comparative study to investigate the relative impacts of biocides and nanoparticles on stream water microbial communities. The goal of study 1 was to investigate the impact of three types of biocides and three types of nanoparticles (NPs) on the microbial diversity in a hydraulic fracturing impacted stream. Here we hypothesized that biocides would more strongly alter the microbial community composition than nanoparticles.

Additionally, many studies have sought to investigate the mechanisms of biocide resistance. However, very few studies have sought to characterize the development of resistance to nanoparticles. To date, diverse mechanisms have been shown for the development of resistance to biocides including increased expression of efflux pumps.

However, until recently few studies investigated the mechanism for resistance to silver nanoparticles. In a recent study a physical mechanism for resistance was proposed (expression of flagellin proteins leading to Ag-NP aggregation). This study proposed a purely phenotypic mechanism for Ag-NP resistance. To address the potential for distinct mechanisms of resistance to DBNPA and Ag-NP we performed an experimental evolution experiment to examine the potential for the development of resistance to these antimicrobials and provide a direct comparison between adaptations acquired for resistance to DBNPA and Ag-NPs. The goal of study 2 was to investigate the mechanism of bacterial resistance to silver nanoparticles (Ag-NPs) and biocides (DBNPA). Here we hypothesized that bacteria would more rapidly develop resistance to DBNPA compared to Ag-NP and that there would be distinct mechanisms for resistance between the DBNPA- and Ag-NP-adapted *E. coli*.

Finally, there are conflicting reports about the impact of natural organic matter on the stability and impact on the antimicrobial activity of nanoparticles. Some studies have shown that NOM can increase the aggregation of NPs, while others have shown a stabilizing effect. Therefore, we sought to understand how different types of organic matter can affect the antimicrobial activities and aggregation state of Ag-NPs.

Furthermore, we sought to compare the relative impact of NOM on biocide antimicrobial activity. The goal of study 3 was to investigate how four types of natural organic matter (NOM) influence the antibacterial properties of Ag-NPs and DBNPA. Here we hypothesized that nanoparticles and biocides will have decreased antimicrobial activity in

presence of environmentally relevant concentrations of natural organic matter (NOM), but will retain substantial antimicrobial activity.

This work will expand our understanding of the environmental impacts of biocides and nanoparticles by providing a direct comparison of these two common classes of antimicrobials.

# Chapter 2

## Biocides More Strongly Alter Microbial Communities in Hydraulic Fracturing Impacted Stream than Metal Oxide Nanoparticles

### 2.1 Abstract

Our study goal was to investigate the impact of biocides and nanoparticles (NPs) on microbial diversity in a hydraulic fracturing impacted stream. Biocides and NPs are known for their antimicrobial properties and for controlling microbial growth. Previous work has shown that biocides can alter the microbial community composition of stream water and may select for biocide-resistant bacteria. Additional studies have shown that nanoparticles can also alter microbial community composition. However previous work has often focused on the response to a single compound. Here we provide a more thorough analysis of the microbial community response to three different biocides and three different nanoparticles. A microcosm-based study was undertaken that exposed stream microbial communities to either biocides or NPs at a concentration of 16.7 mg/L. We tracked the changes in pH, lactate dehydrogenase (LDH) activity, microbial abundance, and microbial community composition. Our results showed a dramatic decrease in bacterial abundance with different types of nanoparticles, but an increase in microbial abundance in biocide-amended treatments. This increase in microbial

abundance in biocide treatments may suggest the presence of biocide-resistant bacteria in these streams. The microbial community composition (MCC) was distinct from the controls in all biocide and NP treatments, which resulted in differentially enriched taxa in the treatments compared to the controls. Our results indicate that NPs slightly altered the MCC compared to the biocide-treated microcosms. After 14 days, the MCC in the nanoparticle-treated conditions was similar to the MCC in the control. Conversely, the MCC in the biocide-treated microcosms was distinct from the controls at day 14 and distinct from all conditions at day 0. This finding may point to the use of NPs as an alternative to biocides in some settings.

## 2.2 Introduction

Biocides and nanoparticles are known for their antimicrobial properties and are used in controlling microbial growth (Maillard, 2005, Fernando et al., 2018a, Fernando et al., 2018b). If released to the environment, biocides and nanoparticles have the potential for transient and long-term effects on the health of the environment. Biocides are chemical substances used in industrial and household applications to control a wide range of microorganisms (Fink, 2013). The common use of biocides in diverse industries is due in part to their effectiveness and low cost (Guardiola et al., 2012, Levy, 2002). Quaternary ammonium compounds (QACs), glutaraldehyde (GA), Triclosan (TCS), Triclocarban (TCC), chlorine dioxide, and other biocides are commonly used in both household and

industrial applications (Levy, 2002). The widespread use of biocides and their release to the environment has led to ecological problems (Kahrilas et al., 2015).

Of particular interest to our study is the use of biocides in the oil and gas industry, specifically, hydraulic fracturing (HF). HF is the process where highly pressurized water, sand, and a mixture of chemicals are injected into oil and gas harboring shales to release the oil and gas. Biocides are commonly used in hydraulic fracturing to control microbial growth and prevent biofouling. Hydraulic fracturing activity has been shown to alter the response of stream microorganisms to biocides (Mumford et al., 2018, Campa et al., 2018, Campa et al., 2019a). The biocide 2, 2-dibromo-3-nitrilopropionamide (DBNPA) is used in the paper and oil and gas industries for disinfection of industrial water systems and equipment (Chattopadhyay et al., 2004, Siddiqui et al., 2017). Glutaraldehyde (GA) and DBNPA are two of the most commonly used biocides in hydraulic fracturing operations (Kahrilas et al., 2015). The release of biocides such as GA and DBNPA into aquatic environments can cause shifts in the microbial community composition through the inactivation of certain microbes. For example, (Mumford et al., 2018) demonstrated the potential for biocides to decrease iron reduction rates (Mumford et al., 2018). Glutaraldehyde amendment also resulted in changes to microbial community structure in stream microbial communities. In a microcosm-based study, differences were observed in the microbial community response to GA depending on the level of hydraulic fracturing activity in the watershed along with past contamination, with streams previously exposed to hydraulic fracturing wastewater being more resistant to GA

addition (Campa et al., 2018). Furthermore, it has been proposed that biocide use associated with hydraulic fracturing operations could lead to antimicrobial resistance in streams adjacent to HF operations (Campa et al., 2019b).

Nanoparticles (NPs) are substances with nanoscale diameters. The design and shape of NPs play an important role in the effect of these particles (Liu et al., 2012). Engineered nanoparticles, such as silver (Ag), titanium dioxide (TiO<sub>2</sub>), and zinc dioxide (ZnO) have antimicrobial properties (Paterson et al., 2011, Li et al., 2008). Metal oxides NPs and other metals, such as silver and copper, are commonly used to control microbial activity (Wang et al., 2017). Metal and metal oxides of NPs have been reported to be toxic to microbes through diverse mechanisms (Slavin et al., 2017). These mechanisms include the production of reactive oxygen species (TiO<sub>2</sub>, ZnO), compromising of the cell envelope (ZnO and Ag), among other mechanisms (Slavin et al., 2017). Similarly, silica nanoparticles are considered safe antimicrobial agents due to silica being natural in many environments (Adams et al., 2006, Kim et al., 2017). TiO<sub>2</sub>, especially as nanoparticulate anatase, is thought to be an interesting antibacterial agent with notable photocatalytic behavior (Krug., 2008). Also, the stability of NPs in solutions is important for the antimicrobial properties of NPs specifically on causing bacterial cell membrane damage (Kumari et al., 2014).

While many studies have examined the antimicrobial properties of NPs in controlled lab environments, previous studies have also shown that NPs, such as TiO<sub>2</sub> NPs, caused a shift in microbial community structure and diversity in soil and stream environments (Battin et al., 2009, Moll et al., 2017, Ward et al., 2019). In addition, NPs have been shown to affect some of the bacteria that responsible for the removal of nitrogen and phosphorus from the environment and cause an essential decrease in aquatic microbial diversity and change in the composition of microbial species (Liu et al., 2018, Ward et al., 2019, Londono et al., 2017). One study showed that the addition of silver nanoparticles (Ag-NP) changed microbial diversity and community composition compared to the controls where no Ag-NP was added (Ward et al., 2019). While there are fewer reports of bacterial resistance to nanoparticles, a recent study examined the potential for *E. coli* to develop resistance to Ag-NP (Panacek et al., 2018). This study demonstrated that after 20 transfers in the presence of Ag-NP, *E. coli* became at least 10 times more resistant to Ag-NP than the parental strain. They also demonstrated that overexpression of flagellin proteins resulted in aggregation of Ag-NP leading to the enhanced tolerance of the Ag-NP. The authors of this study found that purified flagellin resulted in NP aggregation and since NP activity is associated with particle size, this aggregation resulted in decreased NP efficacy.

Few studies have directly compared the impact of biocides and NPs on natural microbial communities in the context of previous hydraulic fracturing contamination. Here, we sought to better understand the environmental effects of biocides and nanoparticles by

comparing the effects of biocides and NPs on microbial abundance and community composition. A microcosm-based approach was used, where stream microbial communities were exposed to both biocides or NPs, and changes in cytotoxicity measures, microbial abundance, and microbial community composition were tracked. Previous work has shown that biocides strongly and rapidly alter microbial community composition (Campa et al., 2019a, Campa et al., 2018) Other studies have shown that Ag-NP can strongly impact microbial community composition. We hypothesized that biocides will result in a more strongly altered microbial community composition relative to NPs. The objective of the study was to investigate the impact of biocides and nanoparticles on natural microbial communities in one hydraulic fracturing-impacted stream.

### **2.3 Materials and methods**

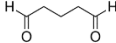
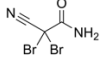
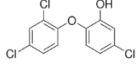
The biocides used in this study were 2, 2-dibromo-3-nitrilopropionamide (DBNPA) (molecular weight: 241.87 g/mol, Sigma-Aldrich), Triclosan (molecular weight: 289.54 g/mol, Sigma-Aldrich), and Glutaraldehyde (molecular weight: 100.12 g/mol, Sigma-Aldrich). Stock solutions of each were prepared at a concentration of 100 mg/L and dissolved in ethanol (Table 2.1).

The nanoparticles used in this study were commercial preparations of metal oxide nanoparticles (US Research Nanomaterials, Inc. 3302 Twig Leaf Lane, Houston, TX

77084, USA, 99.9% TiO<sub>2</sub> with 18 nm, 99.95% ZnO with 18 nm, and 99.5% SiO<sub>2</sub> with 18nm) all of the nanoparticles were spherical in shape. Molecular weight of TiO<sub>2</sub> is 79.87 g/mol. Molecular weight of ZnO is 81.38 g mol<sup>-1</sup>. Molecular weight of SiO<sub>2</sub> is 60.08 g/mol (Table 2.1).

Table 2.1

The biocides or NPs used in this study.

Antimicrobial	Antimicrobial type	Chemical Structure	Chemical Formula
<b>Glutaraldehyde (GA)</b>	Biocide		C <sub>5</sub> H <sub>8</sub> O <sub>2</sub>
<b>2, 2-dibromo-3-nitrilopropionamide (DBNPA)</b>	Biocide		C <sub>3</sub> H <sub>2</sub> Br <sub>2</sub> N <sub>2</sub> O
<b>Triclosan (TCS)</b>	Biocide		C <sub>12</sub> H <sub>2</sub> Cl <sub>3</sub> O <sub>2</sub>
<b>Titanium oxide (TiO<sub>2</sub>)</b>	Nanoparticles	O=Ti=O	TiO <sub>2</sub>
<b>Zinc oxide (ZnO)</b>	Nanoparticles	Zn=O	ZnO
<b>Silicon dioxide (SiO<sub>2</sub>)</b>	Nanoparticles	O=Si=O	SiO <sub>2</sub>

### 2.3.1 Microcosm set up

Stock solutions of nanoparticles were prepared at concentration 100 mg/L in sterile Milli-Q water and sonicated in an ultrasonic bath (Sonicator) for 20-30 min and stored in a refrigerator and used within a week. Surface water was obtained from Lower Greys Run,

PA. The water for culturing was collected in sterile 500 ml plastic bottles (Figure 2.1; Figure. S2.3.1.1.). The bottles were shipped on ice to Michigan Technological University on ice and stored at 4 °C until the microcosm was set up after a week. Thirty mL of stream water was placed into sterile serum bottles in triplicate. One set of bottles was used as a control with no amendment. The controls were used to track the normal growth of the microbial cells without nanoparticles or biocides to understand the bottle effect. This condition served as a negative control to control for changes in microbial community diversity and composition that resulted from other factors than treatment with antimicrobials. Other sets of microcosms were set up where nanoparticles or biocides were added to the water samples. Five ml of the 100 mg/L stock of nanoparticles or biocides was added to 25 ml of stream water to make 16.7 mg/L as the final concentration. The working concentration for all treatments were as follows: 0.069 mM for DBNPA, 0.057 mM for triclosan, 0.166 mM for glutaraldehyde, 0.21 mM for TiO<sub>2</sub>, 0.21 mM for ZnO, and 0.28 mM for SiO<sub>2</sub>. Our experimental design controlled for gravimetric concentration. Previous studies into the impacts of biocides or nanoparticles on microbial communities have used gravimetric concentrations (Campa et al., 2018, Campa et al., 2019b, Ward et al., 2019) Therefore, controlling for gravimetric concentration allows for comparison with previous work. However, this design allows for us to test if high molar concentrations of NPs have stronger effects on microbial community diversity and composition. We chose these concentrations of biocides and nanoparticles based on previous studies that have shown that similar or lower concentrations of antimicrobials resulted in effects on the microbial community (Ward et

al., 2019, Battin et al., 2009, Drury et al., 2013, Gnanadhas et al., 2013, Vikram et al., 2015c). All conditions were set up in triplicate. The bottles were incubated aerobically at 25°C in the dark. Bottles were sacrificially sampled at the given time points. The water was filtered through a 0.2 µm pore size, polyethersulfone (PES) membrane with a 47 mm diameter using a vacuum pump. The filters were retained for DNA extraction. Time zero samples were collected after the addition of antimicrobials and after all microcosms were set up. Therefore, there were slight differences in the time of exposure after the addition of the antimicrobials until the time zero conditions were frozen. Filtered water was kept for the measurement of pH and LDH activity. Measurements were taken every 0, 1, 7, and 14 days.



1. Lower Grays Run, PA.

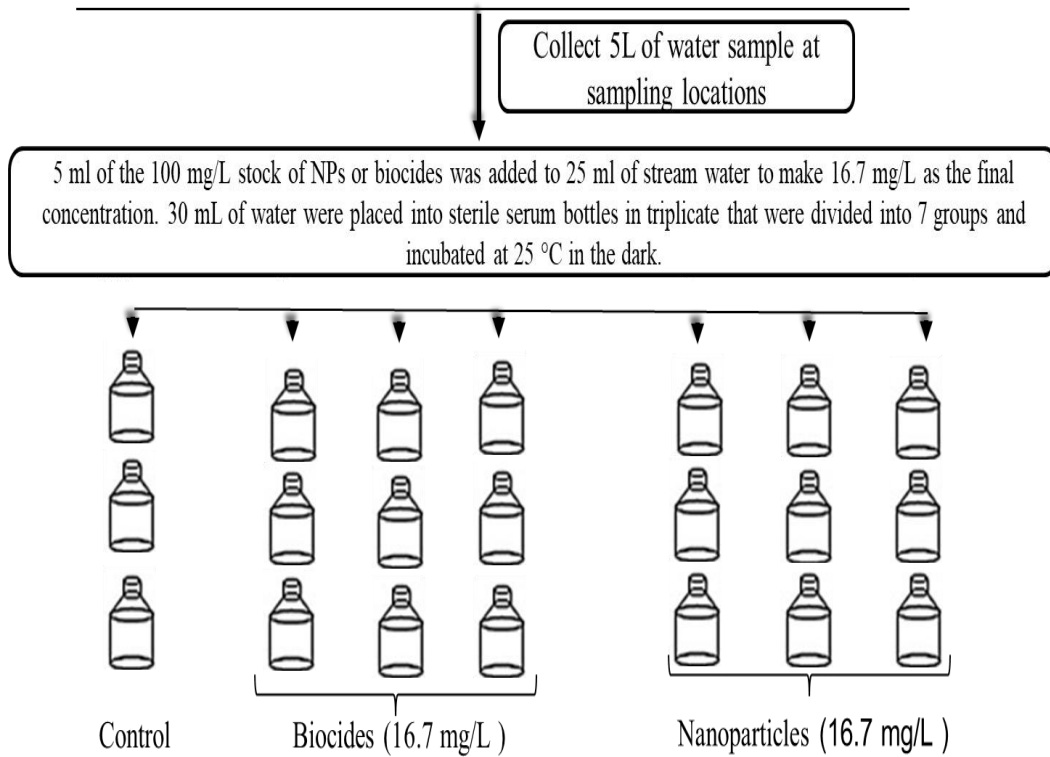


Figure 2.1 Microcosm set up of nanoparticles and biocides stock solution with the Lower Greys Run, PA surface water.

### 2.3.2 Nanoparticle characterization

The size and charge of nanoparticles in stream water were determined throughout the experiment. Size and zeta potential were determined using a Malvern zetasizer at 25°C. The zetasizer measures particle and molecular size using dynamic light scattering (DLS) and zeta potential and electrophoretic mobility using electrophoretic light scattering. The size distribution and charge of the nanoparticles were determined from the average independent size (d. nm) measurements. The average size distribution was determined for each replicate. The size of the nanoparticles was determined based on intensity. The average of the particle size distribution and zeta potential for most treatments were measured three independent times. TiO<sub>2</sub> day 0, ZnO day 0, SiO<sub>2</sub> day 0, TiO<sub>2</sub> day 7 are only shown as the average size distribution of three independent measurements on the zeta sizer and reported as the average distribution. For all other samples, each independent measurement is reported allowing for standard deviation and stander error to be reported (Table S2.4.1.1, and Table S2.4.1.2).

Nanoparticles were also characterized by Transmission Electron Microscopy (TEM) to confirm the studied particles' size and shape. To perform TEM, we pipetted 5 µl from 16.7 mg/L of nanoparticles incubation bottles at day 0 onto a carbon-coated grid. Samples were examined by TEM images using a FEI 200kV Titan Themis STEM microscope at an accelerating voltage of 80 kV (FEI company, USA). The specimens were prepared for each NPs in a closed tube.

### **2.3.3 pH measurements**

The pH of the microcosms was measured in order to determine the change in the pH of stream water as a result of treatment. The pH of a system can impact the microbial community composition (Hou et al., 2017). The pH measurements were taken for the filtered water every 0, 1, 7, and 14 days. The pH was measured using Fisherbrand™ accumet™ AB250 pH/ISE Benchtop calibrated with a three-point standard curve. A Shapiro-Wilk test was used to determine if the pH data were normally distributed. Since the data was not normally distributed, a Kruskal-Wallis test was used to compare between time and treatments and evaluate the significance relative to the control of experimental results ( $P < 0.05$  was considered significant). Dunn's significance difference test for multiple comparisons of means was used as a post hoc test to evaluate the significance of experimental results ( $P < 0.05$  was considered significant). For the Dunn test p-values were corrected for multiple comparisons using a Benjamini-Hochberg false discovery rate correction.

### **2.3.4 Membrane permeability assessment - lactate dehydrogenase assay (LDH)**

Lactate dehydrogenase (LDH) measurements estimate the viability of bacterial cells by detecting the damage of bacterial cell membrane structure (Kumari et al., 2014). LDH is an intracellular enzyme. A high concentration of LDH outside of the cell is an indication of cellular damage and cytotoxicity. The LDH enzyme is present in the anaerobic metabolic pathway in all tissues such as plants, animals, etc. LDH functions in the

conversion of lactate to pyruvate by reducing the NAD<sup>+</sup> to NADH and vice versa (Farhana and Lappin, 2021). The filtrate from each microcosm was saved and used to measure cytotoxicity. LDH was measured following standard methods. LDH was measured as follows: 100  $\mu$ L from each filtered water bottle were mixed with 30 mM sodium pyruvate, and 2.8 mL of 0.2 M Tris-HCl. Then 100  $\mu$ L of 6.6 mM NADH were added to the mixtures. LDH activity was measured by tracking absorbance at 340 nm using a UV-vis spectrophotometer (Kumari et al., 2014). The LDH measurements were taken for the filtered water collected from the microcosms after 24 hr. A Shapiro-Wilk test was used to determine if the LDH data were normally distributed. The data was not normally distributed, therefore a Kruskal-Wallis test was used to determine if there was a significant difference between treatments at different times as well as if there were differences between nanoparticle or biocide conditions at different times. A Dunn test was used as a post hoc test to determine which conditions and times were their significant differences. For the Dunn test p-values were corrected for multiple comparisons using a Benjamini-Hochberg false discovery rate correction.

### **2.3.5 DNA extraction**

DNA was extracted from the water filters using the Zymobionics DNA extraction kit. Sterilized scissors and forceps were used to cut the 47 mm filters in half in a sterile petri dish. The Zymobionics DNA extraction kit protocol was followed according to the manufacturer's specifications (D4301, Zymo Research Corporation, Irvine, CA USA).

### 2.3.6 Bacterial abundance analysis (qPCR)

Abundance of the 16S rRNA gene were determined by using quantitative Polymerase Chain Reaction (qPCR). We used gene copies of the 16S rRNA gene as a proxy for microbial abundance. qPCR was performed as previously described in (Techtman et al., 2017). The qPCR reaction set up as follows: 10 $\mu$ l of SYBR® Green RT-PCR master mix, 0.5  $\mu$ l of each primer (20  $\mu$ M) Bact341F and Uni519R primers (Jorgensen et al., 2012), 2  $\mu$ l of Environmental DNA, and 7  $\mu$ l Sterile nuclease-free water. Reactions were prepared in white 96 well PCR plates that have been sterilized by autoclaving. The amplification was carried out in a StepOnePlus™ Real-Time PCR System thermocycler (ThermoFisher Scientific Waltham, MA USA). The following temperature protocol was used: 95°C for 15 min and 35 cycles of 95°C for 15 sec, 58°C for 30 sec, and 72° C for 30 sec. The CT values or threshold cycle is the cycle number at which the fluorescence generated within a reaction crosses the fluorescence threshold, which provides the amount number of generated gene amplicon product were converted to a number of copies using a standard curve based on the standards described in (Techtman et al., 2017). The concentration values were converted to log CT and log(copies) and followed the equation  $y = -11.932x + 20.312$  with an  $R^2$  of 0.9594 for our standard curve. A Shapiro-Wilk test for normality was used to determine if the qPCR gene copies data were normally distributed. The data was not normally distributed, so a Kruskal-Wallis Test was used to evaluate the significance of experimental results ( $P < 0.05$ ). A Dunn's test significance difference test for multiple comparisons of means obtained was used as a post hoc to evaluate the significance of experimental results ( $P < 0.05$ ). Comparisons were performed between

treatments and the control as well as to see if there were significant differences between biocide- and NP-amended treatments and the control.

### **2.3.7 Microbial community composition analysis (16S rRNA) gene sequencing**

The microbial community composition profile was determined using 16S rRNA gene sequencing of the environmental DNA. The 16S rRNA gene was amplified to profile changes in taxonomic diversity in these microcosms. The total reaction volume was 25  $\mu$ L. The reaction setup was (12.5  $\mu$ L Phusion® High-Fidelity PCR Master Mix (Thermo Fisher Scientific, Waltham, MA, USA), 515YF and 926R primers were used to amplify the V4-V5 region with 0.4  $\mu$ M concentration in a 96 well PCR plate (Parada et al., 2016). The amplification was carried out in a thermocycler with the following protocol: 95 °C for 3 min, 25 cycles of 95 °C for 30 sec, 55 °C for 30 sec, 72 °C for 30 sec, followed by one cycle of 72 °C for 5 min. PCR clean-up was done on the initial amplicon. Following the Illumina MiSeq 16S rRNA metagenomic library prep guides (Illumina, San Diego, CA), AxyPrep MAG PCR clean-up beads (Corning, Big Flags, NY, USA) were used for the PCR cleanup process. The final product was eluted in 25  $\mu$ L 10 mM Tris buffer at a pH of 8. Sequencing adapters and indexes were added with a second PCR, where 5  $\mu$ l were added from the first PCR reaction, and different index forward and reverse primers were added to each reaction then performed an 8 cycle PCR. The indexed PCR product was purified using the AxyPrep MAG PCR clean-up beads. Finally, 16S rRNA gene sequencing was done using the Illumina MiSeq (Illuming, SanDiego, CA). The

concentration of each of the cleaned 16S rRNA PCR reactions was determined using PicoGreen™. We pooled all our samples with the same concentration into one pool and diluted the pool to 1.5 nM. Then we followed the MiSeq v2 600 cycle kit (2 x 300) protocol.

All data analysis was performed in R. Raw sequencing reads were demultiplexed by the Illumina MiSeq platform. The DADA2 package was used to remove primer nucleotides, merge paired-end reads, quality filtered, and cleansed of internal standard phiX. To account for true biological variation within our samples, DADA2 was used to infer ASVs (amplicon sequence variants) and remove chimeric sequences through a Needleman-Wunsch global alignment. From 408549 paired-end input reads, 403744 nonchimeric reads passed filtering parameters and were used as ASVs for analysis in this study. Taxonomy of ASVs was assigned through DADA2 with a rapid assignment naive Bayesian classifier using the SILVA v132 training set(Callahan et al., 2016).

Only samples with more than 1000 reads were used in downstream analyses. Due to low sequencing yields, this resulted in a substantial number of treatments being removed from the dataset. Therefore, we compared the microbial community composition for each treatment on days 0 and 14 of the experiment to analyze the impact of treatment on microbial community composition. For day 0 only the control, triclosan, TiO<sub>2</sub>, ZnO, and SiO<sub>2</sub> treatments had more than 1000 reads and were included in our analysis. Diversity

analyses were performed using phyloseq (McMurdie and Holmes, 2013). Alpha diversity was determined through rarifying the ASV table 100 times to the lowest number of sequences per sample (1111 reads). Shannon diversity, inverse Simpson, and observed ASVs were determined for each of the 100 tables. The average diversity for the 100 tables was calculated. A Shapiro-Wilk test was used to determine if the data was normally distributed. Both Inverse Simpson and Observed ASVs were normally distributed so an ANOVA was used to assess significance in the diversity between Nanoparticles and Biocides at the two times. The Shannon diversity data was not normally distributed so a Kruskal Wallis test was used to see if there was a significant difference in the Shannon between Nanoparticles and Biocides at the two times.

To assess differences in microbial community composition, we performed a Principle Component Analysis (PCoA) based on a Bray Curtis dissimilarity matrix from an ASV table rarified to 1111 sequences per sample. To determine if there were significant differences in the microbial community composition between nanoparticles and biocide treatments, a PERMANOVA of Bray Curtis dissimilarity using the `adonis2` program in the `vegan` package in R. Differential abundance was performed using DESeq2 (Love et al., 2014) to identify ASVs that were enriched in either the NP or biocide treatments at day 14. ASVs were considered enriched if they had a log<sub>2</sub> fold change of greater than 2 and an adjusted p-value of < 0.05.

## 2.4 Results

### 2.4.1 Metal oxide nanoparticles size and stability

To study the stability of NPs at a gravimetric concentration of 16.7 mg/L in the stream water and their aggregation behavior, the size and zeta potential analysis were performed at days 0,1,7, and 14 (Table.2.1, Table S2.4.1.1, and Table S2.4.1.2). Throughout the experiment, the mean of the size distribution of TiO<sub>2</sub> NPs decreased in size from 667.6 nm on day 0 to 280.13 nm on day 14. Similarly, the mean size distribution of the ZnO NPs decreased from 397.7 nm on day 0 to 280.13 nm on day 14. With SiO<sub>2</sub> NPs there was an increase in mean size distribution from 387.9 nm on day 0 to 548.63 nm on day 14. Zeta potential has been used as an indicator of dispersion stability. With all NPs, the zeta-potentials were highly negative, which suggests that they are stable in the water samples. The zeta potentials were less than -18.7 mV which represents the dispersion of particles. The size of the NPs in the 16.7 mg/L solutions of the three nanoparticles and stream water was also measured using TEM (Figure.2.2).

Table. 2.2

Showing the average of three measurements of the mean NPs size, zeta potential, and their standard error in Lower Grays water treated samples over time (n=3) (average  $\pm$  standard error).

Type of Nanoparticles / Days	TiO <sub>2</sub>		SiO <sub>2</sub>		ZnO	
	Size	Zeta Potential	Size	Zeta Potential	Size	Zeta Potential
	(d.nm)	(mV)	(d.nm)	(mV)	(d.nm)	(mV)
<b>Day 0</b>	667.6	-23	387.9 $\pm$ 5.8	-18.1	397.7	-25.2
<b>Day 1</b>	457.9 $\pm$ 7.7	-24.67 $\pm$ 0.32	541.4 $\pm$ 37.8	-21.5 $\pm$ 1.2	343.2 $\pm$ 1.7	-21.3 $\pm$ 1.2
<b>Day 7</b>	269.9	-18.7 $\pm$ 0.76	460.83 $\pm$ 20.9	-28.8 $\pm$ 1.9	203.76 $\pm$ 3	-27.3 $\pm$ 2.9
<b>Day 14</b>	280.13 $\pm$ 5.1	-24.03 $\pm$ 0.9	548.63 $\pm$ 16.1	-24.3 $\pm$ 2.2	398.86 $\pm$ 15.7	-18 $\pm$ 1.8

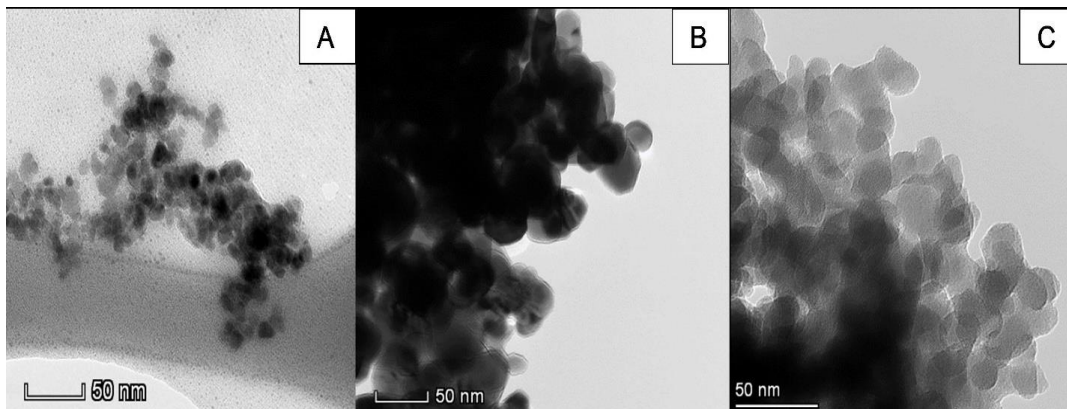


Figure 2.2 Transmission electron microscopy photomicrograph of (A) TiO<sub>2</sub> NPs stock solution, (B) ZnO NPs stock solution, (C) SiO<sub>2</sub>NPs. stock solution scale bars = 50 nm.

#### 2.4.2 Change in pH over time and treatment

There was a significant difference in the pH in the NPs and biocide treatments and at different times (Kruskall Wallis test p-value = 1.654e-08) (Fig.2.3, Table S2.4.2.1).

Despite the overall significant difference, there were only slight changes in the pH.

When comparing the pH at time 0 and Day 7, significant differences were seen for SiO<sub>2</sub> (Dunn test adjusted p-value = 0.019) and Triclosan (Dunn test adjusted p-value = 0.015).

When comparing the pH between Day 0 and Day 14, triclosan showed a significant difference (Dunn test p-value = 0.021) (Table S2.4.2.1). In general, the pH level of the metal oxide NPs looked similar to the control. On the other hand, in our study biocides tended to lower the pH, especially with glutaraldehyde.

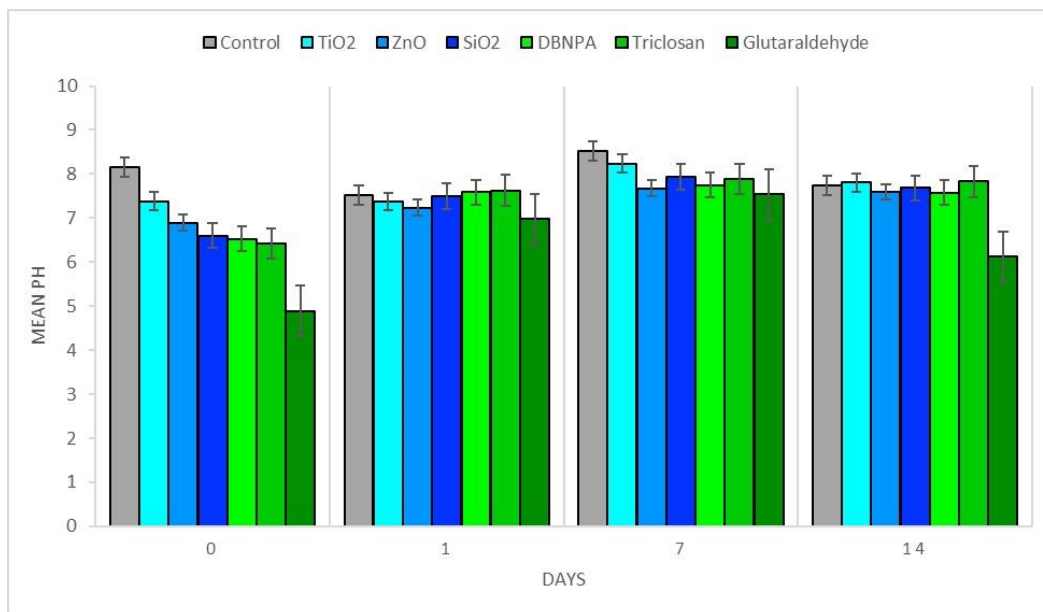


Figure. 2.3 pH measurements of NPs and Biocides in Lower Grays Run, PA. Showing change in pH over time and treatment.

### 2.4.3 Cytotoxicity effects of biocides and nanoparticles on bacterial membrane permeability (LDH)

LDH measurements were obtained from filtrate at all time points following established protocols (Kumari et al., 2014) by measuring an OD340 using the filtered water for both NPs, biocides, and the control samples (Figure.2.4). TiO<sub>2</sub> was the only treatment to give a higher LDH level than the control on day 1. No significant differences were observed for any of the treatments in comparison to the control on day 1. The LDH level for triclosan, glutaraldehyde, DBNPA, ZnO, and SiO<sub>2</sub> were all less than the control at 24 hours (Table S2.4.3.1). On day 7 and day 14, all of the treatments had high levels of LDH activity.

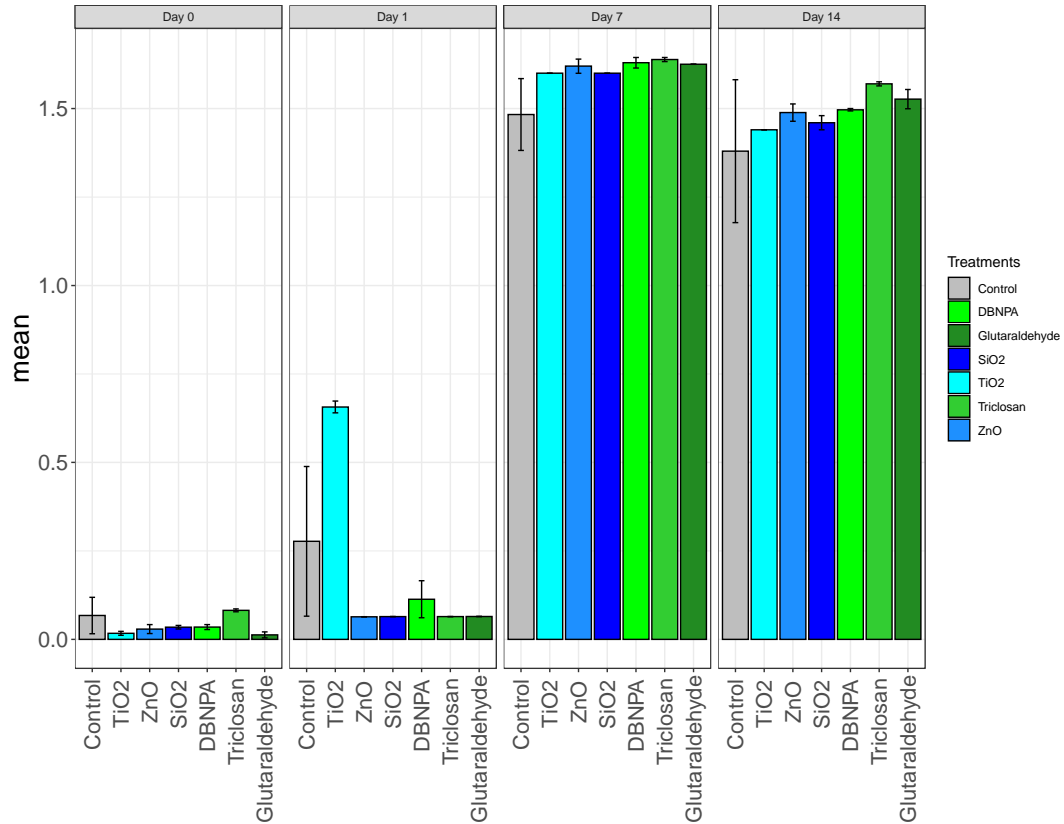


Figure 2.4 Showing relative LDH and the standard error for 16.7 mg/L concentration of biocides and NPs (n=3)

#### 2.4.4 Effect of NPs and biocides on 16S rRNA gene copies

The change of the 16S rRNA gene abundance was determined by using real-time qPCR (Figure. 2.5 and Table.S2.4.4.1). During PCR amplification, we used the copies of the 16S rRNA gene as a proxy for the bacterial abundance changes with different treatments. We compared the microbial abundance between treatments and the control. Additionally, we showed the change in 16S rRNA copies as a function of time for each treatment. Overall, between day 0 and day 14, there was an increase in microbial abundance in the biocide treatments. On the other hand, the microbial abundance in NPs treatments looked

similar to the control as it decreased over time. However, the bacterial abundance with GA had the greatest change in the number of copies from  $8.54 \times 10^3 (\pm 1.53 \times 10^3)$  to  $2.99 \times 10^7 (\pm 9.97 \times 10^6)$  copies/ml from day 0 to day 14 out of all of the treatments. For the biocides, the DBNPA treatments showed the least change in abundance over the experiment with a change of  $7.48 \times 10^3$  to  $1.29 \times 10^5$  copies/ml between day 0 and day 14. The Triclosan treatments showed the least change in abundance over the experiment with a change of  $1.18 \times 10^4$  to  $1.12 \times 10^8$  copies/ml between day 0 and day 14. In contrast, the bacterial abundance with  $\text{SiO}_2$  had the smallest change in the number of copies of any of the NPs treatments from  $1.02 \times 10^7$  to  $5.43 \times 10^4$  copies/ml observed from day 0 to day 14.  $\text{TiO}_2$  had a change in the number of copies of the 16S rRNA gene over the experiment from  $2.29 \times 10^6$  to  $1.41 \times 10^4$  copies/ml. ZnO had the greatest change in the number of copies of the 16S rRNA gene over the experiment from  $3.94 \times 10^7$  to  $2.81 \times 10^4$  copies/ml. In general, the gene copies at time zero for the biocide treatments were lower than the gene copies at time zero for the control and nanoparticles. This difference may be due to the activity of the biocides during the time from the addition of the antimicrobials to when the samples were filtered, which was longer for the nanoparticles samples. On day 7, the microbial abundances were similar between the NPs and biocide treatments. The biocides treatments on average increased by 2.7 log from day 0 to day 14. The nanoparticle treatments on average decreased by 2.8 log from day 0 to day 14. The increase of microbial abundance in biocide treatments over time might suggest the presence of resistant bacteria in these streams. There was a significant difference in the gene copies when comparing time and treatment (Kruskal Wallis p-

value = 0.00116). However, when using the Dunn test there were no significant differences between day 0 and day 14 for any of the treatments based on p values adjusted for multiple comparisons (Table.S2.4.4.2).

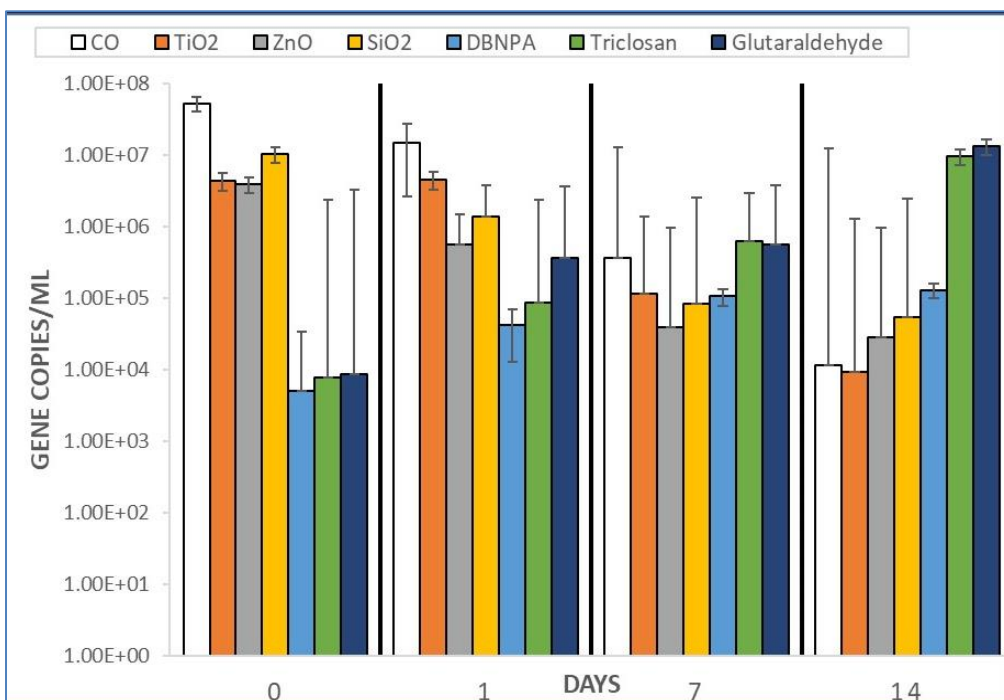


Figure 2.5 Showing the plots of the mean  $\pm$  standard deviation of microbial abundance changes over time to compare the effect of nanoparticles and biocides in Lower Grays Run, PA samples.

## 2.4.5 Microbial community structure

### 2.4.5.1 Changes in alpha diversity in biocide and nanoparticle treatments

Overall NP microcosms had higher evenness and richness than biocide treatments after 14 days of incubation. On day 0 the control, all three nanoparticle treatments, and the

triclosan treatment all had similar diversity. After incubation, the triclosan and glutaraldehyde treatments had lower diversity than the control and nanoparticle treatments (Figure.2.6). The DBNPA treatment at 14 days had high Shannon diversity, Inverse Simpson's diversity, and observed ASVs, which were similar to the control and the nanoparticle treatments. When comparing the diversity of biocide treatments with NPs and control, there were no significant differences between biocides and NP for any of the three alpha diversity metrics tested. (Kruskal Wallis p-value 0.3914 for Shannon, ANOVA p-value 0.496 for inverse Simpsons, and 0.748 for richness respectively) (Table.S2.4.5.1).

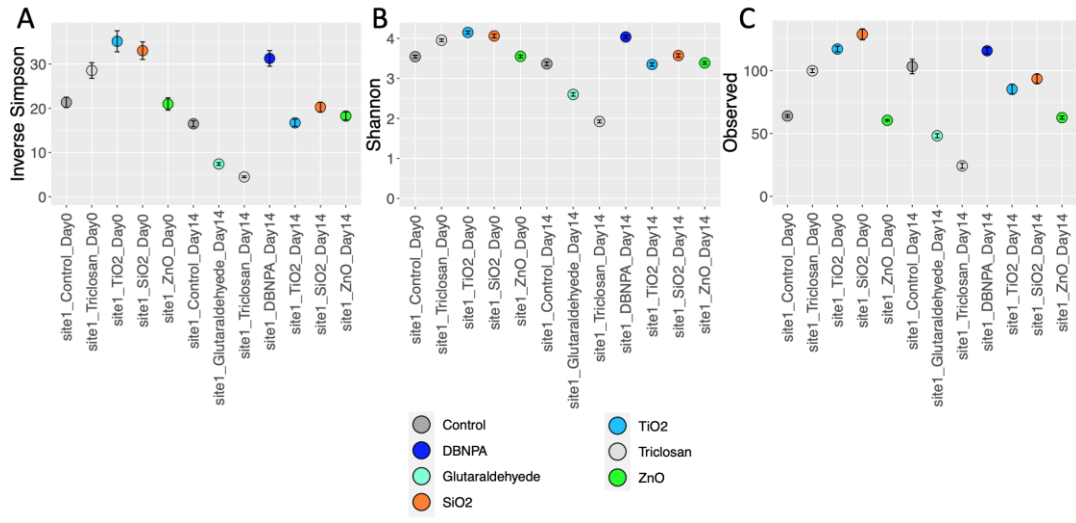


Figure 2.6 Three different richness and evenness alpha diversity estimates, (A) Inverse Simpsons, (B) Shannon, and (C) richness (observed ASVs). Represent the differences in alpha diversity on day 0 and day 14 to compare the effect of NPs and biocides in Lower Grays Run, PA samples.

#### **2.4.5.2 Principal coordinate analysis (PCoA):**

PCoA analysis of a Bray Curtis dissimilarity matrix from the rarified ASV table showed three distinct groups (1) the initial time points, (2) triclosan and Glutaraldehyde at day 14 and (3) NPs, and control at day 14 (Figure.2.7). The PCoA analysis shows that all of the nanoparticles, the control, and triclosan (the only one of the initial biocide treatments to have sufficient sequences) clustered together at time zero. This indicates that the microbial community composition of the starting communities was similar despite the initial difference in microbial abundances. After 14 days of incubation, a divergence in community composition was observed between the triclosan and glutaraldehyde compared to the NPs and the control. On day 14, the three nanoparticles and the control clustered together, whereas the biocide treatments were distant from the control and each other. This finding suggested there was a change in the microbial community between biocide and NPs samples, which indicates that biocides alter the microbial community composition more strongly than the nanoparticles. Interestingly the DBNPA treatment at day 14 clustered more similarly to the initial time points. This could be in part due to the short half-life of DBNPA and water (Campa et al., 2019a). Permutational multivariate analysis of variance (PERMANOVA) was used to test the hypothesis that the microbial community composition in the biocide treatments was significantly different from the nanoparticle treatments at different time points (PERMANOVA P-value 0.009, degrees of freedom 5,  $R^2$  0.613) (Table 2.3).

Table 2.3

Permutational multivariate analysis of variance (PERMANOVA) of Bray Curtis dissimilarity of Lower Grays Run, PA samples comparing nanoparticle and biocide treatments days 0 and 14.

<b>Comparison</b>	<b>No. of degrees of freedom (Df)</b>	<b>Sums of Squares (Sums of Sqs)</b>	<b>R<sup>2</sup></b>	<b>F. statistic value (F. Model)</b>	<b>P-value Pr(&gt;F)</b>
<b>Nanoparticles vs. Biocides</b>	5	2.2640	0.61366	1.9061	0.009
<b>Residuals</b>	6	1.4253	0.38634		
<b>Total</b>	11	3.6893			

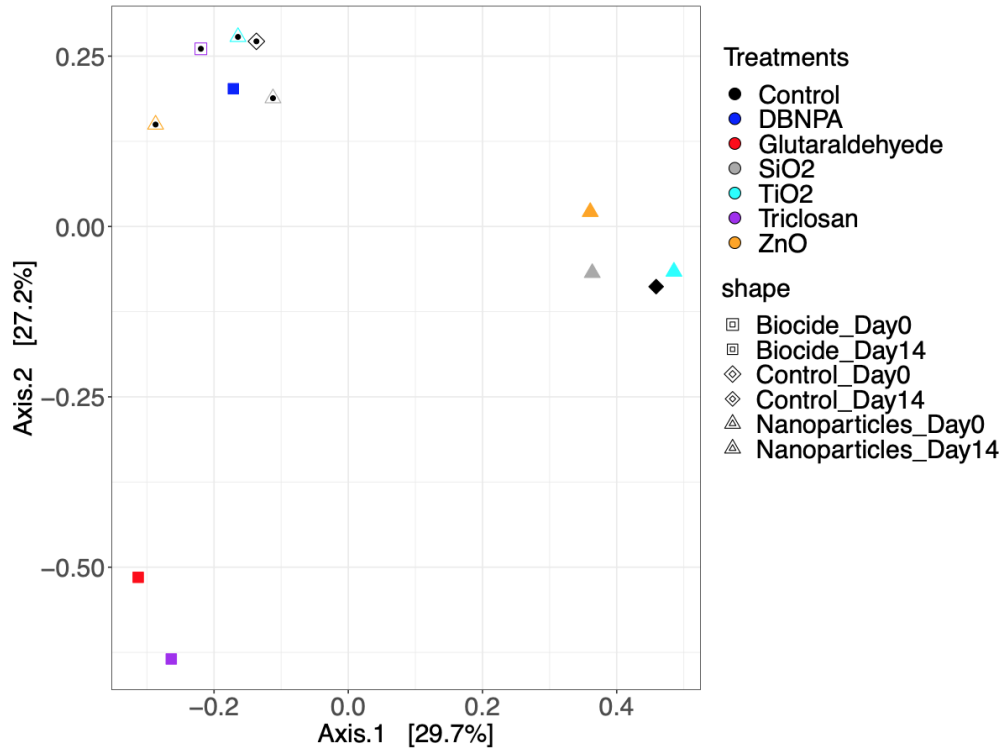


Figure 2.7 Principal coordinate analysis (PCoA) of Bray Curtis Dissimilarity of the rarified ASV table of microcosms from Lower Grays Run, PA samples with 16.7 mg/L concentration of three metal oxides NPs and biocides. This is showing the dissimilarity of the microbial community on day 0 (open symbols) and day 14 (closed symbols). Treatments are shown in different colors

#### **2.4.6 Differentially enriched taxa between NPs and biocides microcosm:**

To better understand which taxa were differentially abundant in the different treatments, we analyzed the community composition of each treatment at the taxonomic level of order. The change in the taxonomic diversity measured by the relative abundance in each taxonomic order for all treatments is shown in (Figure.2.8). At initial time points, the communities in all samples were relatively similar. The communities had high levels of Betaproteobacteria, Pseudomonadales, Flavobacteriales, and Cytophagales. After 14 days, there were changes in the taxonomic composition of all treatments. In the control, the bacterial population was primarily Betaproteobacteriales with Chitinophageles as the second most abundant order, and Salinisphaerales was the third most abundant. Similar trends were observed in the three NPs. The Cytophagales showed higher relative abundance with SiO<sub>2</sub> NPs treatment than the control. The population of Sphingomonadales in SiO<sub>2</sub> NPs treatments was also higher than the other NPs. On the other hand, in the SiO<sub>2</sub> treatments, there was a reduction in the Betaproteobacteriales abundance compared to the control and NPs microcosms. Pseudomonadales were dominant members of the microbial community in the triclosan and glutaraldehyde treatments. The second most abundant group in the three biocide microcosms was Xanthomonadales. Despite the short half-life of DBNPA (63 hours at a pH of 7) (EPA, 2012), there was a distinct microbial community composition in the DBNPA treated microcosms with members of the Cytophagales and the Flavobacteriales being higher abundance compared to the control and other biocide treatments.

We performed differential abundance analysis using DESeq2 on day 14 samples to identify the differentially abundant taxa between biocides and nanoparticles. Fifteen ASVs were determined to be significantly enriched in either the nanoparticles or the biocide treatments (Table.S2.4.6.1). Eleven ASVs were significantly enriched in the biocide treatments and four ASVs were enriched in the nanoparticle treatments. Four of the ASVs enriched in the biocide treatments were annotated as Pseudomonadales. Five of the ASVs enriched in the biocide were annotated as Xanthomonadales. The remaining three ASVs were annotated as members of the Burkholderiales (Delftia, Janthinobacterium, and Herbaspirillum). The four ASVs enriched in the nanoparticle treatments were members of the Burkholderiales and Sphingomonadales. These findings confirm the overall observations from the taxa plots (Figure.2.8).

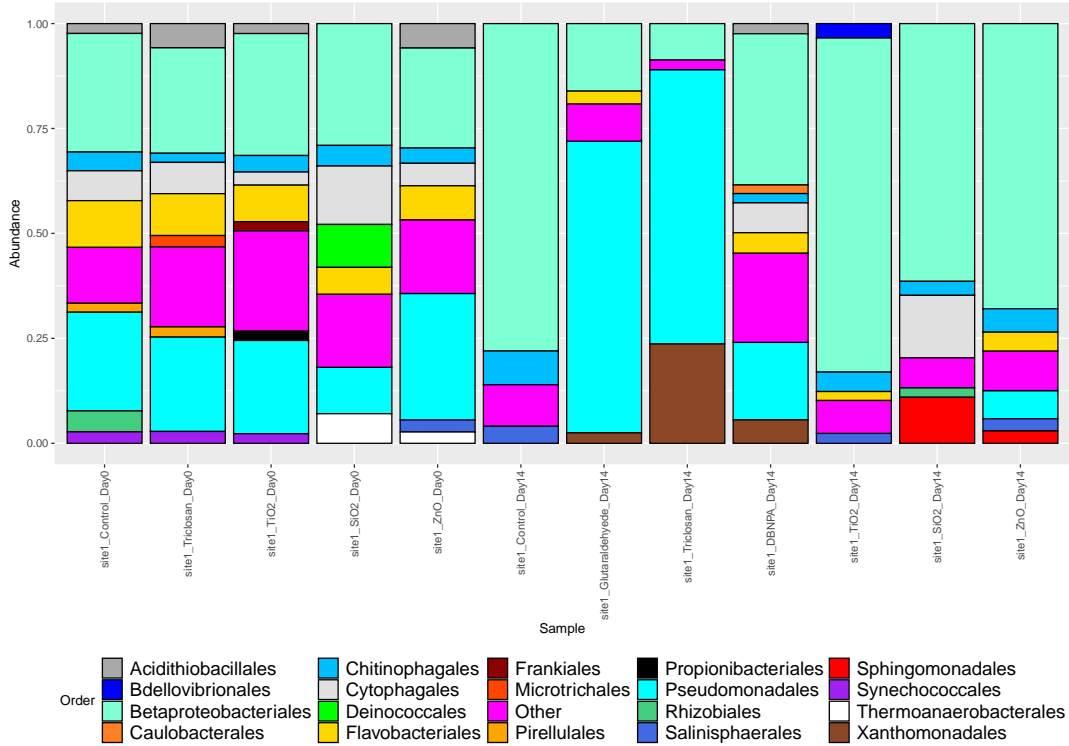


Figure 2.8 Bar graph of taxonomic diversity shows the relative abundance of bacterial order with those classes represented with different colors. This figure shows the relative abundance of bacterial orders on day 0 and day 14 for Lower Grays Run, PA samples incubated with three metal oxide nanoparticles, and biocides at 16.7 mg/L concentration for all treatments.

## 2.5 Discussion

The objective of this study was to investigate the provide a comparative study of the impact of biocide and NPs on natural microbial communities in a hydraulic fracturing impacted stream. We hypothesized that biocides will result in a more strongly altered microbial community composition relative to NPs.

### 2.5.1 Stability of NPs in stream water

The characteristics of metal oxide NPs in water are shown in table.2.1. While TEM images of the NPs stock suspension showed similar size to the commercial reported values (Fig.2.1), the average size distribution of the nanoparticles, were much larger than the reported size with an average size from 203.7– 667.6. This finding suggests that the NPs aggregated in water due to having diameters larger than 100 nm size. This aggregation of NPs may decrease the antimicrobial efficacy (Slavin et al., 2017). However, this trend of NPs aggregating in natural water is similar to what has been observed previously, where researchers observed larger metal oxide nanoparticles size with 200-800 nm range than the commercial size when they add them to water samples (Zhang et al., 2008). The zeta potential of all metal oxide NPs in the water sample was negative.

### **2.5.2 The change in pH of microcosms as a result of treatment**

On day 0 and day 14, glutaraldehyde (GA) had the lowest pH level of all of the treatments ( $4.9 \pm 0.02$  to  $6.1 \pm 0.2$ ) which indicates a more acidic condition in this treatment. Previous studies have found a similar change in pH in GA amended microcosms (Campa et al., 2018). Glutaraldehyde can be biodegraded under aerobic conditions to glutaric acid, which could affect the pH of these microcosms.

### **2.5.3 The cytotoxicity of NPs & biocides**

The NPs were selected in this study due to their antibacterial properties (Kadiyala et al., 2018). Previous work demonstrated that concentrations of  $\text{TiO}_2$  as low as 5.3 mg/L affected the microbial communities (Battin et al., 2009). Additionally, Ag NPs were shown to be effective at concentrations as low as 10 mg/L (Ward et al., 2019). Our results show that  $\text{TiO}_2$  NPs had the highest cytotoxic effect compared to other NPs and biocides based on high levels of LDH activity at 24 hours in the  $\text{TiO}_2$  treatments. It has previously been reported that some NPs target the membrane of some bacteria conferring the antimicrobial properties of NPs (Bondarenko et al., 2018). In particular,  $\text{TiO}_2$  has been shown to cause membrane damage to cells (Joost et al., 2015). Therefore, we expected that some NPs would result in increased LDH activity due to destabilizing of membranes, which would result in releases of LDH.  $\text{TiO}_2$  NPs are known for their UV-induced antimicrobial activity (Ripolles-Avila et al., 2019). It was surprising to see such

antimicrobial activity for TiO<sub>2</sub>, especially under dark conditions. However, previous work has shown that TiO<sub>2</sub> can generate radicals in the dark (Kumari et al., 2014). Therefore, this high LDH activity could be due to non-UV radical generation. This activity could damage the cell membrane and increased the permeability of the bacterial cell membrane and cell death.

The 16s rRNA gene abundance results showed that between day 0 to day 14 there were increases in microbial abundance in each of the biocide treatments. Conversely, microbial abundance decreased from day 0 to day 14 for the NPs samples as well as the control. This increase in microbial abundance over time in biocide-treated samples is similar to previous reports of increased gene copies in later time points of glutaraldehyde amended microcosms (Campa et al., 2018). This increase in gene copies may suggest the ability of biocides to select resistant bacteria. While the increase of microbial abundance may also be due to microbes utilizing the biocides as a carbon source. However, for a microbe to metabolize a biocide, it must be resistant to the biocide. We saw the highest change in bacterial abundance was with glutaraldehyde treated microcosms. Previous work showed that cell abundance increased at later time points in GA amended microcosms from other hydraulically impacted streams (Campa et al. 2018). This increase in cell abundance was attributed to the biodegradation of GA and the increase of glutaric acid (Campa et al., 2018). The increase of glutaric acid reported in the previous study was observed after day 7. In contrast to the results for the biocide-amended

treatments, the microbial abundance of NP-treated samples showed similar trends to the control microcosms of decreasing microbial abundance over time.

#### **2.5.4 The effects of NPs & biocides on bacterial community composition and diversity**

Alpha diversity analysis indicated there was a change in the richness and evenness of the communities within some of the biocide microcosms after 14 days compared to NP microcosms, which were similar to the control as well as compared to the initial conditions. Shannon diversity showed decreases in evenness and richness in glutaraldehyde and triclosan treatments compared to the others. Campa et al 2018 found that the addition of GA resulted in a decrease in diversity. The extent of the decrease in diversity was affected by the previous contamination state. Streams impacted by HF often showed less of a decrease in diversity in response to GA addition. Our results show that GA and triclosan result in a decrease in diversity matches their results.

Our results also demonstrated a strong impact of biocide addition on microbial community composition. In our study, we observed dramatically altered microbial community composition in biocide-amended microcosms. In particular, Pseudomonadales were enriched in the presence of both GA and TCS compared to time zero, the control, and other NP treatments. This enrichment in Pseudomonadales could be due to some Pseudomonadales having resistance to biocides. A recent study demonstrated

that *Pseudomonas aeruginosa* and *Pseudomonas fluorescens* employ efflux pumps to resist glutaraldehyde (Vikram et al., 2015a). Additionally, another study had suggested the mechanisms of resistance to TCS by using efflux pumps (Carey and McNamara, 2014). The Pseudomonadales in these streams may be employing mechanisms such as efflux pumps to survive biocide treatments.

Nanoparticle treatments showed increases in both Cytophagales and Sphingomonadales. This finding is in line with previous studies on the impact of pulsed addition of Ag NP on wetland microbial communities. In Ward et al 2019, they found that the addition of Ag NP resulted in increases in members of the Cytophagales after the first few days (Ward et al., 2019). Ward et al (2019) found that a member of the Cytophagales, *Flectobacillus*, dominated the pulsed treatments after the first few days. *Sphingomonas* were also found to be one of the key indicator organisms of Ag-NP addition. Ag-NPs have distinct properties from the metal oxide nanoparticles used in this study. These findings suggest that there may be common taxa that are resistant to NP in aquatic environments.

Hydraulic fracturing activity is a critical issue for environmental and public health and can present risks for ground and surface water contamination. Hydraulic fracturing methods depend on injecting fluid, which includes water, sand, and other chemicals including biocides. Previous work has demonstrated that hydraulic fracturing activity can affect the response of stream communities to biocide exposure. Nanoparticles are an appealing alternative antimicrobial. Our results demonstrate a dramatic decrease in

bacterial abundance with different types of nanoparticles. Conversely, microbial abundance increased for all of the biocide treatments over time. This may suggest the presence of biocide-resistant bacteria in these streams as well as the ability of some taxa to use the biocides as a carbon source. Biocides strongly impacted the microbial community composition of freshwater. We observed changes in microbial taxa in response to antimicrobial additions that were similar to previous studies in other systems, suggesting some common microbial responses to antimicrobials in aquatic settings. Even though, the different molar exposure concentrations between NPs and biocides, this difference in concentration is further confirmation that the nanoparticles have less of an effect on the microbial community as they are present at much higher concentrations than the biocides were in these microcosms. Here we investigated NPs that are potentially more “environmentally friendly” than the commonly used antimicrobial silver NPs. While, there are some concerns about the risk of nanoparticle release into the environment, here we demonstrate that the NPs chosen in our study have minimal effect on the microbial community. Our results support the idea that nanoparticles may be a promising antimicrobial for diverse industrial applications.

# Chapter 3

## Experimental evolution to investigate the mechanism of biocide and nanoparticle resistance

### 3.1 Abstract

Antimicrobials such as nanoparticles and biocides are used in many different settings to control microbial growth. We used *E. coli* to study the process where growth in low concentrations of antimicrobials can select for resistance to Ag-NPs and DBNPA. Our study goal was to investigate the mechanism of bacterial resistance to silver nanoparticles (Ag-NPs) and biocides (DBNPA). We determined the minimal inhibitory concentrations (MIC) of these two antimicrobials against *E. coli*. We then performed an experimental evolution study where *E. coli* was growing in low concentrations of the antimicrobials and transferred ten times. We then tracked the changes in lactate dehydrogenase (LDH) activity, reactive oxidative species (ROS), growth curves, importance of efflux, and genome sequencing between the adapted strain and parental strains. Our results showed that *E. coli* can rapidly develop resistance to Ag-NPs and DBNPA after growth in low concentrations of the antimicrobials. The expression of efflux pumps plays important role in both DBNPA and Ag-NPs resistance. Multiple gene mutations occurred in the adapted strains that may confer resistance to both Ag-NPs and DBNPA. Moreover, we found

changes in the DNA for flagellar and efflux pump genes in both the *E. coli* adapted to Ag-NPs and in the *E. coli* adapted to DBNPA. Our study provides insights into the mechanisms of adaptation and resistance to antimicrobials by repeated exposure at sub MIC concentrations and selection of mutants capable of growth at higher antimicrobial concentrations. Our results suggest that there is a different mechanism to resist nanoparticles than biocides. The mechanism of resistance to Ag-NPs might be related to flagellin production while the efflux pump seems to be associated with resistance to DBNPA. There is limited knowledge regarding the development of microbial resistance to biocide and NPs on a molecular level. This information is required to stop the spread of antimicrobial-resistant bacteria. This work seeks to clarify the mechanisms of resistance to these biocides.

### **3.2 Introduction**

Antimicrobials are used in several settings to control microbial growth (Doron and Davidson, 2011). These antimicrobials can take the form of antibiotics, biocides, and antimicrobial nanoparticles (Wang et al., 2017b, Kampf, 2018). Antimicrobial resistance is a major challenge that must be addressed as an increasing number of microorganisms are becoming resistant to commonly used antimicrobials (Ventola, 2015). Much work has been invested in studying the mechanisms of antimicrobial resistance (Prestinaci et al., 2015). The focus of these studies has been how bacteria develop resistance to commonly used antibiotics due to the need to understand the spread of antibiotic-resistant

pathogens (Davies and Davies, 2010). However, others have begun to investigate the ability of bacteria to develop resistance to other antimicrobials such as biocides (Davies and Davies, 2010). Nanoparticles have been proposed as a promising new alternative antimicrobial that may help to deal with antibiotic resistance (Vallet-Regí et al., 2019, Lee et al., 2019)

Nanoparticles show great promise to revolutionize many industries including medical products, and microbial control (Zhu et al., 2014, Khan et al., 2019, Mende, 2015, Pal et al., 2011). Metal oxides NPs and other metals such as silver and copper are commonly used to control microbial activity (Wang et al., 2017b). silver NPs (Ag-NPs) exert antimicrobial activity through diverse mechanisms such as induction of Reactive Oxygen Species (ROS) leading to cell damage and the release of Ag<sup>+</sup> ions which can damage cell membranes or interact with thiol groups (-SH) of proteins (Nisar et al., 2019).

Biocide is another class of antimicrobial chemicals that have been used in industrial and household applications to kill a wide range of microorganisms (Fink, 2013). 2,2-dibromo-3-nitrilopropionamide (DBNPA) is a common, effective, and low-cost biocide that is used in many industrial settings (Campa et al., 2019b, Guardiola et al., 2012a, Levy, 2002a). DBNPA functions through the inactivation of key proteins through reactions with thiol groups in proteins. The widespread use of biocides and their release to the environment has led to ecological problems (Kahrilas et al., 2015a). Biocides can be

released to the environment and persist at sub-MIC concentrations, which can lead to the development of resistance to these commonly used biocides (Grant and Bott, 2005, Condell et al., 2012, MD, 2007).

### **3.2.1 Mechanisms of resistance to biocides and nanoparticles**

The presence of biocides at sub-minimum inhibitory concentrations may select for bacteria that are resistant to these biocidal compounds (Fahimipour et al., 2018).

Previous studies have shown that when bacteria are exposed to low doses of biocides, they can very rapidly develop resistance to those biocides (Braoudaki and Hilton, 2004, Capita et al., 2019). Also, it has been reported that overuse of biocides in hospitals can increase the amount of antibiotic-resistant bacteria (Russell, 1999).

Efflux pumps are one of the ways that bacteria use to remove toxic substances such as biocides from the cell (Munita and Arias, 2016). Efflux pumps can pump biocides out of the cell before they can act upon the cell components (Soto, 2013). Efflux pumps need energy such as ATP or the proton motive force for the transfer of the substrate outside the cells (Webber, 2002). Many studies have demonstrated that bacteria such as *E. coli*, *Pseudomonas aeruginosa*, and *Pseudomonas fluorescens* employ efflux pumps to resist biocides such as QACs, triclosan, and glutaraldehyde (Levy, 2002b, J.Y.Maillard, 2007, Vikram et al., 2015c). The fact that overexpression of efflux pumps is also a mechanism

for antibiotic resistance, suggests that there is potential for the development of cross-resistance to biocides and antibiotics by bacteria.

Nanoparticle resistance is less well understood. One recent study demonstrated that bacteria could become resistant to NPs by increasing the aggregation of NPs and thus decreasing their ability to interact with the cell (Panacek et al., 2018). In this study, it was shown that overexpression of flagella increased the aggregation of Ag-NP and thus decreased the toxicity and increased the MIC of Ag-NPs. However, the authors of this study concluded that despite the change in expression of the protein flagellin, they were not able to detect genetic changes in the adapted *E. coli* strains. Further work is needed to understand the mechanisms of bacterial resistance to NP in a more generalizable manner.

Here we performed an experimental evolution study to adapt *E. coli* (gram-negative) for resistance to Ag-NPs and DBNPA by repeated exposure of *E. coli* to sub MIC concentrations of antimicrobials. We used a combination of biochemical, physiological, and genetic tools to investigate the mechanism of bacterial resistance to these antimicrobials in the adapted strains relative to the parent strain. We hypothesized that bacteria will more quickly acquire resistance to biocides relative to NPs and the objective was determining the potential for biocides and nanoparticles to select for antimicrobial resistance.

### **3.3 Materials and methods**

#### **3.3.1 Chemicals.**

The biocides used in this study was 2, 2-dibromo-3-nitrilopropionamide (DBNPA) (molecular weight: 241.87g mol<sup>-1</sup>, Sigma-Aldrich). Stock solutions of each were prepared at a concentration of 1 mmol/L in ethanol.

The nanoparticles used in this study were commercial preparations of metal nanoparticles (US Research Nanomaterials, Inc. 3302 Twig Leaf Lane, Houston, TX 77084, USA, Silver Nano powder water dispersion with 15 nm 1000mg/L (9.2 mM)) the nanoparticles were spherical in shape. The concentrations of silver NPs stock solution in Mueller Hinton broth that was used in all the studies was (1 mM concentration).

#### **3.3.2 Bacterial strains and growth conditions.**

*E. coli* (ATCC 700609) was the strain we used in this study and Mueller Hinton broth (MH) was the growth media. Bacteria were grown at 37 °C (Panacek et al., 2018).

#### **3.3.3 Stability of nanoparticles in growth medium.**

Here we performed an experimental evolution experiment with one strain of bacteria and two types of antimicrobials. Bacterial resistance was detected by determining the minimum inhibitory concentration of NPs and biocides. The distribution, shape, and size of the NPs were confirmed by Electron microscopy (E.M) and Dynamic light scattering

(DLS). Zeta Potential measured at 25 °C using a ZetaSizer for nanoparticle charges. The size of the nanoparticles was determined by taking the average of the size distribution as determined by intensity.

### **3.3.4 Experimental evolution study to adapt *E. coli* to biocides and NPs- minimal inhibitory concentrations MIC.**

Exposure to sub-minimal inhibitory concentrations MIC of NPs or DBNPA can select for microbes with increased resistance to NP as per published protocol (Panacek et al., 2018). *E. coli* was grown in a variety of concentrations (2, 5, 15, 25, 45, 65,85, 100,150, and 200 mg/L) of Ag-NPs (45, 65,85, 100,150, 200, 250, 300, 400, 500, 600, 700, 800, 900, 1000, 1250, and 1500 mg/L) of DBNPA with three replicates. Cultures were inoculated at a concentration of  $10^7$  CFU/ml (colony-forming units per ml) as determined by viable plate counts and grown in 96 well plates. The MIC was determined by measuring the OD600 for each culture and identifying the concentration at which there is no observable growth. The three concentrations before the MIC were pooled and regrown in a medium without antimicrobial. The subculture was then subjected to the same range of concentrations of NP or biocide to determine the MIC of the adapted strain. Each concentration was inoculated with  $10^7$  CFU/ml of *E. coli*. Each MIC was considered one transfer. The MIC was tracked as a function of a number of transfers to determine the rate of increase in MIC for biocides relative to NPs. All experiments performed in a microplate and OD 600 was read for bacterial culture after 24 hours of growth at 37 °C in the incubator shaker at 120 rpm (Tiwari et al., 2018, Panacek et al., 2018). Ten successive culture steps

were applied in this study. The data obtained in all tests were compared with the MIC of the parent which was used as a control.

### **Growth rate determination for adapted versus parent strain.**

Growth curves of the DBNPA and Ag-NPs adapted strains and the parent *E. coli* were determined in Mueller Hinton broth without any antimicrobial chemicals. Bacteria were grown in a 96 microplate and incubated in a shaker at 120 rpm, and OD was measured by UV-spectrophotometer at 600 nm every 2 hours at 37°C (Tiwari et al., 2018). Doubling times, growth rates, and growth yields were determined for each strain. Here we determined the growth rate ( $\mu$ ) using the equation  $\mu = (\ln(\text{OD}_{\text{TF}}) - \ln(\text{OD}_{\text{T0}})) / (\text{T}_{\text{F}} - \text{T}_{\text{0}})$  where  $\text{OD}_{\text{TF}}$  is the  $\text{OD}_{600}$  at a later timepoint,  $\text{OD}_{\text{T0}}$  is the  $\text{OD}_{600}$  at an initial timepoint and  $\text{T}_{\text{F}}$  is the time final time and  $\text{T}_{\text{0}}$  is the time of the initial measurement. The timepoints were chosen to be within the logarithmic growth phase of the cultures. To determine generation time, we used the equation  $g = (\ln(2)/\mu)$ . Growth yield was determined by measuring the highest OD observed for each culture.

### **3.3.5 Morphology and interaction with bacterial cells with nanoparticles.**

**Specimen Preparation for Scanning Electron Microscopy:** The specimens were prepared from the adapted strains with their parent strains.

**Fixation:** 1 ml from each sample was fixed in 2% (v/v) glutaraldehyde in 0.1M. PSB buffer at pH 7.2 for a period of 4 hours. It was then kept overnight in the same buffer at a temperature of 4°C. The buffer was replaced by a cold 2% (w/v) osmium tetra-oxide in 0.1M PSB buffer at pH7.2 and kept for 3 hours at room temperature. The sample was washed 3 times for a period of 15 minutes each in the same buffer and then washed twice for a period of 15 minutes each in distilled water.

**Dehydration:** The specimen was dehydrated using ethanol by changing the serial concentration at 30% (v/v) for 15 minutes at room temperature, then at 50% (v/v) for 15 minutes, at 70% (v/v) for 15 minutes, or at 70% (v/v) containing 2% uranyl acetate for a period of 12 hours, at 90% (v/v) for 15 minutes and then finally at a concentration of 100% (v/v) for a period of 30 minutes. Each sample was kept in 0.5 ml of 100% ethanol in a closed tube. Samples were examined via electron microscopy.

### **3.3.6 Study the mechanism of the resistant bacteria to biocide and NPs**

**Treatments used for the study:** To better understand the mechanism of resistance we compared the adapted strains with the parent strain. The conditions tested were illustrated in Table.3.1. We tested the cytotoxic response to NPs and biocides by measuring LDH activity, ROS, we also tested the effect of efflux pumps on acquired resistance, and global genetic changes by whole genome sequencing.

Table 3.1

Conditions tested to investigate the physiological response to antimicrobials.

<b>Name</b>	<b>Strain</b>	<b>Antimicrobial Treatment</b>	<b>Concentration Category</b>	<b>Concentration (mg/L)</b>
<b>P</b>	Parent	None	Control	0 mg/L
<b>A-NP</b>	Ag-NP Adapted	None	Control	0 mg/L
<b>A-bio</b>	DBNPA Adapted	None	Control	0 mg/L
<b>P-L-NP</b>	Parent	Ag-NP	Low	2 mg/L
<b>P-L-bio</b>	Parent	DBNPA	Low	45 mg/L
<b>A-L-NP</b>	Ag-NP Adapted	Ag-NP	Low	2 mg/L
<b>A-H-NP</b>	Ag-NP Adapted	Ag-NP	High	100 mg/L
<b>A-L-bio</b>	DBNPA Adapted	DBNPA	Low	45 mg/L
<b>A-H-bio</b>	DBNPA Adapted	DBNPA	High	900 mg/L

### **3.3.7 Cytotoxicity effects of biocides and nanoparticles -lactate dehydrogenase assay (LDH)**

To estimate the cytotoxicity of the antimicrobials on *E. coli* and detect the damage of bacterial cell membranes, we tested the lactate dehydrogenase (LDH) activity in response to different treatments for different strains. LDH is an intracellular enzyme (Kumari et al., 2014). Therefore, detection of LDH activity in the supernatant is an indication of cellular damage and cytotoxicity. To measure LDH, subsamples of culture were centrifuged after 24 hours and we took 100  $\mu$ L from the supernatant of each different test tubes. The supernatants were mixed with 30 mM sodium pyruvate, and 2.8 mL of 0.2 M Tris-HCl. Then 100  $\mu$ L of 6.6 mM NADH were added to the mixtures. LDH activity was measured by tracking absorbance at 340 nm using a UV-vis spectrophotometer (Kumari et al., 2014).

### **3.3.8 Cytotoxicity effects of biocides and nanoparticles - reactive oxidative species (ROS)**

To understand the stress response of the bacterial cells when exposed to the biocide/NPs, we measured reactive oxidative species (ROS). The resistant strains are expected to have lower ROS than their parent (Mostafa M., 2018, Tiwari et al., 2018). Measurements of ROS production by bacterial cells were done according to a published protocol (Tiwari et al., 2018). We obtained 100  $\mu$ l of either the adapted cultures or parental strains grown in the presence of the antimicrobial after 24 hours. Cells harvested by centrifuging at

10,000 x g for 10 min. We collected the pellet, and mixed it with 2% Nitro Blue Tetrazolium (NBT) solution, and incubated it in the dark for 1 hour. The cells were again collected by pelleting the cells by centrifugation. The pellet was washed with Phosphate-buffered saline (PBS) and then centrifuged at 8000 x g for 2 min. The pellet was then washed with methanol and centrifuged at 8000 x g for 2 min. To damage the bacterial cell membrane, we added 2 M KOH and to dissolve the formazan crystals we added 50% DMSO solution and incubated for 10 min. After centrifuging at 8,000 x g for 2 min the supernatant we transferred to a microplate and the absorbance read at 620 nm. The control was bacterial cultures without antimicrobials and uninoculated bacterial media was taken as blank.

### **3.3.9 Study the mechanism of the resistance - The impact of efflux pumps on conferring antimicrobial resistance**

Previous research has shown that increased expression of efflux pumps is associated with an increased biocide resistance (Blanco et al., 2016). In this task, we confirmed the role of efflux pumps in the resistance mechanism of biocides (DBNPA) and nanoparticles (Ag-NP). To determine the impact of efflux pumps in biocide and nanoparticle resistance, we treated the cells with efflux pump inhibitors and measured changes in growth in the presence of antimicrobials in the efflux pump inhibited treatment relative to the non-inhibited. This was done following previously published protocols (Vikram et al., 2015b) with some modifications. We used 1-(1-naphthylmethyl)-piperazine (NMP)

“arylpiperazine compound” as efflux pump inhibitors (EPIs). 1-(1-Naphthylmethyl)-piperazine (NMP) consider a chemosensitizer due to its ability to inhibit AcrAB and AcrEF efflux pumps (Anes et al., 2019)

The *E. coli* strains were grown with three concentrations of the (NMP) (15, 45, and 85 mg/L). The absorbance was recorded at 570 nm and the mean  $\pm$  SD with three biological replicates (Anes et al., 2019).

### **3.3.10 Study the mechanism of the resistance - Genome-wide analysis of the adapted strains**

**DNA extraction:** DNA was extracted from adapted versus parental strains using the Zymobiomics DNA extraction kit. The Zymobiomics DNA extraction kit protocol was followed according to the manufacturer’s specifications (D4301, Zymo Research Corporation, Irvine, CA USA).

**Genome Sequencing:** DNA was sent to the Microbial Genome Sequencing Center (MIGS Center, Pittsburgh, PA) for Illumina sequencing. A 2 x 150 bp sequencing run was performed on an Illumina NextSeq.

**Genome Processing and Variant Calling:** Raw reads were quality filtered using trimmomatic version 0.36 (Bolger et al., 2014). The leading 3 and trailing 3 nucleotides

were trimmed from the reads. Quality was filtered using a four base-pair window and a quality cutoff of a Phred quality score of 15. Sequences less than 36 bp long were removed. Quality filtered data were mapped against the *E. coli* K-12 substr MG1655 genome using bowtie2 (Langmead and Salzberg, 2012). Variants were called using samtools (Li et al., 2009) to include only variants that had a quality of greater than 30. Variants found in the adapted strains but not in the parent strain were identified using the intersect command in bedtools (Quinlan and Hall, 2010). Variants in the two adapted strains were summarized and annotated using snpEff (Cingolani et al., 2012).

## **Statistics**

A Shapiro-Wilk test for normality was used to determine if the data was normally distributed. IF the data was not normally distributed, a Kruskal-Wallis Test was used to evaluate the significance of experimental results ( $P < 0.05$ ). A **Dunn's test** significance difference test for multiple comparisons of means obtained was used as a post hoc to evaluate the significance of experimental results ( $P < 0.05$ ). Comparisons were performed between treatments and the control as well as to see if there were significant differences between biocide- and NP-amended treatments and the control.

## 3.4 Results

### 3.4.1 Silver nanoparticles size and stability

The stability of silver NPs (1 mM concentration) in the MH media and their aggregation behavior was determined by measuring the size and zeta potential of the NPs after 24 hours (Table. 3.4.1). The average size distribution of the silver NPs was  $39.97 \pm 0.53$  nm after 24 hours in MH medium. Zeta potential has been used as an indicator of dispersion stability. The zeta-potential was negative ( $-14.9 \pm 1$  mV), which suggests it is stable in the media and represents the dispersion of particles. The size of the silver NPs in the 1 mM solution was also measured using TEM (Fig.3.1). These sizes are similar to those stated for the commercial preparations used. These commercial preparations were reported to be 18 nm and our measured values were approximately 40 nm. This indicates that these Ag-NP are stable in the Mueller Hinton broth used for the growth of *E. coli*.

Table 3.2

Relative Ag-NPs size, zeta potential, and their standard error over time (n=3) (average  $\pm$  standard error).

<b>The average Silver- Nanoparticles stability in Mueller Hinton broth</b>		
<b>Days</b>	<b>Size (d. nm)</b>	<b>Zeta Potential (mV)</b>
<b>Day 0</b>	44.06 $\pm$ 0.53	-8.12 $\pm$ 1.28
<b>Day 1</b>	39.97 $\pm$ 0.53	-14.9 $\pm$ 1

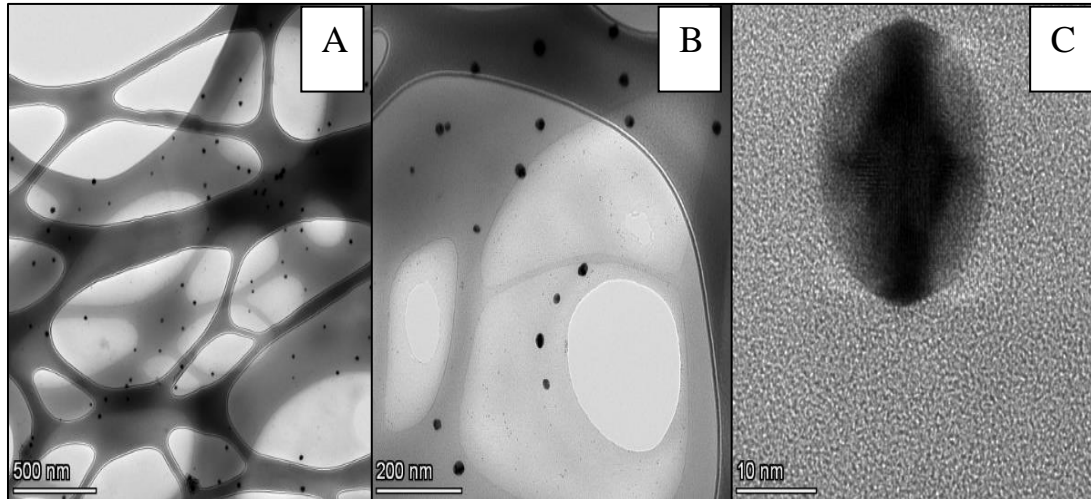


Figure 3.1 Transmission electron microscopy photomicrograph of Ag-NPs stock solution (A) Scale bars= 500 nm, (B) Scale bars = 200 nm, (C) Scale bars = 10 nm.

### 3.4.2 Experimental evolution study to adapt *E. coli* to DBNPA and Ag-NPs

Minimum inhibitory concentrations (MICs) were determined for Ag-NPs and DBNPA against the *E. coli* parent. The initial MICs were 5 mg/L for Ag-NP and 65 mg/L for DBNPA. After ten transfers the MIC of Ag-NP for *E. coli* changed from 5 to 150 mg/L from the beginning to the end of the experiment (Figure 3.2; Table.S.3.4.2.1). On the other hand, the MICs of DBNPA changed from 65 to 1250 mg/L from the beginning to the end of the experiment (Figure 3.2). The MIC of the DBNPA adapted strain was significantly different from the MIC of the parent after the fifth cultivation step (Kruskal Wallis p-value = 0.0007, Dunn. test  $P \leq 0.018$ ) (Table.S.3.4.2.2). The MIC of the DBNPA-adapted *E. coli* after five transfers was 500 mg/L compared to the MIC of the parental strain of 50 mg/L. This is in contrast to the Ag-NP adapted strain whose MIC only significantly increased from the parent after the eighth transfer. The MIC of Ag-NP against the parent was 5 mg/L. After eight transfers, Ag-NP had a MIC of 150 mg/L against the Ag-NP adapted strain (Figure 3.2; Figure 3.4; Table.S.3.4.2.1). This finding indicates that *E. coli* can more rapidly acquire resistance to DBNAP than to Ag-NP. In both cases, there is a significant increase in the MIC over the course of 10 transfers. *E. coli* increased resistance to DBNPA by a factor of 27 times and to Ag-NP by a factor of 30. These findings indicate that *E. coli* rapidly adapts to both antimicrobials.

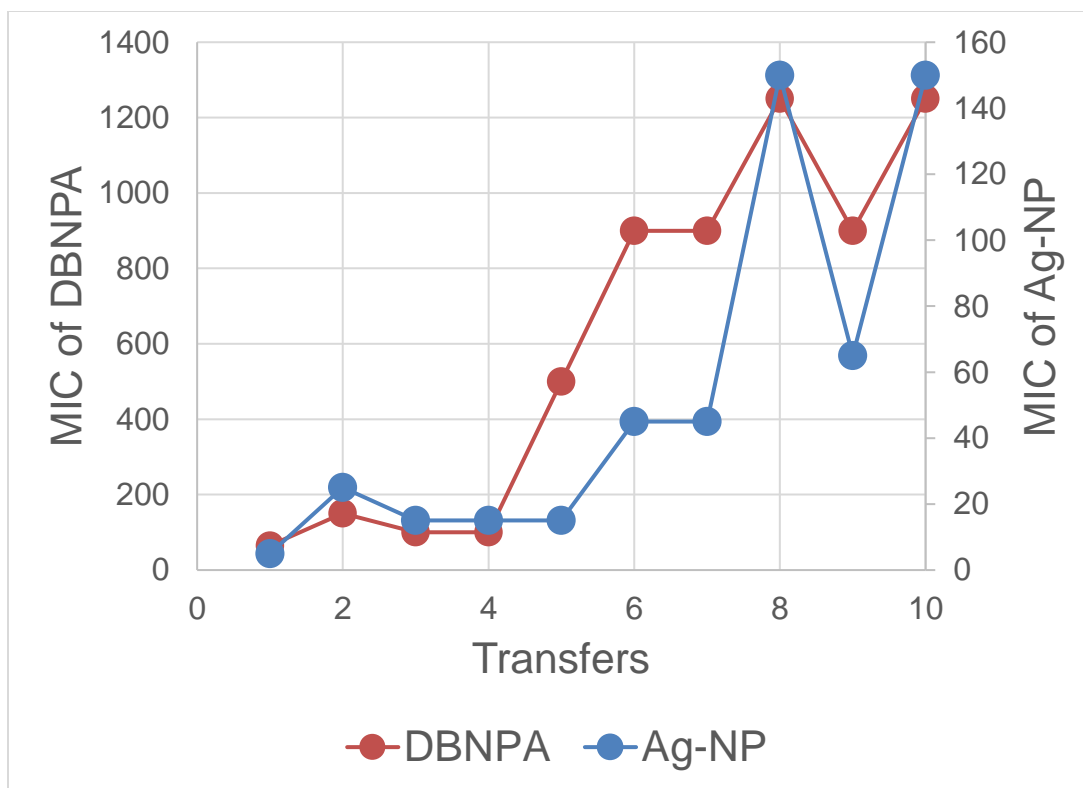


Figure 3.2 Minimum inhibitory concentrations of silver NPs & DBNPA as determined for *E. coli* after each of 10 consequent culture steps. The DBNPA MIC is shown in red and the Ag-NP MIC is shown in blue.

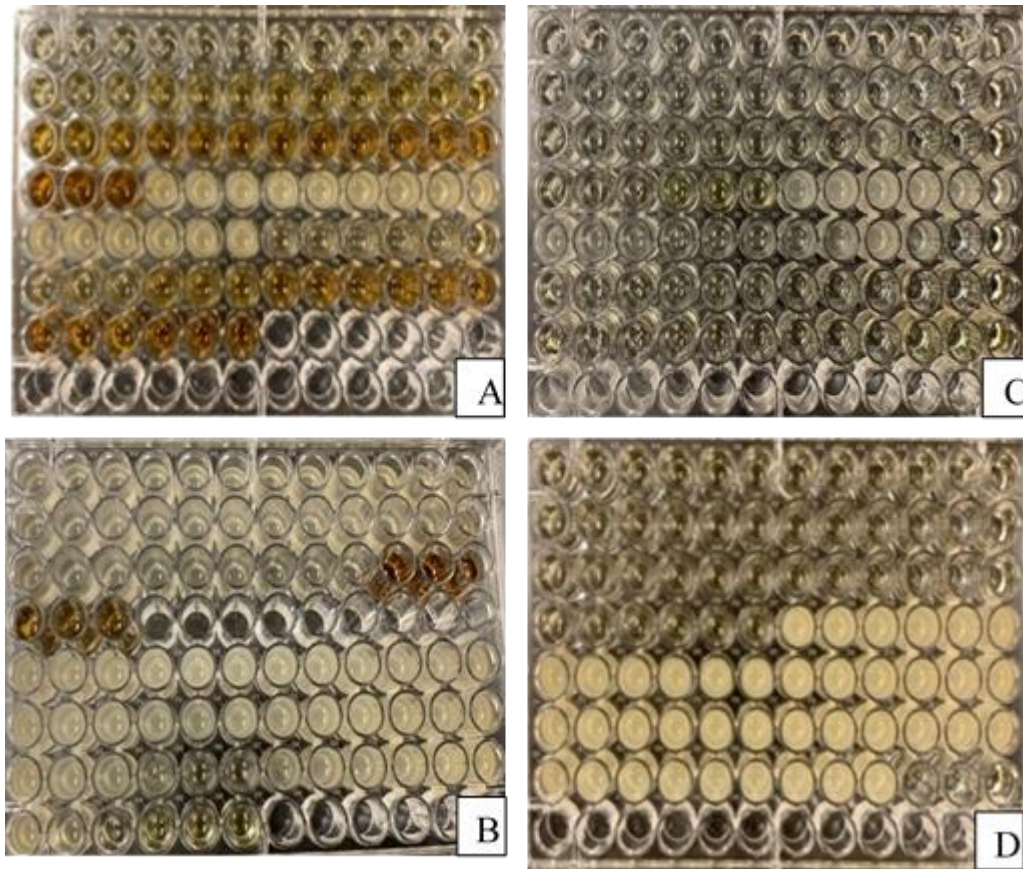


Figure 3.3 Example of a MIC plate from the experimental evolution study to adapt and parent *E. coli* and to different concentrations of DBNPA and Ag-NPs. (A) Showing the MIC of parent *E. coli* (P) with Ag-NPs, (B) Showing the MIC of Adapt *E. coli* (A-NP) with Ag-NPs, (C) Showing the MIC of parent *E. coli* (P) with DBNPA, (D) Showing the MIC of Adapt *E. coli* (A-NP) with DBNPA.

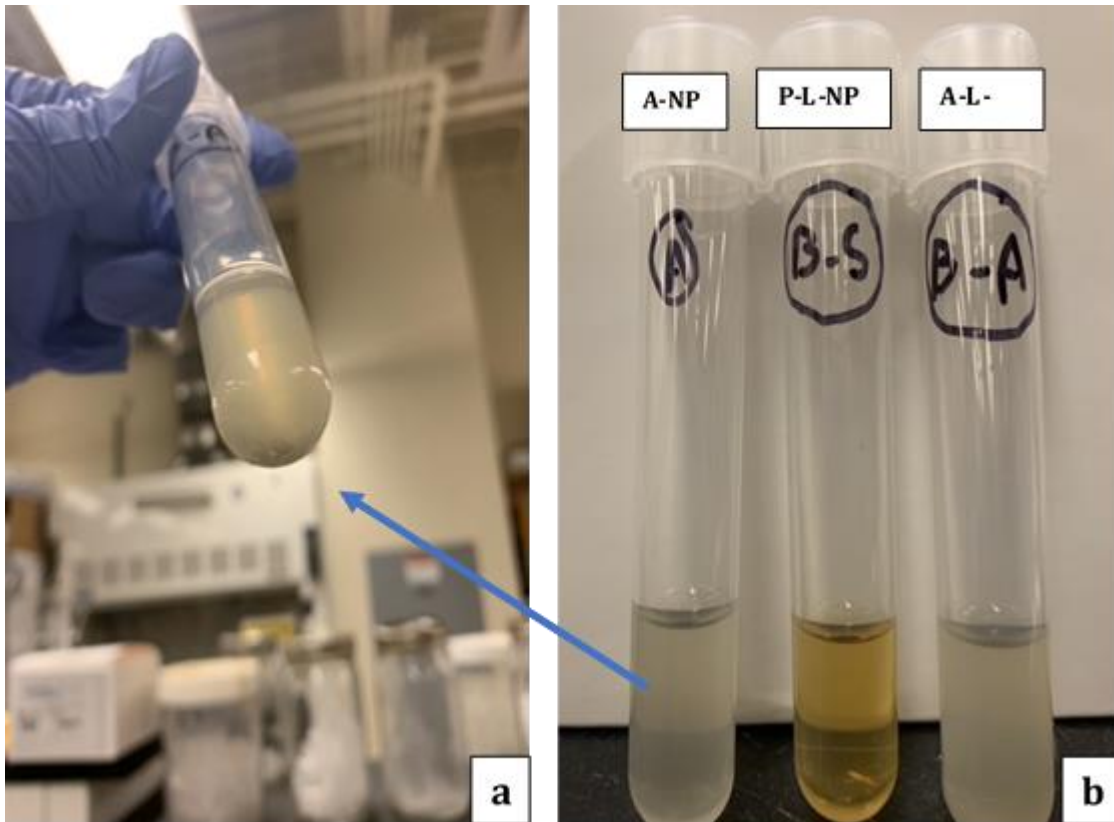


Figure 3.4 The images demonstrate the aggregation and precipitation of silver NPs after 48 hours of incubation with silver NPs. (a, left) The tube on the left side of the picture contains 'adapt *E. coli* without silver NPs (A-NP). (b, right) The first tube on the right side of the picture contains 'adapt *E. coli* without silver NPs (A-NP). The second tube on the right side of the picture contains parent *E. coli* and to below the maximum MIC (5 mg/L) of silver NPs (P-L-NP). The third tube on the right side of the picture contains adapt *E. coli* cultivated to below the maximum MIC (150 mg/L) of silver NPs (A-L-NP).

### **3.4.3 Effects of DBNPA and Ag-NPs to *E. coli* cells morphology**

We demonstrated the Ag-NPs aggregation after culturing with the present and adapt *E. coli* of in the microplates and in the bottom of the test tube (Figure 3.3 & Figure 3.4). Scanning electron microscopy (SEM) was used to investigate the interaction Ag-NPs with *E. coli* (Figure 3.5). In (Figure 3.5.B) shows the size and shape of Ag-NPs that clustered on the surface of the *E. coli* after we treated it with a low concentration of Ag-NPs. *E. coli* after treated with a low concentration of DBNPA showed in (Fig.3.5.C).

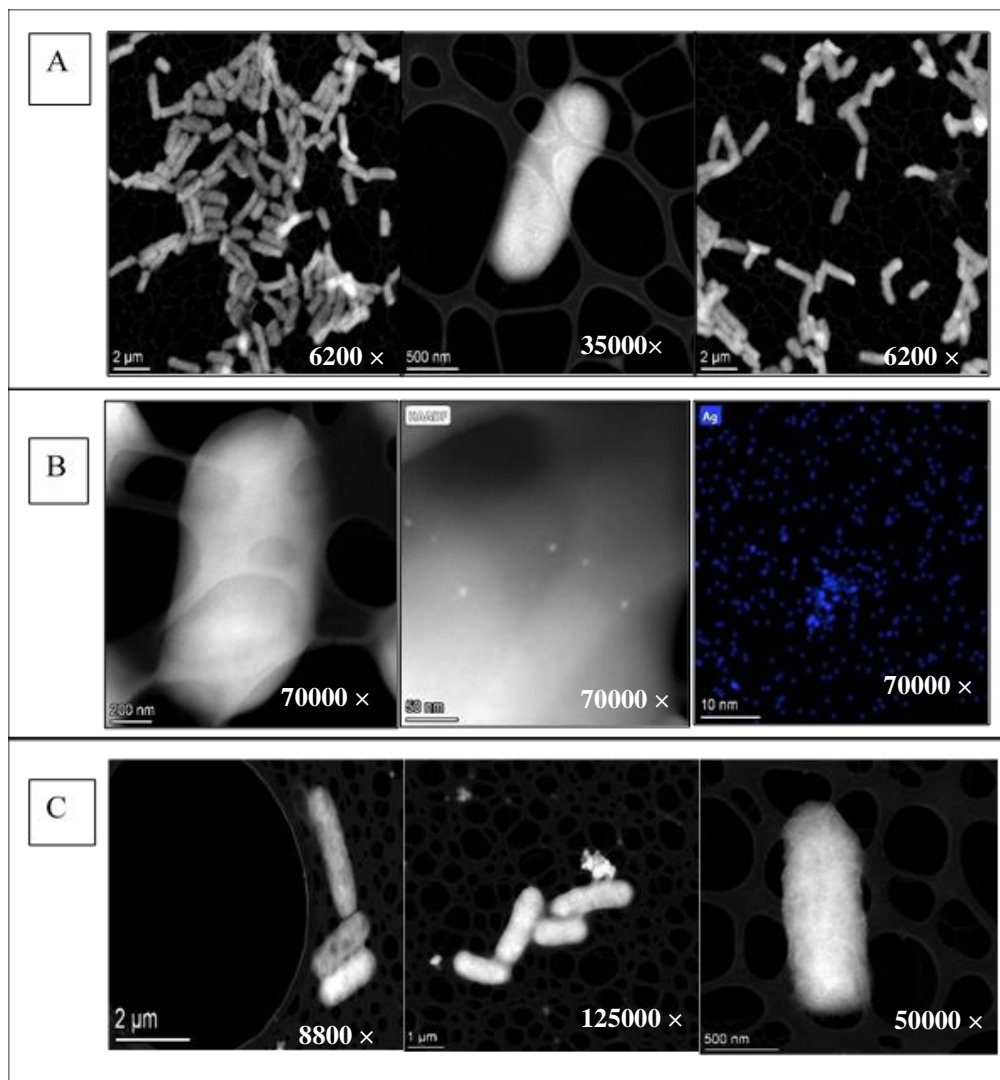


Figure 3.5 Scanning electron microscopy (SEM) showing interactions of Ag-NPs and DBNPA with (A) Parent *E. coli*, (B) Adapt *E. coli* with 2 mg/L of Ag-NPs (C) Adapt *E. coli* with 45 mg/L DBNPA.

### 3.4.4 Impact of adaptation on the growth of *E. coli* in the absence of antimicrobials

To investigate the potential for there to be fitness costs associated with adaptation to antimicrobials, we measured the growth parameters of the two adapted strains of *E. coli* in comparison to the parent strain. The growth curves for adapted and parent *E. coli* in the absence of antimicrobials were determined by measuring OD<sub>600</sub> at 0, 2, 4, 6, 8, 16 hours (Figure 3.6; Table.S.3.4.4.1; Table.S.3.4.4.2). The growth curves in Figure 3.6, shows that parent *E. coli* reached a higher density (OD 600 of  $0.539 \pm 0.004$ ) compared to a maximum OD 600 of  $0.237 \pm 0.037$  for the DBNPA adapted strain and  $0.273 \pm 0.045$  for the Ag-NP adapted strain. These differences were significant for both the DBNPA-adapted strain (t-test p-value = 0.0047) and Ag-NP (t-test p-value = 0.0092) compared to the parent (Table.S.3.4.4.3). Additionally, there were minor changes in the growth rate observed between the parental and the adapted strains. The parent had a specific growth rate of  $1.72 \pm 0.08 \text{ hr}^{-1}$  while the DBNPA adapted strains had a specific growth rate of  $1.472 \pm 0.119 \text{ hr}^{-1}$  and the Ag-NP strain had a specific growth rate of  $1.58 \pm 0.029 \text{ hr}^{-1}$ . The adapted bacteria for both DBNPA or Ag-NPs showed similar overall growth yields and growth rates.

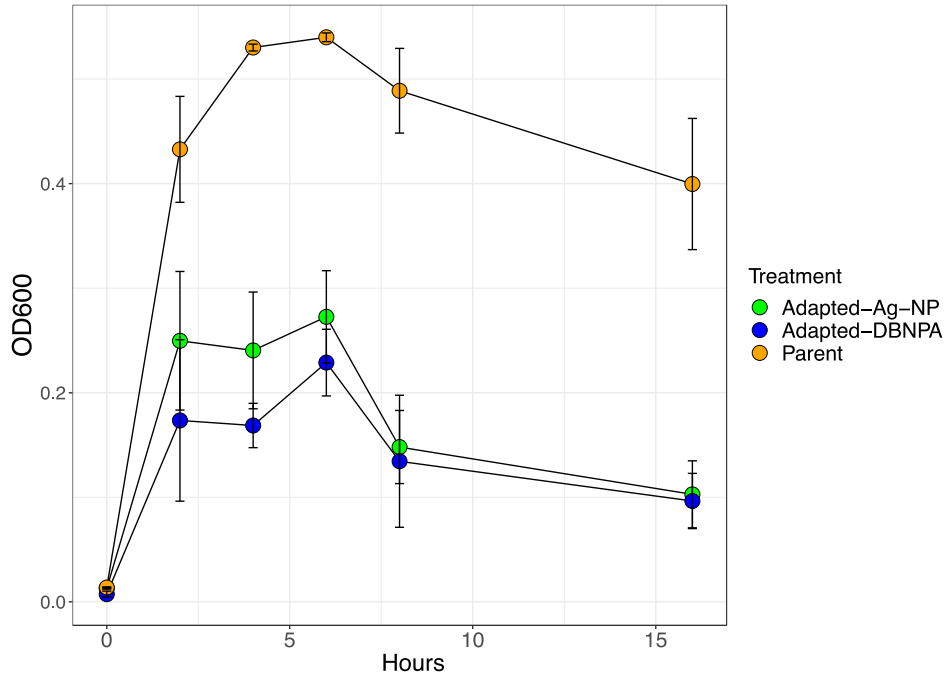


Figure 3.6 Growth curves for the parent *E. coli* (blue) and DBNPA-adapted (red) and Ag-NP adapted *E. coli* (green) after 24h incubation (n=3) and the data showed as mean and error bars represent standard error.

### 3.4.5 Cytotoxicity effects of DBNPA and Ag-NPs on bacterial membrane permeability (LDH) and reactive oxidative species (ROS)

LDH measurements were obtained after 24 hours of incubation by measuring OD340 using three replicates of each of the chosen strains. We determined response to two concentrations of antimicrobials in order to determine if there was a difference in the cytotoxic effects of biocides and nanoparticles on the adapted and parental *E. coli*. The low concentrations were chosen to represent the sub MIC concentration for the parental strain. These low concentrations were 2 mg/L for Ag-NPs and 45 mg/L for DBNPA. The high concentrations were chosen to represent the sub MIC concentrations for the parental strain. These

concentrations were 100 mg/L for Ag-NPs and 900 mg/L for DBNPA. Because the parental is not able to grow at the high concentration, we only tested the parental strain at the low concentrations. As a control, we determined the LDH activity for the parental and the two adapted strains in the absence of antimicrobials (Figure 3.7; Table.S3.4.5.1). The parental strain showed high LDH levels when exposed to low concentrations of biocides and nanoparticles. However, the parental strain showed high LDH activity even in the absence of antimicrobials. The highest LDH activities were seen with the parental strain with and without antimicrobials. The lowest LDH level was the DBNPA-adapted strain (A-bio) and the DBNPA-adapted strain at a low concentration of biocides (A-L-bio). However, the parent strain had a higher LDH level than the Ag-NP adapted strains (A-NP) and DBNPA-adapted strains (A-bio) for both NPs and DBNPA respectively and that difference was significant (Shapiro-Wilk p-value = 0.0004, Kruskal-Wallis p-value = 0.001) (Table.S.3.4.5.2).

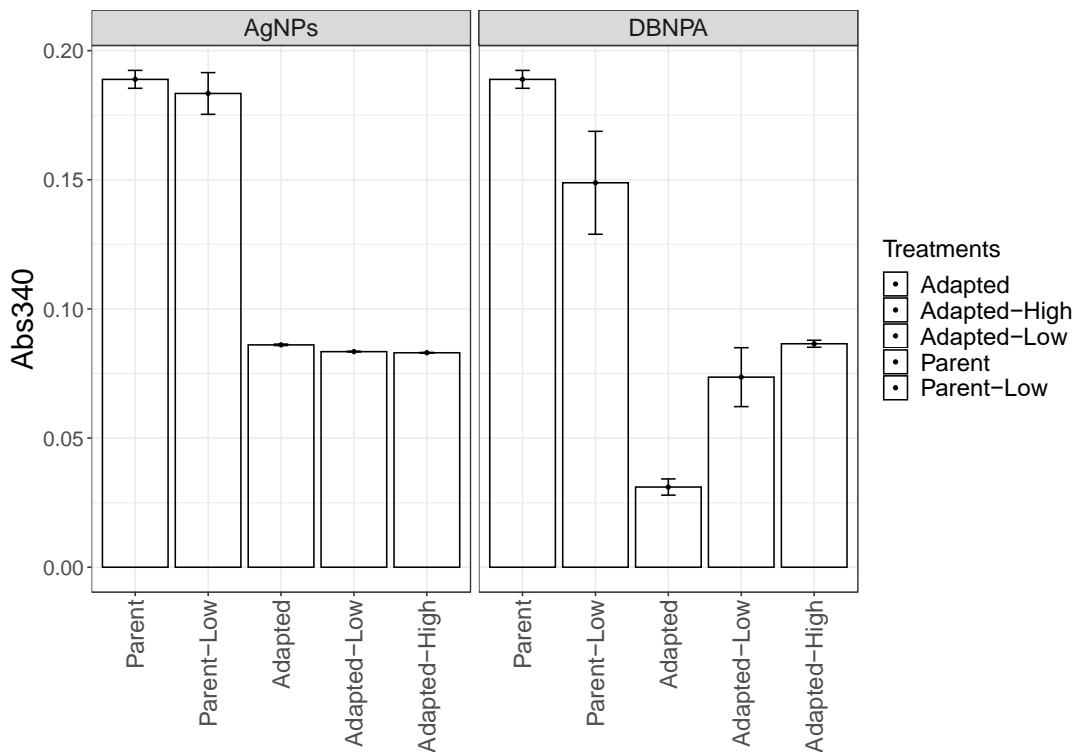


Figure 3.7 Showing relative LDH of Ag-NPs and DBNPA on the tested bacteria for the conditions illustrated in Table.3.1 after 24h incubation (n=3). Colors represent the different treatments. Error bars are standard errors. The same parental strain without antimicrobials (P) as measured from the same triplicate conditions are shown in both groups of data for sake of comparison.

Reactive oxygen species (ROS) measurements were obtained after 24 hours of incubation in triplicate of each of the conditions described above (Figure 3.8; Table S3.4.5.3). In contrast to the LDH measurements, the parental strain in the absence of antimicrobials demonstrated relatively low ROS levels. In the presence of the antimicrobials, the parental strain with a low concentration of Ag NPs (P-L-NP) exhibited significantly higher ROS levels (Shapiro-Wilk p-value = 0, Kruskal-Wallis p-value = 0.03) compared to the adapted strain with low concentrations of Ag NPs (A-L-NP) (Table S3.4.5.4). The glutathione and protein-bound sulfhydryl groups “the membrane proteins” may interact

with Ag NPs and affect the lipid peroxidation “antioxidant enzymes indicative” leads to cell oxidative damage (McShan et al., 2014). On the other hand, the ROS levels for the adapted strains in the presence of low and high concentrations of nanoparticles were either lower or the same as the adapted strains without antimicrobials. There was a significant difference between the parent strain with a low concentration of DBNPA (P-L-bio) compared to the adapted with low concentrations of DBNPA (A-L-bio) (Kruskal-Wallis p-value = 0.039) (Table S3.4.5.4). The parent with a low concentration of nanoparticles showed lower ROS levels (Average = 0.2) than the parent with a low concentration of DBNPA (Average =0.3) (Table S3.4.5.4).

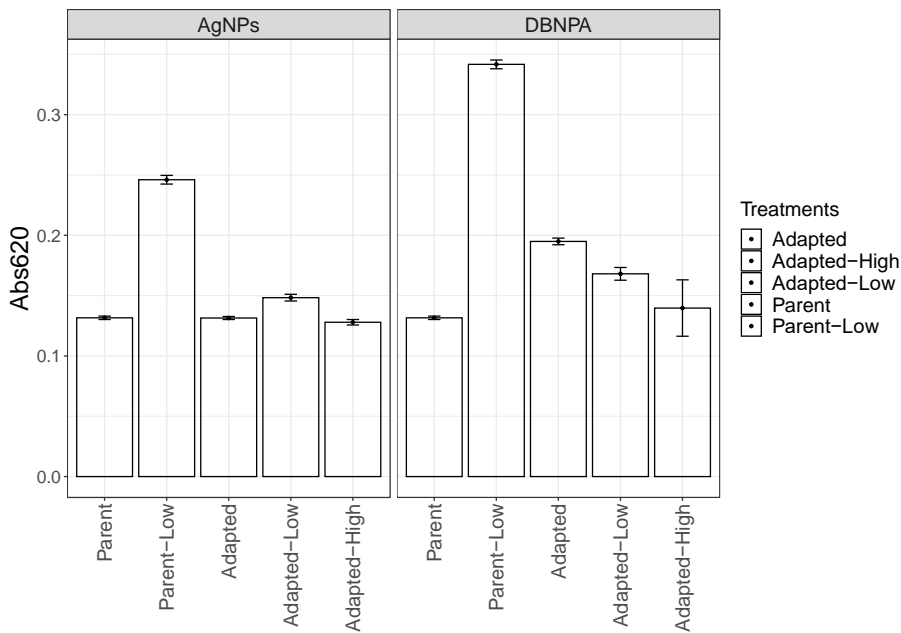


Figure 3.8 Showing relative ROS of Ag-NPs and DBNPA on the tested bacteria for the conditions illustrated in Table.3.1 after 24h incubation (n=3). Colors represent the different treatments. Error bars are standard errors. The same parental strain without antimicrobials (P) from the same triplicate conditions are shown in both groups of data for sake of comparison.

### 3.4.6 Role of efflux pumps in acquired resistance to DBNPA and Ag-NPs

Based on previous studies, we hypothesized that efflux pumps may play a key role in biocide resistance. Here we used 1-(1Naphthylmethyl)-piperazine (NMP) as an efflux pump inhibitor to examine the impact of inhibiting efflux on the effectiveness of biocides. The treated bacteria were incubated for 24 hours with either Ag-NPs or DBNPA in the presence of three concentrations of NMP (15, 45, 85 mg/l) based on similar concentrations used by (Vikram et al., 2015c). As a control, the bacteria were grown without any NMP. Another control was the parent *E. coli* strain with NMP but no antimicrobials to determine if NMP is inhibitory to the growth of *E. coli*. OD570 after 24 hours was measured as an indication of growth. If efflux pumps were important for antimicrobial resistance, then in NMP treated conditions, the antimicrobials would be more effective and there would be decreased growth as shown in a decrease in OD570. In general, both strains exhibited increased sensitivity to antimicrobials in NMP-treated conditions compared to the untreated strains (Figure 3.9; Figure 3.10). For example, there was a significant difference in the growth of the Ag-NP and DBNPA-adapted strains with NMP and without NMP especially with concentrations of 45 and 85 mg/L NMP and no significant difference at 15 mg/L NMP concentration compared to the parent (Shapiro-Wilk p-value = 0) (Table.S3.4.6.2). Similar significant differences were found with adapted *E. coli* to DBNPA with 85 mg/L NMP compared to the parent without NMP (Shapiro-Wilk p-value = 0, Kruskal-Wallis P = 0.015) (Table.S3.4.6.2). The adapt *E. coli* to Ag NP with 85 mg/L NMP (Shapiro-Wilk p-value = 0, Kruskal-Wallis P = 0.014) compared to the parent (Table.S3.4.6.2). There also appears to be

some growth inhibition as a result of the 85 mg/L NMP treatment on *E. coli* as the parent showed a decrease in OD<sub>570</sub> (average =0.8) in the 85 mg/L conditions in the absence of antimicrobials (Table.S3.4.6.1).

Overall, there appears to be some impact of efflux pumps in the presence of both antimicrobials. The *E. coli* adapted to Ag-NP exhibited an effect of NMP where the condition with no NMP had an OD of 0.38 ( $\pm 0.07$ ) and at 85 mg/L NMP had an OD<sub>570</sub> of 0.28 ( $\pm 0.08$ ) (Table.S3.4.6.1). A similar trend was seen for the adapt *E. coli* DBNPA treatment where the parent with no NMP grew to an OD of 0.51( $\pm 0.17$ ), but in 45 mg/L of NMP, the OD was 0.38( $\pm 0.16$ ) (Table.S3.4.6.1). These show that the parent relies in part on efflux pumps to be able to tolerate low concentrations of antimicrobials. Similar trends were seen for the adapted strains. At high concentrations of Ag-NP, the adapted strain grows to high ODs. However, at 45 mg/L NMP, the OD dropped in the presence of high concentrations of Ag-NP. Similarly, for the high DBNPA concentrations, the *E. coli* were able to grow to high ODs at 15 mg/L of NMP, at 45 mg/L NMP the OD was different than in the 15 mg/L treatment. Interestingly the ODs were higher for the DBNPA-adapted strain with 15 mg/L than at 0 mg/L NMP.

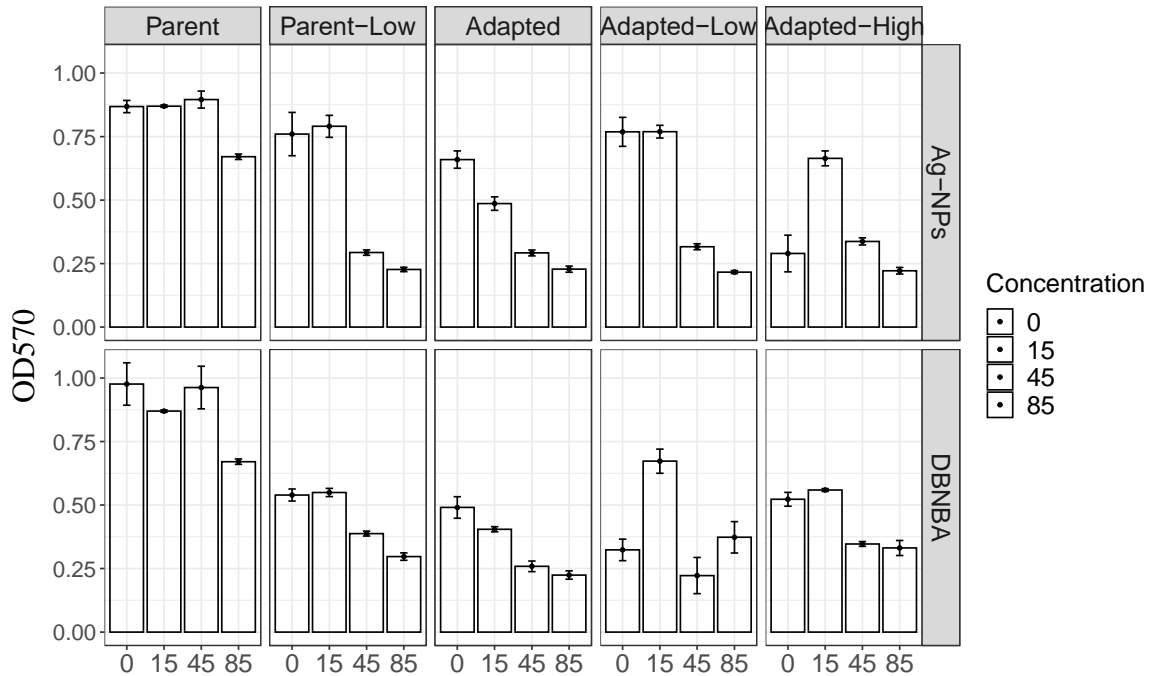


Figure 3.9 Showing the effect of efflux pump inhibitors (EPLs) 1-(1Naphthylmethyl)-piperazine (NMP) on the tested bacteria for the conditions illustrated in Table.3.1 after 24h incubation (n=3). Showing the effect of different concentrations of (NMP) against adapted and parent *E. coli* treated with Ag-NPs. Showing the effect of efflux pump inhibitors (EPLs) 1-(1Naphthylmethyl)-piperazine (NMP) on the tested bacteria for the conditions illustrated in Table.3.1 after 24h incubation (n=3). Showing the effect of different concentrations of (NMP) against adapt and parent *E. coli* treated with DBNPA.

### 3.4.7 Study the mechanism of the resistant bacteria to DBNPA and Ag-NPs- Genome-wide analysis of the adapted strains

To determine the genetic differences between *E. coli* adapted to Ag-NPs and DBNPA in relation to the parental *E. coli* strain, we sequenced their genomes. The snpEff program was used to classify mutations based on their impact. High impact mutations would include frameshifts, a gain of stop or loss of start codons, as well as large insertions and deletions. The high-impact mutation genes were compared between the adapted strains

and the parental strain. Overall, 265 variants were identified in the Ag-NP adapted strain relative to the parental strain. Of these mutations, 179 were SNPs, and 86 were insertion or deletions. The DBNPA-adapted strain had 222 variants identified relative to the parental strain. Of these mutations, 153 were SNPs and 69 were insertion or deletions. When compared together 136 mutations were identified to be shared between the two adapted strains and 141 and 97 were found only in the Ag-NP adapted strains and the DBNPA-adapted strain, respectively. These mutations ranged in predicted impacts. For example, in the Ag-NP-adapted strain, 12 mutations were considered high impact mutations. Two mutations were shown to be non-sense mutations and 37 mutations were missense mutations in the Ag-NP-adapted strain. Similarly, the DBNPA-adapted strain had 13 high-impact mutations, with 2 non-sense mutations and 38 missense mutations.

Both adapt strains had mutations in genes associated with lipid A biosynthesis, Sugar utilization, transport systems, and flagellin genes, and drug-metabolite efflux induced transcriptional regulators. Mutations were identified in some outer membrane proteins, Flagellin, Putative, or transporter genes, more in the adapted *E. coli* to Ag-NPs than adapted *E. coli* to DBNPA. On the other hand, more mutations were observed in Qin prophage 3B and drug-metabolite efflux genes in the DBNPA-adapted *E. coli* compared to Ag-NP-adapted *E. coli*. Pseudogenes had been identified in adapted *E. coli* to DBNPA genomes with unknown function (Figure 3.11; Chapter3-Supplemental Dataset-Genome).

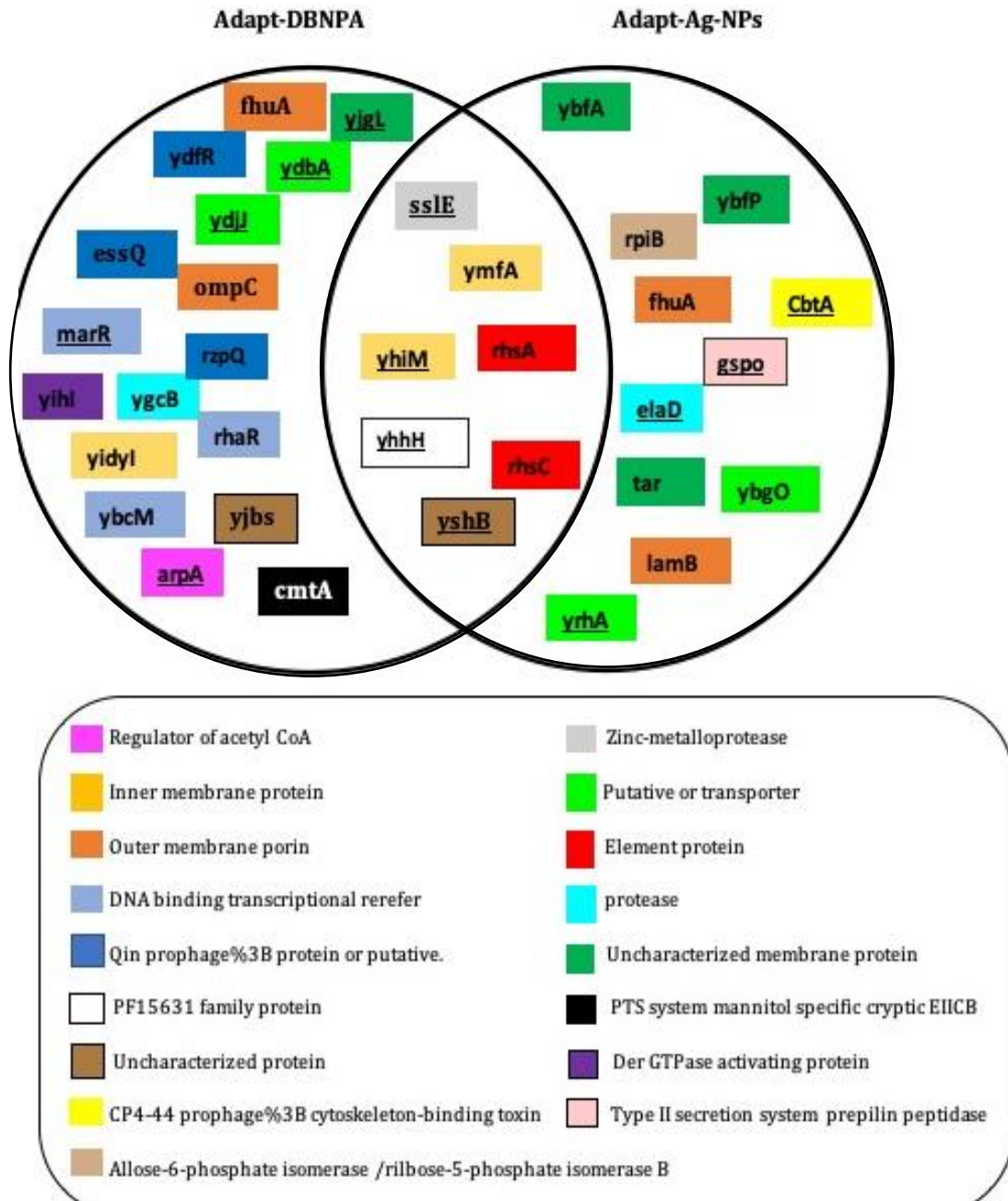


Figure 3.10 A Venn diagram summary of identified gene mutations that were considered the high and moderate impact of the *E. coli* adapted to Ag-NPs and DBNPA from the genome sequenced in this study. The underlined genes indicate genes with high impact and the rest had moderate impacts.

As previous studies have shown a role for either flagellin or efflux pumps in resistance to Ag-NP and biocides respectively, we focused on mutations in and near those genes. In Table 3.3, we showed a summary of comparative observed mutations of similar efflux pump and flagellin genes on whole-population genomic sequencing of adapted *E. coli* to Ag-NPs and DBNPA. Mutations in or near flagellin genes occurred more with adapted *E. coli* to Ag-NPs while adapted *E. coli* to DBNPA had more mutations in and near efflux pump genes (Table 3.3; Chapter3-Supplemental Dataset-Genome).

Table 3.3

Summary comparison between mutations found near efflux pumps and flagellin genes on adapted *E. coli* to Ag-NPs and DBNPA to *E. coli* Parent genome sequenced in this study. The predicted strength of the mutation is shown next to the gene name. Modifier indicates mutations that occurred near a gene or a mutation with a minimal effect on the gene sequence. Low effect impact indicates one or many codons are changed.

<b>Gene / Function / Gene impact</b>	<b>Ag-NP Adapted</b>	<b>DBNPA Adapted</b>
<b>Efflux pump Genes</b>		
<b>EmrB /multidrug efflux pump membrane subunit/ variants impact (MODIFIER)</b>	-	+
<b>EmrD /multidrug efflux pump/ variants impact (MODIFIER)</b>	-	+
<b>EmrE/multidrug/betaine/choline efflux transporter / variants impact (MODIFIER)</b>	-	+
<b>EmrA / multidrug efflux pump membrane fusion protein/ variants impact (MODIFIER)</b>	-	+
<b>marB / multiple antibiotic resistance protein/ variants impact (MODIFIER)</b>	+	-
<b>mdtM /multidrug efflux pump/bile salt:H (+) antiporter/Na (+):H (+) antiporter/K (+):H (+) antiporter/ variants impact (MODIFIER)</b>	-	+
<b>mdtN/putative multidrug efflux pump membrane fusion protein/ variants impact (MODIFIER)</b>	-	+
<b>MdtO /putative multidrug efflux pump subunit/ variants impact (MODIFIER)</b>	-	+
<b>mdtP /putative multidrug efflux pump outer membrane channel/ variants impact (MODIFIER)</b>	-	+

<b>Flagellin Genes</b>		
<b>FliC /Flagellar filament structural protein / variants impact (LOW)</b>	+	+
<b>FliD /Flagellar filament capping protein / variants impact (MODIFIER)</b>	+	+
<b>FliS /Flagellar biosynthesis protein / variants impact (MODIFIER)</b>	+	-
<b>FliT /Flagellar biosynthesis protein / variants impact (MODIFIER)</b>	+	-
<b>flgK / flagellar hook-filament junction protein 1/ variants impact (MODIFIER)</b>	+	-
<b>flgL / flagellar hook-filament junction protein 2/ variants impact (MODIFIER)</b>	+	-
<b>fliY / Flagellar motor switch phosphatase/ variants impact (MODIFIER)</b>	+	+

### 3.5 Discussion

With the increased use of antimicrobials such as biocides and nanoparticles, there is an increased risk for the development of microbial resistance to these antimicrobials.

Exposure to low concentrations of antimicrobials in the environment has the potential to select strains of bacteria that are capable of growing in the presence of these sub-minimum inhibitory concentrations. Here we used an experimental evolution study to examine the mechanisms of acquired resistance to these two types of antimicrobials. We investigated the physiological and genetic mechanisms for acquired resistance. Our experimental evolution study was used to select strains of the gram-negative bacterium *E. coli* that were resistant to Ag-NPs and DBNPA. Our experimental evolution provided insights into mechanisms of adaptation and resistance to antimicrobials by repeated exposure at sub MIC concentrations and selection of mutants capable of growth at higher concentrations. We investigated the mechanisms of resistance by using different pathways to help us confer anti-microbial resistance in *E. coli*.

Previous work performed an experimental evolution study on the ability of *E. coli* to develop resistance to Ag-NPs (Panacek et al., 2018) In this previous study, they found that *E. coli* increased its resistance to Ag-NP by at least ten times after twenty transfers. Our results are in line with this, in that our adapted *E. coli* was 30 times more resistant to Ag-NP after ten transfers. Our work also showed that *E. coli* very rapidly develop resistance to DBNPA. The DBNPA adapted strain more rapidly developed resistance the

antimicrobial compared to the Ag-NP-adapted strain. This rapid development of resistance is similar to what has been observed in similar experimental evolution studies with antibiotics. Specifically, one study showed a rapid increase in the MIC of *Acinetobacter baumannii* after short periods (Panacek et al., 2018).

To understand the mechanism of resistance, we first investigated the physiological effect of DBNPA and Ag-NPs antimicrobial activity on adapted and parental *E. coli*. Previous work has shown that the antimicrobial activity of Ag-NP is due to the nanoparticles penetrating the cell membrane, which can result in changes to the permeability of cell membranes, increase reactive oxygen species, as well as an interruption to cellular processes through the release of silver ions (Wang et al., 2017b). In some cases, the release of silver ions from Ag-NPs can also interrupt protein activity through interactions with thiol groups (Prabhu and Poulouse, 2012). The mechanism of action for DBNPA on the other hand involves the reaction with sulfhydryl groups of proteins which more generically inhibits metabolism and growth (Yin et al., 2020, Bajpai, 2015). Based on these mechanisms we expected that Ag-NPs will have an effect on the bacterial cell envelope while DBNPA will affect the cell growth. Our results demonstrated that LDH levels were lowest in the DBNPA-adapted strains compared to the parent or Ag-NPs adapted *E. coli*. It was reported that Ag-NPs have physicochemical properties that let them aggregate on the bacterial cell membrane and cause membrane damage resulting in cell leakage (Qing et al., 2018, Yin et al., 2020, Dakal et al., 2016) (Figure.3.7). However, our results show that there is little difference in the parent with and without

Ag-NP as well as little difference in the Ag-NP adapted strains with high and low concentrations of Ag-NP compared to the adapted strain without Ag-NP. The LDH data seems to suggest that cell damage and leakage of the LDH is not a major mechanism of Ag-NP cytotoxicity.

To further investigate the physiological response to antimicrobials we investigated the potential role of ROS in the antimicrobial activity of these antimicrobials. Several studies had previously reported that ROS was involved in the antimicrobial activity of Ag-NP and other antimicrobial NPs (Yin et al., 2020, Dakal et al., 2016). To leverage the experimental evolution study, we compared the ROS production in response to both antimicrobials by the parent and the adapted strains. Our results confirm the previous work that shows that ROS production results from exposure to Ag-NP. Interestingly, when the *E. coli* strain adapted to Ag-NP was exposed to high concentrations of Ag-NP, the ROS levels were similar to those of the parental *E. coli* without Ag-NP. This finding indicates that part of the resistance mechanism to Ag-NP is the ability to cope with ROS levels. Interestingly, a similar pattern was observed for the DBNPA adapted strains. The increase in ROS levels caused by Ag-NPs was significantly higher than DBNPA (Figure.3.8).

The second level of investigation was studying a potential biochemical mechanism for response to these antimicrobials. Previous studies have shown that bacteria can become

resistant to the biocide glutaraldehyde through overexpression of efflux pumps (Levy, 2002b, J.Y.Maillard, 2007). Efflux pumps are the way that bacteria use to pump toxic substances outside their cells (Webber, 2002). However, many prokaryotic species use efflux systems to resist biocides (Levy, 2002a, J.Y.Maillard, 2007, Webber, 2002). Efflux systems have been shown to help some bacteria resist chlorhexidine, QACs, and phenolics. For example, *E. coli* used efflux systems to resist triclosan (J.Y.Maillard, 2007, Levy, 2002a). Additionally, efflux pumps are important for the development of resistance to glutaraldehyde by *Pseudomonas* spp (Vikram et al., 2015c). In addition to biocide resistance, it was reported that putative multidrug-resistant pump in pathogenic *E. coli* is involved with penicillin G resistance (Soto, 2013). Other studies have shown a relationship between a mutation in efflux pumps encoding genes such as *emrD*, *emrE*, and *mdtE* and antibiotic resistance (Soto, 2013). In our study, we used an efflux pump inhibitor to identify if efflux pumps are important in resistance to DBNPA and Ag-NP. Our work shows that inhibition of efflux pumps results in increased sensitivity to both DBNPA and Ag-NP for the parent and adapted strains. However, efflux pumps appear to play a more important role in biocides than resistance to Ag-NPs.

The third angle of the investigation was studying the genetics level. As we mentioned above, previous studies related to Ag-NP resistance have suggested that there was no change in the bacterial genome when the strain was adapted to silver nanoparticles (Panacek et al., 2018). This previous study suggested that only phenotypic changes were needed for resistance to Ag-NP. We analyzed the whole-genome sequence of the *E. coli*

adapted to Ag-NPs and DBNPA in order to detect changes in the bacterial genotype during the experimental evolution experiment. In addition to the global analysis of variants acquired during experimental evolution, we also wanted to focus on specific genes such as flagellar or multidrug efflux genes previously implicated in antimicrobial resistance. Our results showed that in contrast to Panacek *et al* (2018) there were many genetic changes in the genomes of the adapted strains, including mutations near flagellar genes in *E. coli* adapted to Ag-NPs. In particular, the following genes were identified as having some modifications, Flagellar biosynthesis protein (FliT) and (FliS) Flagellar filament structural protein (FliC), and Flagellar filament capping protein (FliD), the hook (FlgK) and (FlgL) (Figure 3.11; Table 3.3; Chapter3-Supplemental Dataset-Genome).

In addition, there were changes in the genome of the *E. coli* adapted to DBNPA, including near genes efflux pumps. (Vikram et al., 2015c) demonstrated that expression of efflux pumps was increased in the presence of glutaraldehyde suggesting a role of efflux pump genes in resistance to biocides. In the DBNPA-adapted strain, we found high impact mutations in the *marR* gene which is a repressor of the *marRAB* operon which is the multiple antibiotic resistance operon. This gene cluster encodes the MarA protein which regulates efflux pumps and porin proteins (Sharma et al., 2017) The *mar* regulon is also considered to overlap with oxidative stress response (Myers et al., 2013, Sharma et al., 2017). The presence of this high impact mutation in a regulator of antibiotic resistance might further suggest a mechanism whereby biocide resistance results in cross-resistance to antibiotics. In addition to the high impact mutation in the *marR* gene,

several other efflux pump genes had mutations in or near the genes. The efflux pump genes with identified changes in our study were the multidrug efflux pump membrane subunit (EmrB), (EmrD), multidrug/betaine/choline efflux transporter (EmrE), multidrug efflux pump/bile salt:H (+) antiporter/Na (+):H (+) antiporter/K (+):H (+) antiporter (mdtM), putative multidrug efflux pump membrane fusion protein (mdtN) and (MdtO), and putative multidrug efflux pump outer membrane channel (mdtP). Moreover, there were changes in the genomic DNA between the two adapted strains when compared to each other (Figure 3.11; Table 3.3; Chapter3-Supplemental Dataset-Genome).

Our study demonstrates that *E. coli* can very rapidly acquire resistance to both Ag-NPs and DBNPA. Furthermore, we demonstrate that while there are some distinctions in the mechanism of resistance, we find that there are some common responses and mutations that occur in the strains adapted to these two types of antimicrobials. Our results indicate that adapted strains have lower ROS in the presence of both antimicrobials. Also, they show that efflux pumps contribute in part to the mechanism of resistance for the types of antimicrobials. Our genomic analysis indicates that mutations have occurred throughout the *E. coli* genome during the experimental evolution and while the mutations are shared between the two antimicrobials, there are impactful mutations that only occurred in one of the adapted strains. Our results confirm previous studies that indicate the rapid development of resistance to both biocides and NPs. However, our results suggest that there are genetic mechanisms for resistance to these two antimicrobials.

# Chapter 4

## Impact of different natural organic matter (NOM) on antimicrobial activity of Silver Nanoparticles (Ag-NPs) and 2,2-dibromo-3-nitrilopropionamide (DBNPA) Against *E. coli*

### 4.1 Abstract

In order to understand the environmental fate and industrial applications of antimicrobials, it is important to understand the impact of environmental conditions on their activity. Natural organic matter (NOM) can act to inhibit or stabilize antimicrobials. Our study goal is to investigate the impact of four types of organic matter (OM) on the antibacterial properties of Ag-NPs and DBNPA against *E. coli*. We grew *E. coli* in the presence of sub-MIC concentrations of Ag-NP (5 mg/L) and DBNPA (50 mg/L) in the presence or absence of a range of concentrations of Suwanee River NOM, Upper Mississippi River NOM, Suwanee River humic acids, and Suwanee River fulvic acids. We determined the change in bacterial growth in the presence of antimicrobials and NOM in the liquid medium, the bacterial viability count in the presence of antimicrobials, and the stability of nanoparticles in the growth medium. Our results showed that different types and concentrations of NOM negatively affected the antimicrobial properties of Ag-

NPs and DBNPA against *E. coli*. The extent of effect was different between Ag-NPs and DBNPA. In particular, we found that humic acids most strongly impacted the antimicrobial activity of Ag-NPs. Moreover, we found little change in the size of NPs when they were treated with different concentrations and types of NOM. This finding might indicate that NOM had a limited impact on the stability of Ag-NPs and their antimicrobial activity. The limited effect of NOM on Ag-NP particle size may indicate that NOM binding to NPs may stabilize them. Our study provides evidence for the effects of various concentrations of NOM on the antimicrobial activity of Ag-NPs and DBNPA.

## 4.2 Introduction

Antimicrobials are used to disinfect or sanitize water and water systems. Biocides and nanoparticles are two classes of common microbial control agents (Maillard, 2005, Fernando et al., 2018b, Fernando et al., 2018a). Both of these antimicrobials can be inadvertently released into the aquatic environments and have the potential to alter microbial community structure and function (Felis et al., 2020, Guo et al., 2019, Campa et al., 2019b). There is a concern about the presence of nanoparticles (NPs) and biocides in natural and engineered systems and their interaction with natural organic matter (NOM) (Taghavi et al., 2013, Siddiqui et al., 2017b).

Natural organic matter (NOM) is a chemical complex with different mixtures of molecular weights of organic carbon and is derived from the primary production or

decomposition of organisms such as plants or animals (Hyung and Kim, 2008). Most NOM in the environment has a net negative charge due to carboxylic and phenolic groups. This quality has been taken advantage of in water treatment; to allow for NOM to interact with activated carbon and adsorb to the activated carbon surface (Hyung and Kim, 2008). These electrostatic interactions may also play a role in driving interactions of NOM with other particles such as nanoparticles. Some previous studies have shown that NOM interacts with nanoparticles and can affect nanoparticle stability (Li et al., 2020, Stankus et al., 2011a).

Silver nanoparticles (Ag-NPs) have increasingly been used in applications such as medical products and nano textiles (Millour et al., 2013). There is therefore a greater chance of environmental release of Ag-NP, which raises many concerns about their environmental fate and potential to affect aquatic environments (Millour et al., 2013). The common use of Ag-NP along with the tendency of NOM to interact with nanoparticles make it important to understand the influence of NOM on the antimicrobial activity of Ag-NPs (Fan et al., 2018). Nanoparticles have been proposed as tools for both drinking water and wastewater treatments as means of removing bacterial contaminants from water due to the strong antimicrobial properties of NPs (Yaqoob et al., 2020). For NPs to be useful in water treatment processes, they must be stable and maintain antimicrobial activity in conditions encountered during the treatment process (Lu et al., 2016). NOM can interfere with water treatment processes and is a factor that must be considered when evaluating novel treatment strategies (Zularisam et al., 2006).

As nanoparticle size and stability is often one of the determining factors for the antimicrobial activity of NPs, the effect of NOM on NP size and stability are important to consider. A previous study demonstrated that NPs aggregate in the presence of NOM (Sikder et al., 2020). This aggregation may impact the antimicrobial activity of these nanoparticles as another study has shown that NP size is a major factor affecting antimicrobial activity, with small NPs (size < 100 nm) being more effective antimicrobial agents (Wang et al., 2017b, Wu et al., 2021). Conversely, other studies have shown that gold (Au) nanoparticles are stabilized in the presence of organic matter (Stankus et al., 2011b). Furthermore, other research has shown that different types of NOM or classes of substances within NOM may differentially affect the stability of NPs (Wu et al., 2021). Additionally, recent work demonstrated that interactions between NPs and smaller molecular weight NOM (< 3 kDa) destabilized ferrihydrite NPs, whereas interactions with higher molecular weight NOM led to increased stability (Li et al., 2020). Additional work is needed to understand how these NP-NOM interactions affect the antimicrobial activity of NPs.

On the other hand, many biocides used in water treatment are highly reactive and they may react with functionalities in NOM (Bajpai, 2015). Due to the wide use of biocides in the healthcare industry, the oil and gas industry, as well as in the home, many biocides have been detected in diverse aquatic systems (Kahrilas et al., 2015a). Many of these biocides are not removed during wastewater treatment (J.Y.Maillard, 2007). These

biocides are diluted during the transmission from point of use to the environment, and thus are present at sub MIC concentrations. However, few studies have investigated the interaction between biocides and NOM (Day et al., 1997). In this study, we hypothesized that nanoparticles and biocides will retain antimicrobial activity in presence of environmentally relevant concentrations of natural organic matter (NOM). The objective of this study was to investigate the effect of four types of natural organic matter (NOM) on the antimicrobial activity of Ag-NPs and DBNPA.

### **4.3 Materials and methods**

#### **4.3.1 Chemicals.**

The biocide used in this study was 2, 2-dibromo-3-nitrilopropionamide (DBNPA) (molecular weight: 241.87g mol<sup>-1</sup>, Sigma-Aldrich). Stock solutions of DBNPA were prepared at a concentration of 1 mmol/L in MH broth.

The nanoparticle used in this study was a commercial preparation of Ag nanoparticles (US Research Nanomaterials, Inc. 3302 Twig Leaf Lane, Houston, TX 77084, USA, Silver Nano powder water dispersion with an average size of 15 nm and stock concentration of 1000 mg/L) these commercially available nanoparticles were spherical.

### 4.3.2 Organic matter description

In this study, we chose to investigate the impact of two natural organic matter samples from the International Humic Substances Society. Natural organic matter is a complex mixture. Here we chose to use the well-characterized Suwannee River NOM as well as the Upper Mississippi River NOM. We choose these NOM depending on the International Humic Substance Society (IHSS) standard and reference for interlaboratory comparison (Green et al., 2014). These represent mixtures include humic and fulvic substances as well as protein-like components of the NOM. To contrast the total NOM from Suawanee River and the Upper Mississippi River, we chose to investigate if fractions of the NOM had similar effects on antimicrobial activity. In particular, we investigated the effect of Suwannee River humic acids and Suwannee River fulvic acids on antimicrobial activity. Humic and fulvic acids as representatives of different fractions of NOM. Fulvic and humic acids are common in aquatic NOM with different hydrophilic proprieties, molecular weight (Mw), and their functional groups (Luo et al., 2018). For example, humic acids have a higher MW than fulvic acids (Luo et al., 2018, Boggs et al., 1985). The Suwannee River NOM, as well as the Suwannee River fulvic acids, and the Suwannee River humic acids were isolated from Suwannee River in southeastern Georgia, USA. The Upper Mississippi River NOM was isolated from the Mississippi River in Minneapolis, Minnesota, USA (Perdue, 2013).

### **4.3.3 Bacterial strains and growth conditions.**

*E. coli* (ATCC 700609) was the strain we used in this study and Mueller Hinton broth was the growth media. The cultures were grown at 37 °C (Panacek et al., 2018).

### **4.3.4 Treatments used for the study.**

To determine the effect of organic matter on NP and biocide activity, *E. coli* was grown in the presence of either Ag-NP, DBNPA, or the combination of the two antimicrobials. The concentrations of antimicrobials are based on the MIC determined for the parental strain of *E. coli* from chapter 3. We used the sub-lethal concentrations that we determined in chapter 3 to allow the bacteria to grow in the presence of the antimicrobials. *E. coli* was grown at a range of NOM concentrations (0, 5, 10, 15 mg/L) with three replicates per treatment. These concentrations represent a range of NOM concentrations observed in natural waters from previous studies (Krzeminski et al., 2019). The experiment setup is illustrated in (Table.4.1). The growth of *E. coli* was tested in the presence of multiple NOM types with the two antimicrobials (Ag-NP and DBNPA) as well as the combination. The concentrations of antimicrobials were 2 mg/L for Ag-NP and 45 mg/L for DBNPA. The combination was made by adding 2 mg/L Ag-NPs and 45 mg/L DBNPA. Each condition was set up so that the final volume was 20 ml (Table.4.1).

We tested the growth inhibition in response to NPs and biocides by measuring OD600 after 24 hours, as well as inactivation of *E. coli* through viable plate bacterial colony counts and we used 0 mg/ml of NOM as a positive control to show inhibition of *E. coli* growth by the selected antimicrobials. An increase in growth upon addition of NOM compared to this control would show an effect of NOM on the antimicrobial activity. *E. coli* was also grown without any antimicrobials or NOM as a negative control. This was used to represent the amount of growth in an uninhibited condition. The decrease in growth relative to this negative control indicates the retention of antimicrobial activity

Table 4.1

Conditions tested to investigate the physiological response to antimicrobials.

<b>NOM Description</b>	<b>NOM Concentration</b>				<b>Antimicrobial Treatment</b>		
<b>IHSS Suwannee River- Humic Acid Standard III (3S101H) - (HA)</b>	0 mg/L	5 mg/L	10 mg/L	15 mg/L	Ag-NPs (2 mg/L)	DBNPA (45 mg/L)	Ag-NPs (2 mg/L) + DBNPA (45 mg/L) (v/v).
<b>/IHSS Suwannee River- Fulvic Acid Standard III (3S101F)- (FA)</b>	0 mg/L	5 mg/L	10 mg/L	15 mg/L	Ag-NPs (2 mg/L)	DBNPA (45 mg/L)	Ag-NPs (2 mg/L) + DBNPA (45 mg/L) (v/v).
<b>IHSS Suwannee River- NOM (RO Isolation) (2R101N)- (NOM1)</b>	0 mg/L	5 mg/L	10 mg/L	15 mg/L	Ag-NPs (2 mg/L)	DBNPA (45 mg/L)	Ag-NPs (2 mg/L) + DBNPA (45 mg/L) (v/v).
<b>IHSS Upper Mississippi- NOM (RO Isolation) (1R101N) -(NOM2)</b>	0 mg/L	5 mg/L	10 mg/L	15 mg/L	Ag-NPs (2 mg/L)	DBNPA (45 mg/L)	Ag-NPs (2 mg/L) + DBNPA (45 mg/L) (v/v).
<b>(3S101F) + (1R101N) (3S101H) + (2R101N) Multiple antimicrobials (v/v).</b>	0 mg/L	5 mg/L	10 mg/L	15 mg/L	Ag-NPs (2 mg/L) + DBNPA (45 mg/L) (v/v).		

#### **4.3.5 Bacterial growth in the presence of antimicrobials in the liquid medium**

*E. coli* was grown separately in 50 mL sterilized Mueller Hinton (MH) broth medium and kept in a shaker incubator at 37°C for overnight incubation. On a subsequent day, the fresh *E. coli* was transferred at a 1% inoculum into 20 mL MH broth. Sublethal concentrations of Ag-NPs (2 mg/L) and DBNPA (45 mg/L) were used to test various concentrations of the four NOM samples (0, 5, 10, and 15 mg/L). One treatment was left without organic matter as a control to track the normal growth of the microbial cells without antibacterial agents. The tubes were incubated at 37°C. Optical density measurements OD<sub>600</sub> from each tube were taken after 24 hours.

#### **4.3.6 Bacterial count in the presence of antimicrobials**

In this method, *E. coli* was grown in sub-MIC concentrations of Ag-NPs (2 mg/L) and DBNPA (45 mg/L) with various concentrations (0, 5, 10, and 15 mg/l of the four NOM that used in this study). A known concentration 10<sup>7</sup> CFU ml/l (colony-forming unit) of *E. coli* was inoculated into the MH broth and incubated for 24 hours under the different conditions described in (Table 4.1). After 24 hours, the cultures were then diluted and several dilutions plated on Muller Hinton agar to observe how many bacteria survived the treatment. The plates were then grown at 37°C for 24 hours. After incubation, the number of bacterial colonies on the plates was counted to determine colony forming units

(CFU/ml). The data obtained in all tests were compared with the positive and negative controls.

#### **4.3.7 Stability of nanoparticles in growth medium.**

The size of the particles was confirmed by dynamic light scattering (DLS). We used Mueller Hinton broth as growth media (Panacek et al., 2018). The aggregation of Ag-NPs were tested in different treatments and NOM concentrations, including the absence and presence of NOM and the mixture of DBNPA-NPs-NOM (Table.4.1). After 24 hours we monitored the size of the Ag-NPs to determine the size and aggregation state in each test. The average size distribution was determined for each replicate. The size of the nanoparticles was determined based on intensity.

#### **Statistic**

A Shapiro-Wilk test for normality was used to determine if the data was normally distributed. If the data was not normally distributed, a Kruskal-Wallis test was used to evaluate the significance of experimental results ( $P < 0.05$ ). A Dunn's test of significant difference test for multiple comparisons of means obtained was used as a post hoc to evaluate the significance of experimental results ( $P < 0.05$ ). Comparisons were performed between treatments and the positive and negative controls as well as to see if there were significant differences between biocide- and NP-amended treatments and the controls.

## 4.4 Results

### 4.4.1 The impact of NOM on bacterial growth in the presence of antimicrobials

### 4.4.2 Effect of NOM on the antimicrobial activity of Silver nanoparticles

The growth of bacterial cells in liquid culture media was measured by the optical density at 600 nm (OD<sub>600</sub>) to determine the changes in overall growth yields with or without different NOM. If NOM impacted the antimicrobial activity of the antimicrobials, we would expect to see higher overall ODs with increasing NOM concentrations. The Ag-NP significantly decreased growth (Kruskal-Wallis P=0, Dunn's test P= 0.0045) from OD<sub>600</sub> of 1.38 ± 0.29 in the no antimicrobial treatment (negative control) to OD<sub>600</sub> of 0.29 ± 0.04 in the presence of Ag-NPs (positive control (0 mg/L)) (Figure 4.1; Table.S.4.4.2.1; Table. S.4.4.2.2). With low NOM concentrations, we observed little increase with OD reads between all NOM when it was added to Ag NP treatment, while we observed that high concentrations of NOM resulted in increased overall bacterial yields compared to bacteria with NPs alone (0mg/L of NOM) (Figure 4.1; Table.S.4.4.1). When Suwannee River- Humic Acid Standard III (HA) was added to *E. coli* cultures with Ag-NP, we observed that the OD substantially increased with increasing concentrations of HA. However, within all NOM, Suwannee River- Humic Acid Standard III (HA) at 15 mg/L concentration was the highest in OD (0.9 ± 0.04) compared to an OD of 0.3 ± 0.04 for the positive control when it treated to Ag-NPs (Figure 4.1; Table.S.4.4.2.1; Table.S.4.4.2.2).

Similar trends were observed with the Suwannee River- Fulvic Acid Standard III (FA) and Suwannee River-NOM-(NOM1) with OD ( $0.76\pm0.07$ ,  $0.75\pm0.1$ ) respectively with 15mg/l concentration compared to the positive control OD ( $0.3 \pm 0.04$ ) (Figure 4.1; Table.S.4.4.1; Table.S.4.4.2). The lowest overall OD was with Upper Mississippi-NOM-(NOM2) at 15 mg/l the high concentration with ( $0.66 \pm 0.14$ ) compared to the positive control OD ( $0.3 \pm 0.04$ ) (Figure 4.1; Table.S.4.4.2.1; Table.S.4.4.2.2). These results might indicate that high concentrations of HA and FA with high MW can interrupt the antimicrobial activity of Ag-NPs compared to the positive control as observed by the largest increase in OD upon treatment.

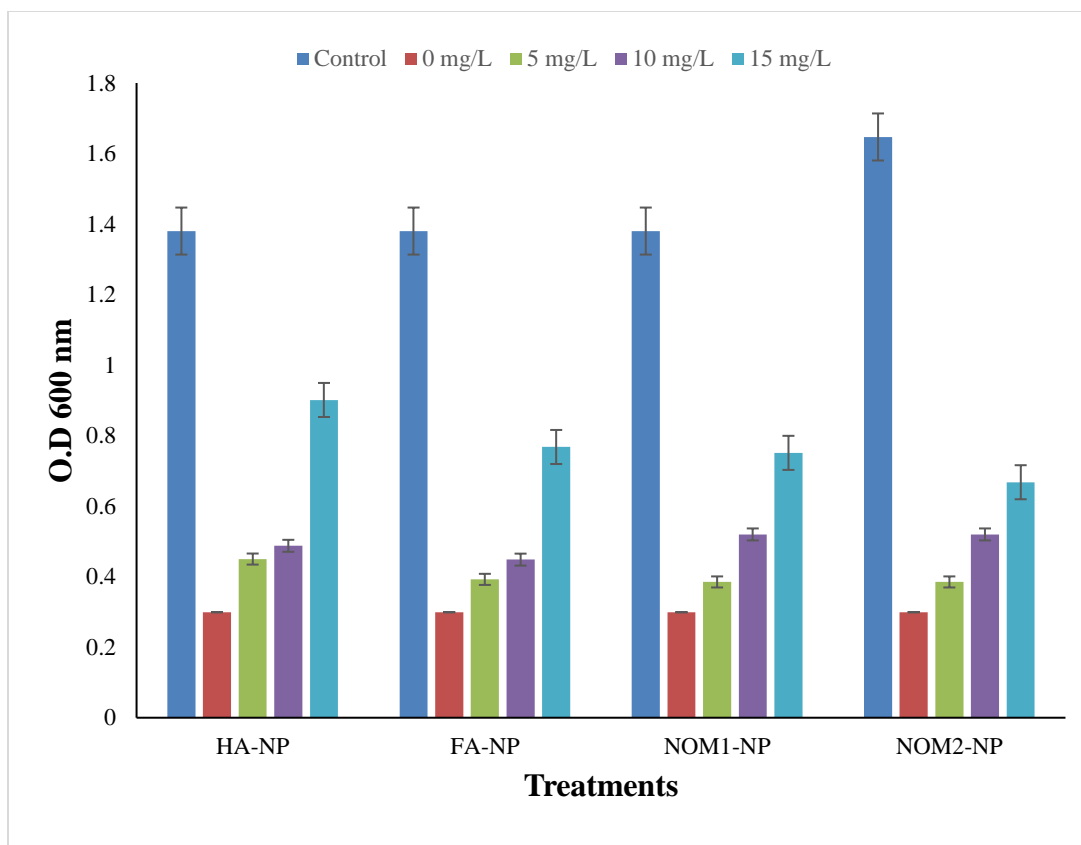


Figure 4.1 Showing silver nanoparticles antimicrobial activity on the bacterial abundance of *E. coli* with different NOM after 24 h incubation (n=3) (average  $\pm$  standard deviation). and the data shown as mean and error bars represent standard deviation. The control (blue) shows *E. coli* abundance only. The NOM treatments show different NOM with three concentrations incubated with (2 mg/L) silver nanoparticles (Table 4.1). The 0 mg/l (red) without NOM from the same triplicate conditions is shown in the groups of data for sake of comparison. The NOM treatments abbreviations are the following: (HA-NP)-Humic Acid with Ag-NPs, (FA -NP)-Fulvic Acid with Ag-NPs, (NOM1-NP)-Suwannee River NOM with Ag-NPs, (NOM2-NP)- Upper Mississippi NOM with Ag-NPs.

#### 4.4.3 Effect of NOM on DBNPA antimicrobial activity

The addition of DBNPA decreased growth from OD<sub>600</sub> of  $(1.38 \pm 0.29)$  in the no antimicrobial treatment to OD to  $(0.7 \pm 0.1)$  in the presence of DBNPA (Kruskal-Wallis  $P=0$ , Dunn's test  $P= 0.02$ ) (Figure 4.2; Table.S.4.4.3.1; Table. S.4.4.3.2). In all of the treatments, there was an increase in OD in treatments with all organic matter at the high concentration (15mg/L) compared to positive control OD  $(0.7 \pm 0.1)$ . There was a similar negative effect on DBNPA antimicrobial activities with different NOM and different NOM concentrations. Unlike the Ag-NP, NOM addition to the DBNPA treatments resulted in a stronger negative effect at lower concentrations of NOM. For example, at 5 mg/L of Upper Mississippi River and Suwanee River NOM, there was a substantial increase in the OD. This increase in OD at a low concentration of NOM might indicate that the antimicrobial properties of DBNPA were more negatively affected by NOM than Ag NP.

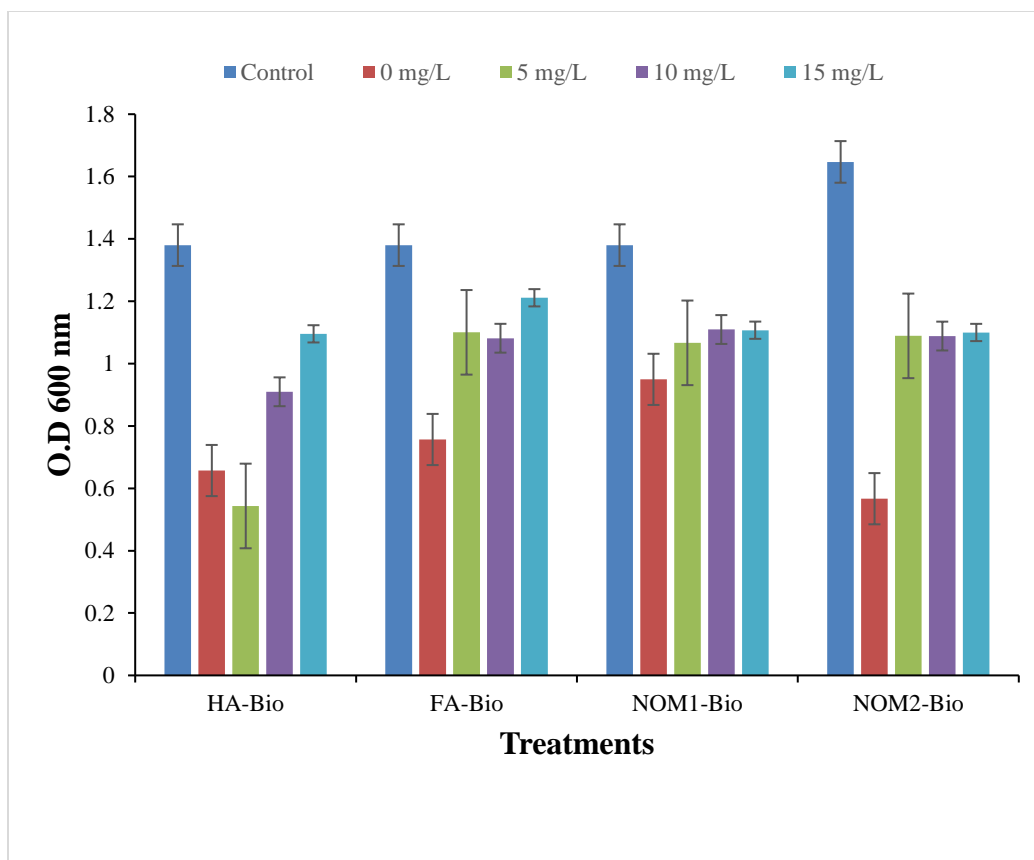


Figure 4.2 Showing DBNPA antimicrobial activity on the bacterial abundance of *E. coli* with different NOM after 24 h incubation (n=3) and the data shown as mean and error bars represent standard deviation. The control (blue) shows *E. coli* abundance only and the 0 mg/l (red) without NOM. The NOM treatments show different NOM with three concentrations incubated with (45 mg/L) DBNPA (Table 4.1). The NOM treatments abbreviations are the following: (HA-Bio)-Humic Acid with DBNPA, (FA - Bio)-Fulvic Acid with DBNPA, (NOM1- Bio)-Suwannee River NOM with DBNPA, (NOM2- Bio)-Upper Mississippi NOM with DBNPA.

#### **4.4.4 Effect of NOM on the combination of Ag-NP and DBNPA antimicrobial activity.**

In the treatments with the mixture of antimicrobials, we observed a decrease in the *E. coli* growth with all mixture treatments at all NOM concentrations relative to the negative control with no antimicrobials (Figure 4.3; Table. S.4.4.4.1). The DBNPA & Ag-NPs decreased growth from OD<sub>600</sub> of  $(1.38 \pm 0.29)$  in the no antimicrobial treatment to OD to  $(0.25 \pm 0.08)$  in the presence of DBNPA & Ag-NPs (Kruskal-Wallis  $P=0$ , Dunn's test  $P= 0.02$ ) (Figure 4.3; Tables.S.4.4.4.1; Table. S.4.4.4.2). This finding suggests higher antibacterial activity when the two antimicrobial agents are combined compared to when we separate Ag-NPs and DBNPA. With all NOM and antibacterial agents, we observed that HA at 15 mg/L with DBNPA and Ag-NPs had the highest OD  $(0.57 \pm 0.48)$ . This finding indicates the negative effect of HA on the Ag NP antibacterial activity even with the presence of DBNPA. The significantly lowest OD in the 15 mg/L NOM treatments  $(0.24 \pm 0.24)$  was Suwannee River-NOM-(NOM1) with DBNPA & Ag-NPs (Kruskal-Wallis  $P=0$ , Dunn's test  $P= 0.03$ ) (Figure 4.3; Tables.S.4.4.4.1; Table. S.4.4.4.2).

Despite the retention of high antimicrobial activity in the presence of NOM when the antimicrobials are combined, there was still an increase in OD relative to the positive control (antimicrobials without NOM). This increase in OD relative to the positive control may suggest that NOM can disrupt NPs and DBNPA antimicrobial activity in MH media, but this negative effect of adding NOM to the combination of Ag-NP and DBNPA is less than the effect of NOM on the individual antibacterial agents.

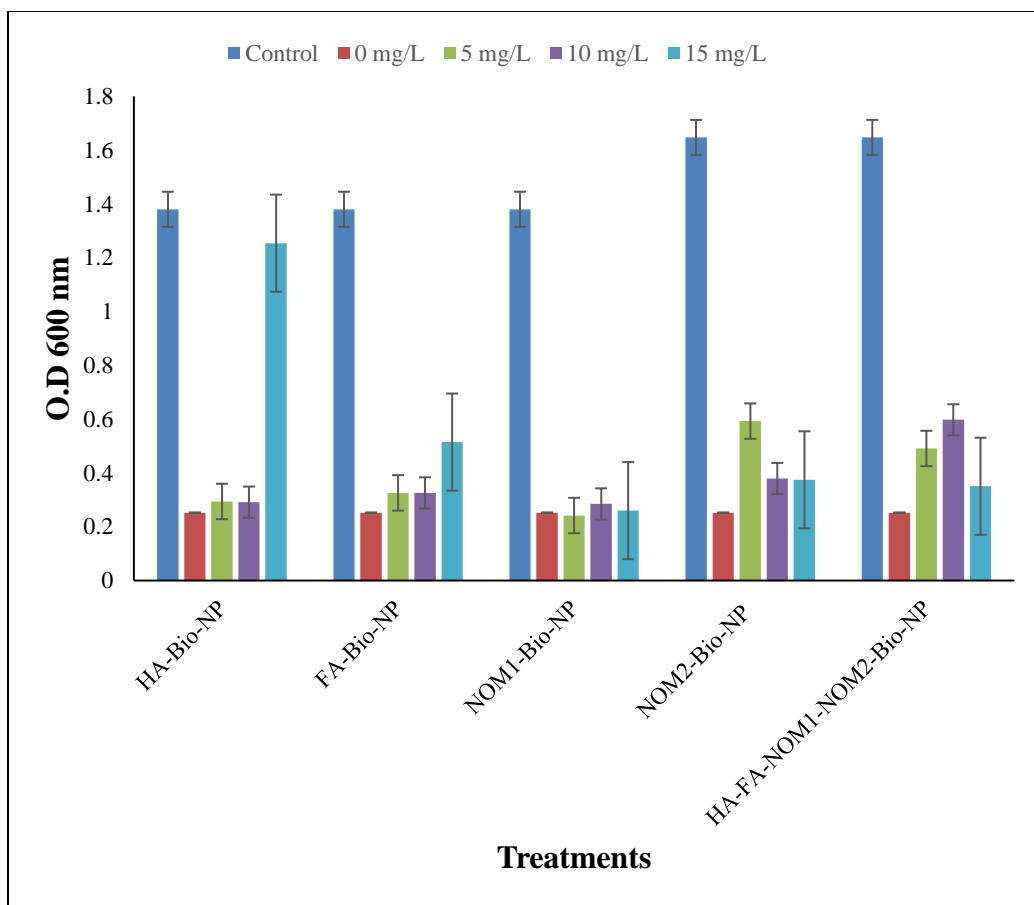


Figure 4.3 Showing the plots of bacterial abundance changes with different NOM. Compared the effect of NOM on a mix of Ag-NPs and DBNPA antimicrobial activity (n=3) (average  $\pm$  standard deviation). The control (blue) shows *E. coli* abundance only. The same 0 mg/l (red) without NOM from the same triplicate conditions are shown in the groups of data for sake of comparison. The NOM treatments show different NOM with three concentrations incubated with (2 mg/L) silver nanoparticles & (45 mg/L) DBNPA (v/v) (Table 4.1). The NOM treatments abbreviations are the following: (HA-Bio-NP)-Humic Acid with Ag-NPs & DBNPA, (FA-Bio-NP)-Fulvic Acid with Ag-NPs & DBNPA, (NOM1-Bio-NP)-Suwannee River NOM with Ag-NPs & DBNPA, (NOM2-Bio-NP)- Upper Mississippi NOM with Ag-NPs & DBNPA, (HA-FA-NOM1-NOM2-Bio-NP)- Humic Acid & Fulvic Acid & Suwannee River NOM& Upper Mississippi NOM with Ag-NPs & DBNPA.

#### **4.4.5 The impact of NOM on bacterial viability count in the presence of antimicrobials**

#### **4.4.6 Effect of NOM on bacterial viability count in the presence of Silver nanoparticles**

Cell viability tests were done to determine the effect of Ag-NPs on inhibiting bacterial viability with and without NOM. Similar trends we observed when comparing viability with the O.D test with all different treatments. When we treated the bacteria with Ag-NPs, we did see that high concentrations of different NOM increase the viable bacterial count number compared to the positive control of bacteria with NPs and no NOM.

Moreover, we observed that the addition of antimicrobials decreased the viable *E. coli* in the positive control (log CFU 8.4) compared to the treatment without Ag-NPs (log CFU 9.5 (Kruskal-Wallis  $P=0$ , Dunn's test  $P= 0.008$ ) (Figure 4.4; Tables.S.4.4.6.1; Table. S.4.4.6.2). The Suwannee River HA at a concentration of 15 mg/L and Ag-NP gave the highest log CFU (8.8) of all of the Ag-NP treatments (Kruskal-Wallis  $P = 0$ , Dunn's test,  $P = 0.0237$ ) compared to the positive control with log CFU (8.4) (Figure 4.4; Table. S.4.4.6.7; Table. S.4.4.6.2). Additionally, a similar trend was observed with FA-NPs and Suwannee River-NOM-(NOM1). On the other hand, the lowest viable count was with Upper Mississippi-NOM-(NOM2) at 15 mg/l with log CFU (8.5) compared to the positive control with log CFU (8.4) (Table. S.4.4.6.2).

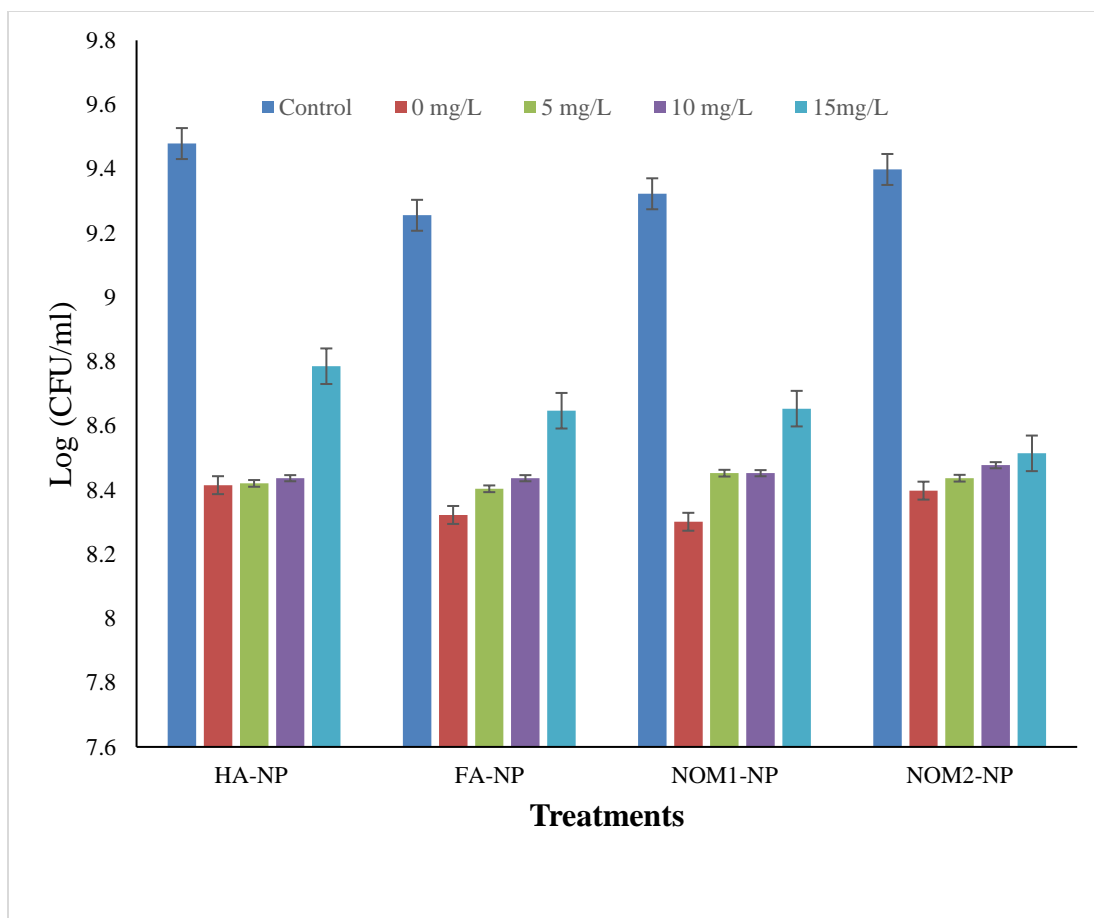


Figure 4.4 Showing silver nanoparticles antimicrobial activity on the bacterial cell viability of *E. coli* with different NOM after 24hrs incubation (n=3) and the data shown as mean and error bars represent standard deviation. The control (blue) shows *E. coli* abundance only. The NOM treatments show different NOM with three concentrations incubated with (2 mg/L) silver nanoparticles. The 0 mg/l (red) without NOM from the same triplicate conditions is shown in the groups of data for sake of comparison. The NOM treatments show different NOM with three concentrations incubated with (2 mg/L) silver nanoparticles (Table 4.1). The NOM treatments abbreviations are the following: (HA-NP)-Humic Acid with Ag-NPs, (FA-NP)-Fulvic Acid with Ag-NPs, (NOM1-NP)-Suwannee River NOM with Ag-NPs, (NOM2-NP)- Upper Mississippi NOM with Ag-NPs.

#### **4.4.7 Effect of NOM on bacterial viability count in the presence of DBNPA**

We observed a decrease in the *E. coli* upon addition of NOM from log CFU of 9.2 when *E. coli* was grown without DBNPA in the no antimicrobial treatment to log CFU of 8.3 in the presence of DBNPA and no NOM in the positive control (Kruskal-Wallis  $P=0$ , Dunn's test  $P= 0.007$ ) (Figure 4.4; Tables.S.4.4.7.1; Table. S.4.4.7.2). With DBNPA, we observed a decrease in the DBNPA antimicrobial activity with the two highest NOM concentrations (10-15 mg/l) (Figure 4.5; Table. S.4.4.7.1). In particular, the highest bacterial counts were observed in the Suwannee River-NOM-(NOM1) 15 mg/L treatment (log CFU= 8.9) compared to the positive control (log CFU= 8.3); Also, the lowest cells count number was with HA at 15 mg/l (log CFU = 8. 47) when HA was added to DBNPA (Table. S.4.4.7.1).

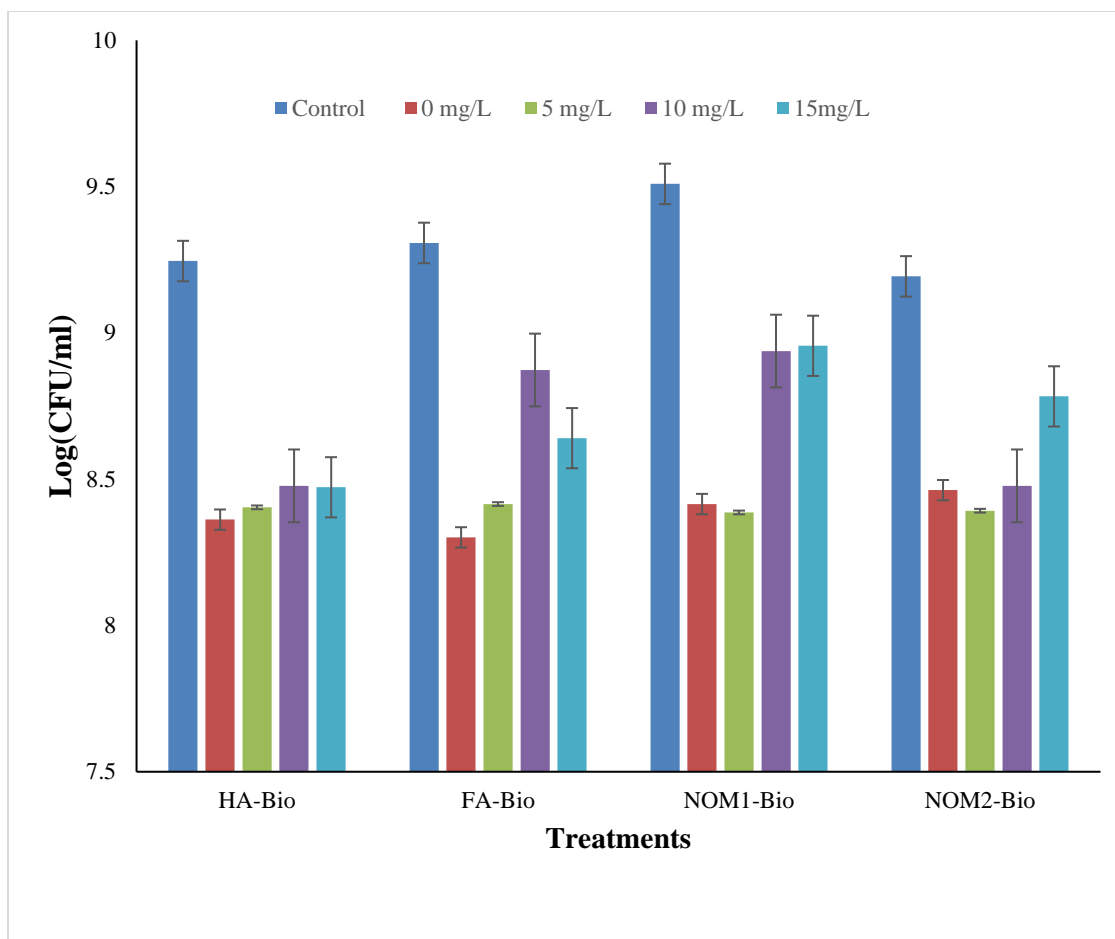


Figure 4.5 Showing DBNPA antimicrobial activity on the bacterial cell viability of *E. coli* with different NOM after 24h incubation (n=3) and the data shown as mean and error bars represent standard deviation. The control (blue) shows *E. coli* abundance only. The NOM treatments show different NOM with three concentrations incubated with (45 mg/L) DBNPA (Table 4.1). The same 0 mg/l without NOM from the same triplicate conditions is shown in the groups of data for sake of comparison. The NOM treatments abbreviations are the following: (HA-Bio)-Humic Acid with DBNPA, (FA-Bio)-Fulvic Acid with DBNPA, (NOM1-Bio)-Suwannee River NOM with DBNPA, (NOM2-Bio)-Upper Mississippi NOM with DBNPA.

#### **4.4.8 Effect of NOM on bacterial viability count in the presence of the combination of Ag-NP and DBNPA**

When comparing the effect of NOM on the combination of antimicrobials, we observed a decrease in the *E. coli* growth in the treatments with both DBNPA and Ag NP from log CFU (9.5) in the no antimicrobial treatment to log CFU (8.3) in the presence of both antimicrobial agents (Kruskal-Wallis  $P=0$ , Dunn's test  $P= 0.006$ ) (Figure 4.4; Tables.S.4.4.8.1; Table. S.4.4.8.2).

In the mixed antimicrobials also, we did not observe much negative effect on antimicrobial activity for both DBNPA or Ag-NPs (Figure 4.6; Table. S.4.4.8.1) with all NOM and antibacterial agents, we observed that FA-bio-NP had significantly the highest reads (log CFU= 8.83) at 15 mg/l compared to the positive control (Kruskal-Wallis  $P = 0$ , Dunn's test,  $P = 0.018$ ), and the lowest was with the combination of all NOM and antibacterial agents that used in this study FA-HA-NOM2-NOM1- DBNPA-Ag-NPs) with (log CFU= 8.3) read (Table. S.4.4.8.1). Similar to the OD results we can say that NOM can negatively affect NPs and DBNPA antimicrobial activity in MH media, but the antimicrobial activity is less impacted in the mixed treatment compared to the individual antibacterial agents.

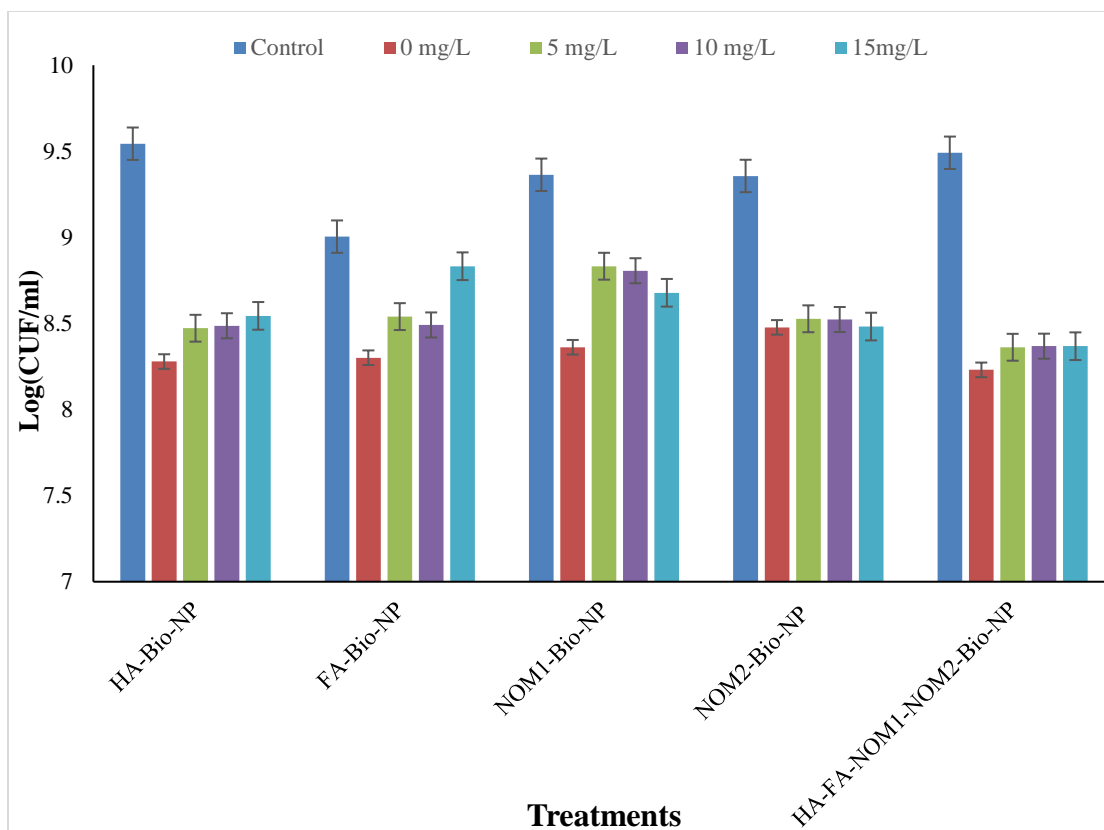


Figure 4.6 Showing the plots of bacterial cell viability changes with different NOM. Compared the effect of NOM on a mix of Ag-nanoparticles and biocides antimicrobial activity (n=3) (average  $\pm$  standard deviation). The NOM treatments abbreviation is illustrated in (Table 4.1). The control (blue) shows *E. coli* abundance only and 0 mg/l (red) without NOM. The NOM treatments show different NOM with three concentrations incubated with (2 mg/L) silver nanoparticles & (45 mg/L) DBNPA (v/v) (Table 4.1). The NOM treatments abbreviations are the following: (HA-Bio-NP)-Humic Acid with Ag-NPs & DBNPA, (FA-Bio-NP)-Fulvic Acid with Ag-NPs & DBNPA, (NOM1-Bio-NP)-Suwannee River NOM with Ag-NPs & DBNPA, (NOM2-Bio-NP)- Upper Mississippi NOM with Ag-NPs & DBNPA, (HA-FA-NOM1-NOM2-Bio-NP)- Humic Acid & Fulvic Acid & Suwannee River NOM & Upper Mississippi NOM with Ag-NPs & DBNPA.

#### 4.4.9 The effect of different NOM on the size and stability of the Silver nanoparticles

To determine if the altered antimicrobial activity of Ag-NPs in the presence of NOM is due to aggregation of Ag-NPs, we studied the changes in the size of the Ag-NPs as the concentration of NOM was increased for all NOM types. The average diameter of silver NPs size distribution was  $44.4 \pm 1.1$  nm after 24 hours for the Ag-NPs in MH media without NOM (Table. S.4.4.9.1). This size distribution is similar to those stated for the commercial preparations used. In general, there was a significant difference between NPs sizes without and with most NOM concentrations ( Kruskal-Wallis  $P = 0.03$ , Dunn's test,  $P = 0.03$ ) (Figure 4.7; Table. S.4.4.9.2). However, the increase in the Ag-NPs size diameter when we added different types and concentrations of NOM was relatively minor (Table. S.4.4.9.1; Table. S.4.4.9.2). The diameter of the particles increased from  $(44.4 \pm 1.1)$  in the 0 mg/L to  $(69.95 \pm 4.7)$  in the HA with 15 mg/L. Moreover, the largest size of Ag-NPs of all the OM tested was HA at 10 mg/l concentration with  $(72.56 \pm 8.32)$  (Table. S.4.4.9.13). The mix NOM with DBNPA showed also, increase in NP size with a similar increase with all concentrations (Figure 4.7; Table. S.4.4.9.1). Upon addition of NOM, for the combined condition, there was an increase in diameter of the Ag-NP from  $(44.4 \pm 1.1)$  in the no-NOM mixed condition to  $(70.18 \pm 7.78)$  in the mixture of DBNPA and Ag-NP with all NOM with 15 mg/L (Figure 4.7; Table. S.4.4.9.3). This finding indicates that despite the relatively high concentration of DBNPA, there was little interaction of the DBNPA and the Ag-NP to increase the size of the Ag-NP.

This minor increase in size may indicate that NOM does not strongly affect NPs stability in MH media. The increase in size does not equal a doubling of the diameter of the particles in the 0 mg/L organic matter conditions. Additionally, despite the relatively high concentrations of DBNPA used in the combined treatment, there was a similar increase in size to the Ag-NP alone. This suggests that the high concentrations of DBNPA do not destabilize the nanoparticles to the point of aggregation.

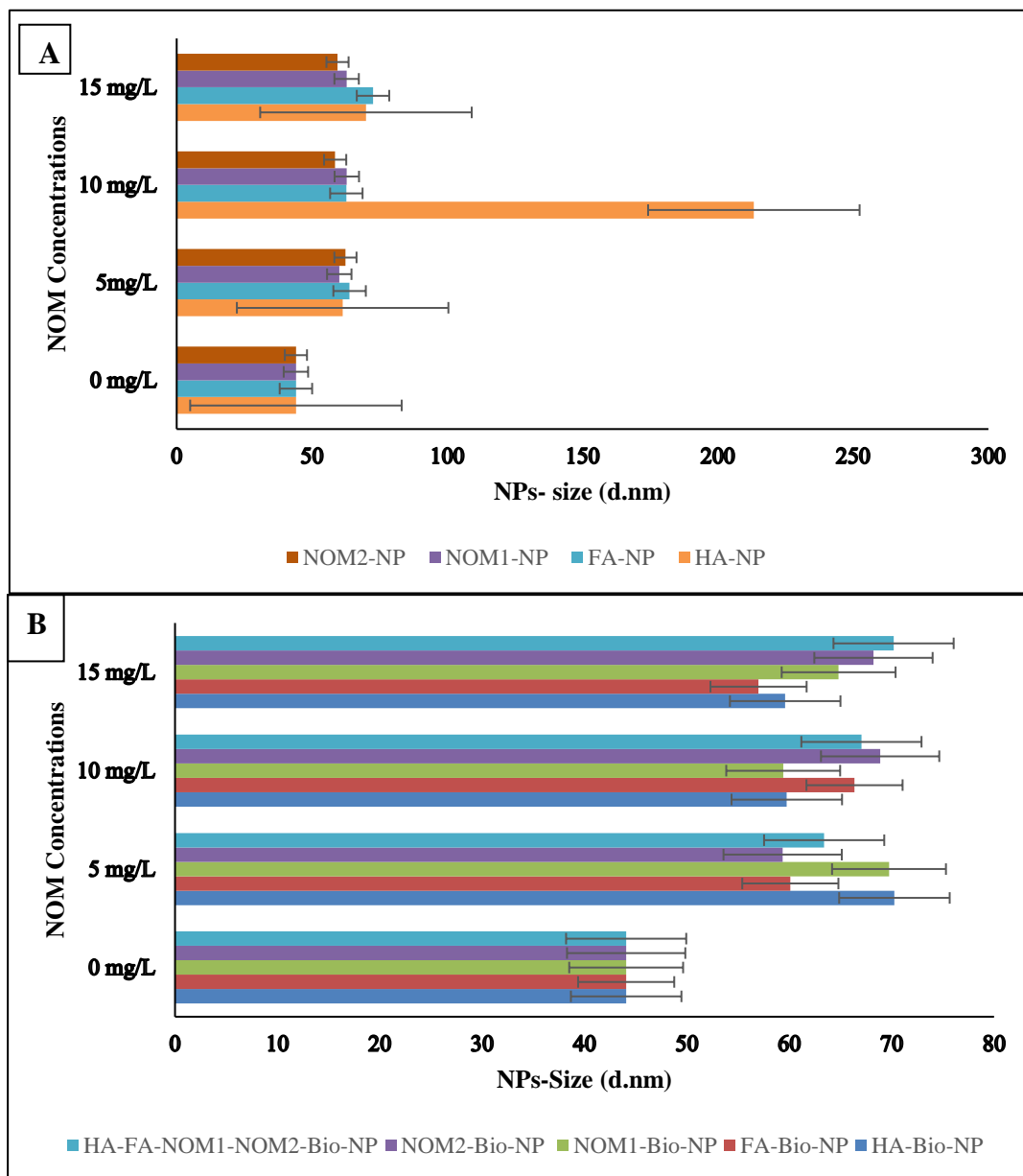


Figure 4.7 Showing relative NPs size distribution was determined based on intensity for each replicate with different NOM in MH media (n=3) (average  $\pm$  standard deviation). Compared the effect of NOM on NPs size. The control is 0 mg/l without NOM and the NOM concentrations show different NOM with three concentrations incubated with (2 mg/L) silver nanoparticles (Table 4.1). **A.** showing the size of Ag-NPs with different NOM under different NOM concentrations without any biocides (DBNPA). The NOM treatments abbreviations are the following: (HA-NP)-Humic Acid with Ag-NPs, (FA-

NP)-Fulvic Acid with Ag-NPs, (NOM1-NP)-Suwannee River NOM with Ag-NPs, (NOM2-NP)- Upper Mississippi NOM with Ag-NPs. **B.** showing the size of Ag-NPs with different NOM and with DBNPA. The NOM treatments abbreviations are the following: (HA-Bio-NP)-Humic Acid with Ag-NPs & DBNPA, (FA-Bio-NP)-Fulvic Acid with Ag-NPs & DBNPA, (NOM1-Bio-NP)-Suwannee River NOM with Ag-NPs & DBNPA, (NOM2-Bio-NP)- Upper Mississippi NOM with Ag-NPs & DBNPA, (HA-FA-NOM1-NOM2-Bio-NP)- Humic Acid & Fulvic Acid & Suwannee River NOM & Upper Mississippi NOM with Ag-NPs & DBNPA.

#### 4.5 Discussion

Our study showed that natural organic matter (NOM) had a negative effect on the antimicrobial activity of both silver nanoparticles and biocides. This effect is different between Ag-NPs and DBNPA due to the different modes of action of each of them. The negative effect on antimicrobial activity also depends on the types, concentrations of NOM, and the types and numbers of antimicrobial agents that present with NOM. Moreover, our results showed that NOM did not substantially alter the particle size of the Ag-NP.

To understand the observed effects of organic matter on Ag-NP or DBNPA antimicrobial activity, it is important to understand the antimicrobial mechanism for Ag-NP or DBNPA against bacteria.

First, Ag-NPs are heavy metal ions that interact with and damage the bacterial cell wall leading to the inactivation of the bacteria (Slavin et al., 2017). It has also been reported that the released silver ions ( $\text{Ag}^+$ ) from Ag-NPs play an important in generating toxicity

to bacterial cells (Qing et al., 2018). However, this interaction between Ag-NPs and bacteria depends on the different surface charges of the bacterial membrane (negative charge) and the positive charge of Ag-NPs which create stronger attractiveness (Abbaszadegan et al., 2015). These interactions are also different between Gram-positive or negative bacteria (Slavin et al., 2017). For example, the *E.coli* tested in this study is Gram-negative which means it has a thinner cell wall (3-4 nm) than other types of bacteria such as Gram-positive (30 nm) (Vila Domínguez et al., 2020, Slavin et al., 2017).

Moreover, one study showed the toxicity mechanism for Ag NPs could be in two ways; First, Ag NPs can enter inside the cell by diffusion and affect the cell by increasing the Reactive Oxygen Species (ROS) production, which leads to damage to proteins and nucleic acids. Second, Ag NPs can interact with membrane proteins such as glutathione and protein-bound sulfhydryl groups and affect the antioxidant enzymes indicative of lipid peroxidation leads to cell oxidative damage (McShan et al., 2014).

The antibacterial effects of NPs also depend on the type, size, and concentration of NPs. The type of NPs play an important role in antimicrobial activity; for example, metal inorganic NPs have high toxicity against microbes compared to carbon NPs (Simonin and Richaume, 2015). The size and the shape of Ag-NPs are also important in the penetration and attachment of the NPs to the bacterial cell membrane; for example, NPs larger than 10 nm gather on the cellular surface and obstruct cellular transportation (Abbaszadegan et al., 2015, Slavin et al., 2017). Usually, smaller NPs should have higher antibacterial activity, due to the large surface-to-volume ratio, but the size is not the only toxicity

factor as many studies have shown larger particles can be harmful to bacteria (Padmavathy and Vijayaraghavan, 2008, Vila Domínguez et al., 2020). The other factors of toxicity can be the different physical features of the NPs, the environment, and the mechanism of defense for the bacteria (Vila Domínguez et al., 2020). One study showed that silver NPs affect *E. coli* by attaching to the bacterial cell membrane and inhibiting the bacterial cellular transport such as nutrient uptake, which leads to cell damage (Gold et al., 2018).

Differing results have been reported about the impact of NOM on NP stability and aggregation. For some NP under some conditions, NOM leads to aggregation. Whereas for other nanoparticles under different conditions, NOM addition can lead to stabilization of NPs. Few studies have investigated the effect of NOM binding on the antimicrobial activity of Ag-NPs.

Our results showed that Ag-NPs retain antibacterial properties even when we add diverse NOM preparations at relatively high concentrations to the bacterial culture. The retention of antimicrobial activity might be due to NOM not affecting the other factors that I mentioned. In most cases the addition of NOM results in decreased antimicrobial activity. The decreased antimicrobial activity of the NPs may be due to adsorption of NOM to the Ag-NPs particles surface in a way that coats the particles and prevents interaction of the particles or release of toxic compound (Delay et al., 2011). NOM coating the Ag-NPs may also explain the little increase of the particle size, which would be in line with the reports of NOM interaction with ferrihydrite nanoparticles (references). Additionally, our results showed that humic acids (HA) had the strongest

negative impact on the Ag-NPs antimicrobial activity. This impact could be due to the physicochemical characteristics of humic acids. It had been reported that the aromatic ring structures, carboxyl groups, and molecular weight play an important role in increasing or decreasing the NPs aggregation or stability (Gutierrez et al., 2020, Luo et al., 2018). However, one study reports that highly aromatic NOM plays an important role in the stability of NPs (Castan et al., 2020). One study confirmed that HA has a higher molecular weight than fulvic acid (FA) also HA is more hydrophilic than FA and that may lead to the low antimicrobial activity of Ag-NPs (Luo et al., 2018). On the other hand, Suwannee River NOM - (NOM1) and Upper Mississippi NOM - (NOM2) had the lowest effect on the antibacterial activity of Ag-NP on *E. coli* growth and survival and that also may explain due to their different physicochemical characteristics than HA or FA. NOM will include the compounds found in humic and fulvic acids as well as other protein-like compounds.

We also investigated the effect of NOM on DBNPA antimicrobial activity. DBNPA is an antimicrobial agent that can inactivate bacteria. DBNPA is known to rapidly hydrolyze in water (Bajpai, 2015). The main targets of DBNPA are sulfur-containing nucleophiles such as glutathione or cysteine, which are found in many microorganisms (Bajpai, 2015). However, this fast hydrolysis in water, its low concentration, and pH are important factors that may reduce the cytotoxicity of DBNPA by altering the half-life of DBNPA (Bajpai, 2015, Campa et al., 2019b). Moreover, these factors and others such as the presence of total organic carbon concentration (TOC) in solution or nucleophilic

reactions under UV light can lead to faster DBNPA degradation into less toxic compounds such as cyanoacetamide (CAM) or monobromonitrilopropionamide (MBNPA) (Campa et al., 2019b). The observed decrease in antimicrobial activity was substantial when NOM was added to DBNPA treatments. This decrease could be due to inactivation of the DBNPA through reaction with sulfur-containing nucleophiles in the NOM rather than the bacterial cell. The unproductive interactions may limit the antimicrobial activity of DBNPA in the presence of high concentrations of NOM.

We lastly investigated the effect of NOM on mixed antimicrobials. In the conditions with a mixture of Ag-NP and DBNPA, we did see a decrease in the bacterial abundance in both measures of OD and viable cells when we add the two antimicrobials agents (Ag-NP & DBNPA). The decrease in the bacterial abundance means that the combination of the antimicrobials leads to effective inactivation of *E. coli*. This is most likely due to the overall increased concentration of antimicrobials in the mixed treatments compared to the individual antimicrobials.

Given these results, it is evident that many factors are involved in impacting the antimicrobial activity of Ag-NPs and DBNPA against *E. coli*. While our studies are a limited investigation impact of NOM on antibacterial activity and aggregation of Ag-NP, our findings support that NOM can negatively affect their antimicrobial activity. Our results show that there is a differential effect of different types and concentrations of

natural organic matter (NOM) on the antibacterial properties of Ag-NPs and DBNPA. Our results indicate that Ag-NP is still stable with a small size distribution within the range of a nanoparticle in the presence of elevated NOM concentrations. Our results also indicate that DBNPA is more strongly impacted by the addition of organic matter than Ag-NP. There is still more work to be done to better characterize the DBNPA-NOM interactions and potential mechanisms for the decreased antimicrobial activity. These findings are important to understanding the interaction of silver nanoparticles and DBNPA with natural organic matter and their effect on nanoparticle stability in aquatic environments.

We cannot rule out the possibility that the decrease in the Ag-NP antibacterial activity in the presence of NOM was due to the aggregation of the nanoparticles, while we observed an increase in NP diameter in addition to NOM. Therefore, it would be worth investigating more physiochemical characterization and seek to more understanding of the influences of each chemical interaction with NPs and NOM in future studies.

Overall, our study demonstrates that natural organic matter (NOM) had a marginal negative effect on the antimicrobial activity of both silver nanoparticles or biocides and that depends on the type and concentrations of the NOM. Moreover, NOM did not substantially Ag-NP particle size. This finding suggests the possibility that NPs may persist in surface water in stable states, which will increase the dangers of toxic NPs in

water. It also may help to inform the use of NPs as methods for water disinfection as the antimicrobials activity of Ag-NPs is decreased in high organic matter conditions. While it's unclear if the decreased activity is due to aggregation or coating of the nanoparticles, our work demonstrates that NOM has an inhibitory effect on the antimicrobial activity of both NPs and biocides.

# Chapter 5

## Conclusions, Implications, & Recommendations for Future Work

### 5.1 Conclusions

Antimicrobials are widely used to control microbial growth in a household, medical, and industrial settings. The environments and mechanisms of resistance are important factors to be investigated to better quantify the effects of the inadvertent release of antimicrobials into the environment. While the environmental impacts and mechanisms of resistance for antibiotics are widely studied, less is known about the environmental impacts and mechanisms of resistance of industrial biocides and antimicrobial nanoparticles. Furthermore, most of the studies into the impacts of biocides and nanoparticles have focused on one particular class of compounds. Here we sought to provide a side-by-side comparison of these two types of antimicrobials. This type of side-by-side comparison allowed for a more thorough analysis of the relative impacts of these two types of antimicrobials on microorganisms. From our study, we conclude that both nanoparticles and biocides are effective antibacterial agents. The unintentional release of biocides and nanoparticles can alter microbial communities in streams and may have the potential for long-term or temporary effects on the environment. Our results show that NPs had less

of an impact than biocides on microbial community composition and microbial abundance compared to the control microcosms from a hydraulic fracturing affected stream.

We also observed that there was an overall increase in microbial abundance in biocide-amended treatments, which follows other studies that have shown increased microbial abundance in microcosms amended with DBNPA and glutaraldehyde. (Campa et al 2018; Campa et al 2019). The observed increase in microbial abundance has been suggested as indicating the presence of biocide-resistant microorganisms that are capable of growing in the presence of biocides and some cases metabolizing the biocides.

In Chapter 3 we began to investigate the ability of exposure of low concentrations of nanoparticles and biocides to select for resistant strains of *E. coli*. The common use of nanoparticles and biocides has led to increased concern of the development of microbial resistance to these antimicrobials; This may give rise to the growth of highly virulent pathogenic bacteria. Whether nanoparticles may select for resistant bacteria has only begun to be investigated and the mechanisms of adaptation and resistance to nanoparticles are poorly understood. The repeated exposure at sub MIC concentrations of antimicrobials can lead to the selection of mutants capable of growth at higher concentrations of antimicrobials. This led us to perform an experimental evolution study to observe acquired mutation in response to the selection of sub-MIC concentrations of

antimicrobials. We observed that *E. coli* more quickly acquire resistance to biocides compared to Ag-NP, with *E. coli* gaining significant resistance to DBNPA more quickly than *E. coli* developed significant resistance to Ag-NP. We also observed that some mechanisms for resistance were shared between the two biocides with a decrease in antimicrobial-induced ROS production being common between both adapted strains. Further, we observed that inhibition of efflux pumps resulted in increased sensitivity to both antimicrobials. The genomic analysis further supported the role of efflux pumps in DBNPA resistance and flagellar proteins being related to the mechanism of resistance to silver nanoparticles. Of particular note is the fact that we found that many mutations were related to the development of resistance. Previous work suggested that resistance to Ag-NPs was solely based on phenotypic changes not related to genetic alterations (Panacek et al., 2018). Our findings clarify that genetic adaptation is possible for both biocide and Ag-NP resistance. Further, we demonstrate that mutations in the multiple antibiotic resistance regulon occurred in the DBNPA-adapted strain. This regulon is important for both antibiotic resistance and oxidative stress response. Therefore, this mutation may be a key mutation conferring resistance to DBNPA in this adapted strain.

Finally, we investigate the effect of interactions with NOM on antimicrobial activity. Nanoparticles and biocides both have been shown to that end up in aquatic systems. However, the impact of environmental conditions on antimicrobial activity is not fully understood. Here we investigated the impact of NOM and different classes of organic matter on antimicrobial activity. It is believed that organic matter can decrease the

efficacy of antimicrobials by altering their stability in the case of NPs or the reaction of the biocides with functional groups on the organic matter in the case of biocides. The results of this study show that the antimicrobial activity of Ag-NPs and DBNPA can be negatively affected by various concentrations of NOM and mixture. However, these results show that these antimicrobials maintain some antimicrobial activity even in the presence of environmentally relevant concentrations of NOM.

Our study provides evidence for the effects of various concentrations of NOM on the antimicrobial activity of Ag-NPs and DBNPA by studying bacterial growth. The results show that NOM had more negative effects on bacterial growth when NOM was added to DBNPA-treated cells compared to Ag-NPs-treated *E. coli*. The effect of NOM depends on their types and concentration of NOM. We found that Suwanee River humic acid had the strongest negative effect on the antimicrobial activity Ag-NP. Moreover, we found that NOM addition did not lead to aggregation of the NPs as the size distribution only marginally increased upon NOM addition. These results seem to indicate that NOM addition inhibits antimicrobial activity through some other mechanism than causing Ag-NP aggregation.

## 5.2 Implications

Given these results, it is evident that many factors can be involved in affecting the antimicrobial activity of Ag-NPs and DBNPA against natural communities and the model bacterium *E. coli*. While our studies are a limited investigation, our findings support the importance of considering the environmental risk of Ag-NPs and DBNPA and performing a direct comparison between these two classes of antimicrobials.

Taken together these studies indicate that NPs show some promise as microbial control agents. Their use may only marginally alter microbial communities if released into the environment. However, repeated exposures of NPs at low concentrations can lead to the development of resistance. Our results also add further support to the potential use NPs in industrial applications due to their relative stability and retained antimicrobial activity in the presence of natural organic matter. This work provides a comparative study of the relative impacts of biocides and nanoparticles.

## 5.3 Recommendations for Future Work

The finding that NPs can lead to less of a change in the microbial community composition in water is worth further study as it may suggest that NPs could be environmentally friendly alternatives to biocides in some settings. Future work could investigate the effect of higher concentrations of NP on stream communities as well as expanding the number of streams tested.

Likewise, it has been proposed that resistance to biocides can lead to cross-resistance to antibiotics. Nanoparticles were proposed as being potential tools to deal with antibiotic-resistant bacteria. However, our findings suggest that bacteria rapidly become resistant to nanoparticles, which is in part due to efflux pumps. Therefore, it would be worthwhile to investigate the potential for nanoparticle resistance to also select for antibiotic resistance.

Furthermore, it would be worth comparing the potential that the DBNPA-adapted strain developed here might also have elevated resistance to Ag-NPs or other biocides. Since many mechanisms for resistance to generic antimicrobials such as biocides and NPs are not compound specific it may be that acquired resistance is more general than tested in this study.

This work provides a comprehensive comparison of the impacts of two commonly used classes of antimicrobials in terms of their impacts on environmental microbial communities and the potential for exposure to lead to resistance. This work aids in our understanding of the uses of these compounds, their potential environmental impacts, and risks.

# Reference List

- ABBASZADEGAN, A., GHAHRAMANI, Y., GHOLAMI, A., HEMMATEENEJAD, B., DOROSTKAR, S., NABAVIZADEH, M. & SHARGHI, H. 2015. The Effect of Charge at the Surface of Silver Nanoparticles on Antimicrobial Activity against Gram-Positive and Gram-Negative Bacteria: A Preliminary Study. *Journal of Nanomaterials*, 2015, 720654.
- ADAMS, L. K., LYON, D. Y. & ALVAREZ, P. J. 2006. Comparative eco-toxicity of nanoscale TiO<sub>2</sub>, SiO<sub>2</sub>, and ZnO water suspensions. *Water Res*, 40, 3527-32.
- ALIAS, A. K. 2012. Colloidal Interactions -food Emulsion-1. *University sains Malaysia*.
- ALVAREZ, P. J. J., CHAN, C. K., ELIMELECH, M., HALAS, N. J. & VILLAGRAN, D. 2018. Emerging opportunities for nanotechnology to enhance water security. *Nat Nanotechnol*, 13, 634-641.
- ANES, J., SIVASANKARAN, S. K., MUTHAPPA, D. M., FANNING, S. & SRIKUMAR, S. 2019. Exposure to Sub-inhibitory Concentrations of the Chemosensitizer 1-(1-Naphthylmethyl)-Piperazine Creates Membrane Destabilization in Multi-Drug Resistant *Klebsiella pneumoniae*. *Frontiers in microbiology*, 10, 92-92.
- BAJPAI, P. 2015. The Control of Microbiological Problems. *Pulp and Paper Industry*, 103-195.
- BATTIN, T. J., KAMMER, F. V., WEILHARTNER, A., OTTOFUELLING, S. & HOFMANN, T. 2009. Nanostructured TiO<sub>2</sub>: transport behavior and effects on aquatic microbial communities under environmental conditions. *Environ Sci Technol*, 43, 8098-104.
- BHATT, I. & TRIPATHI, B. N. 2011. Interaction of engineered nanoparticles with various components of the environment and possible strategies for their risk assessment. *Chemosphere*, 82, 308-317.
- BLANCO, P., HERNANDO-AMADO, S., REALES-CALDERON, J. A., CORONA, F., LIRA, F., ALCALDE-RICO, M., BERNARDINI, A., SANCHEZ, M. B. & MARTINEZ, J. L. 2016. Bacterial Multidrug Efflux Pumps: Much More Than Antibiotic Resistance Determinants. *Microorganisms*, 4, 14.
- BO, Z., AVSAR, S. Y., CORLISS, M. K., CHUNG, M. & CHO, N. J. 2017. Influence of natural organic matter (NOM) coatings on nanoparticle adsorption onto supported lipid bilayers. *J Hazard Mater*, 339, 264-273.
- BOGGS, S., JR., LIVERMORE, D. & SEITZ, M. G. 1985. Humic substances in natural waters and their complexation with trace metals and radionuclides: a review. .
- BOLGER, A. M., LOHSE, M. & USADEL, B. 2014. Trimmomatic: a flexible trimmer for Illumina sequence data. *Bioinformatics*, 30, 2114-2120.
- BONDARENKO, O. M., SIHTMÄE, M., KUZMIČIOVA, J., RAGELIENĖ, L., KAHRU, A. & DAUGELAVIČIUS, R. 2018. Plasma membrane is the target of rapid antibacterial action of silver nanoparticles in *Escherichia coli* and *Pseudomonas aeruginosa*. *International journal of nanomedicine*, 13, 6779-6790.

- BORM, P. J., ROBBINS, D., HAUBOLD, S., KUHNBUSCH, T., FISSAN, H., DONALDSON, K., SCHINS, R., STONE, V., KREYLING, W., LADEMANN, J., KRUTMANN, J., WARHEIT, D. & OBERDORSTER, E. 2006. The potential risks of nanomaterials: a review carried out for ECETOC. *Part Fibre Toxicol*, 3, 11.
- BRAOUDAKI, M. & HILTON, A. C. 2004. Adaptive Resistance to Biocides in *Salmonella enterica* and *Escherichia coli* O157 and Cross-Resistance to Antimicrobial Agents. *Journal of Clinical Microbiology*, 42, 73-78.
- BRUNNER, T. J., WICK, P., MANSER, P., SPOHN, P., GRASS, R. N., LIMBACH, L. K., BRUININK, A. & STARK, W. J. 2006. In Vitro Cytotoxicity of Oxide Nanoparticles: Comparison to Asbestos, Silica, and the Effect of Particle Solubility. *Environmental Science & Technology*, 40, 4374-4381.
- BUSCHOW, K. 2001. Encyclopedia of materials: Science and technology. . *Amsterdam: Elsevier*.
- CALLAHAN, B. J., MCMURDIE, P. J., ROSEN, M. J., HAN, A. W., JOHNSON, A. J. & HOLMES, S. P. 2016. DADA2: High-resolution sample inference from Illumina amplicon data. *Nat Methods*, 13, 581-3.
- CAMPA, M. F., TECHTMANN, S. M., GIBSON, C. M., ZHU, X., PATTERSON, M., GARCIA DE MATOS AMARAL, A., ULRICH, N., CAMPAGNA, S. R., GRANT, C. J., LAMENDELLA, R. & HAZEN, T. C. 2018. Impacts of Glutaraldehyde on Microbial Community Structure and Degradation Potential in Streams Impacted by Hydraulic Fracturing. *Environ Sci Technol*, 52, 5989-5999.
- CAMPA, M. F., TECHTMANN, S. M., LADD, M. P., YAN, J., PATTERSON, M., GARCIA DE MATOS AMARAL, A., CARTER, K. E., ULRICH, N., GRANT, C. J., HETTICH, R. L., LAMENDELLA, R. & HAZEN, T. C. 2019a. Surface Water Microbial Community Response to the Biocide 2,2-Dibromo-3-Nitrilopropionamide, Used in Unconventional Oil and Gas Extraction. *Appl Environ Microbiol*, 85, 01336-19.
- CAMPA, M. F., TECHTMANN, S. M., LADD, M. P., YAN, J., PATTERSON, M., GARCIA DE MATOS AMARAL, A., CARTER, K. E., ULRICH, N., GRANT, C. J., HETTICH, R. L., LAMENDELLA, R. & HAZEN, T. C. 2019b. Surface Water Microbial Community Response to the Biocide 2,2-Dibromo-3-Nitrilopropionamide, Used in Unconventional Oil and Gas Extraction. *Applied and environmental microbiology*, 85, e01336-19.
- CAMPA, M. F., WOLFE, A. K., TECHTMANN, S. M., HARIK, A.-M. & HAZEN, T. C. 2019c. Unconventional Oil and Gas Energy Systems: An Unidentified Hotspot of Antimicrobial Resistance? *Frontiers in Microbiology*, 10.
- CAPITA, R., VICENTE-VELASCO, M., RODRÍGUEZ-MELCÓN, C., GARCÍA-FERNÁNDEZ, C., CARBALLO, J. & ALONSO-CALLEJA, C. 2019. Effect of low doses of biocides on the antimicrobial resistance and the biofilms of *Cronobacter sakazakii* and *Yersinia enterocolitica*. *Scientific Reports*, 9, 15905.
- CAREY, D. E. & MCNAMARA, P. J. 2014. The impact of triclosan on the spread of antibiotic resistance in the environment. *Front Microbiol*, 5, 780.

- CASTAN, S., SIGMUND, G., HUFFER, T., TEPE, N., VON DER KAMMER, F., CHEFETZ, B. & HOFMANN, T. 2020. The importance of aromaticity to describe the interactions of organic matter with carbonaceous materials depends on molecular weight and sorbent geometry. *Environ Sci Process Impacts*, 22, 1888-1897.
- CHATTOPADHYAY, S., HUNT, C. D., RODGERS, P. J., SWIECICHOWSKI, A. L. & WISNESKI, C. L. 2004. Evaluation of biocides for potential treatment of ballast water. BATTELLE MEMORIAL INST COLUMBUS OH.
- CINGOLANI, P., PLATTS, A., WANG LE, L., COON, M., NGUYEN, T., WANG, L., LAND, S. J., LU, X. & RUDEN, D. M. 2012. A program for annotating and predicting the effects of single nucleotide polymorphisms, SnpEff: SNPs in the genome of *Drosophila melanogaster* strain w1118; iso-2; iso-3. *Fly (Austin)*, 6, 80-92.
- CONDELL, O., IVERSEN, C., COONEY, S., POWER, K. A., WALSH, C., BURGESS, C. & FANNING, S. 2012. Efficacy of Biocides Used in the Modern Food Industry To Control *Salmonella enterica*, and Links between Biocide Tolerance and Resistance to Clinically Relevant Antimicrobial Compounds. *Applied and Environmental Microbiology*, 78, 3087-3097.
- COORS, A., VOLLMAR, P., HEIM, J., SACHER, F. & KEHRER, A. 2018. Environmental risk assessment of biocidal products: identification of relevant components and reliability of a component-based mixture assessment. *Environmental sciences Europe*, 30, 3-3.
- COZAD, A. & JONES, R. D. 2003. Disinfection and the prevention of infectious disease. *American Journal of Infection Control*, 31, 243-254.
- DAKAL, T. C., KUMAR, A., MAJUMDAR, R. S. & YADAV, V. 2016. Mechanistic Basis of Antimicrobial Actions of Silver Nanoparticles. *Frontiers in Microbiology*, 7.
- DAVIES, J. & DAVIES, D. 2010. Origins and evolution of antibiotic resistance. *Microbiology and molecular biology reviews : MMBR*, 74, 417-433.
- DAY, G. M., HART, B. T., MCKELVIE, I. D. & BECKETT, R. 1997. Influence of Natural Organic Matter on the Sorption of Biocides onto Goethite, II. Glyphosate. *Environmental Technology*, 18, 781-794.
- DELAY, M., DOLT, T., WOELLHAF, A., SEMBRITZKI, R. & FRIMMEL, F. H. 2011. Interactions and stability of silver nanoparticles in the aqueous phase: Influence of natural organic matter (NOM) and ionic strength. *Journal of Chromatography A*, 1218, 4206-4212.
- DENYER, S. P. 1995. Mechanisms of action of antibacterial biocides. *International Biodeterioration & Biodegradation*, 36, 227-245.
- DORON, S. & DAVIDSON, L. E. 2011. Antimicrobial stewardship. *Mayo Clinic proceedings*, 86, 1113-1123.
- DRURY, B., SCOTT, J., ROSI-MARSHALL, E. J. & KELLY, J. J. 2013. Triclosan exposure increases triclosan resistance and influences taxonomic composition of benthic bacterial communities. *Environ Sci Technol*, 47, 8923-30.

- EPA 2012. Reregistration Eligibility Decision (RED) 2,2-dibromo-3-nitrilopropionamide (DBNPA). *Archived from the original* Retrieved 2012-06-14., p. 179. .
- FAHIMIPOUR, A. K., BEN MAMAAR, S., MCFARLAND, A. G., BLAUSTEIN, R. A., CHEN, J., GLAWE, A. J., KLINE, J., GREEN, J. L., HALDEN, R. U., VAN DEN WYMELENBERG, K., HUTTENHOWER, C. & HARTMANN, E. M. 2018. Antimicrobial Chemicals Associate with Microbial Function and Antibiotic Resistance Indoors. *mSystems*, 3, 200-18.
- FAN, M., WANG, Y., XUE, N., ZHAO, Y., WANG, Z., WANG, M., ZHAO, Y. & GAO, B. 2018. Coagulation of TiO<sub>2</sub> nanoparticles-natural organic matter composite contaminants in various aquatic media: Fluorescence characteristics, flocs properties and membrane fouling abilities. *Separation and Purification Technology*, 205, 113-120.
- FARHANA, A. & LAPPIN, S. L. 2021. Biochemistry, Lactate Dehydrogenase. *StatPearls*. Treasure Island (FL): StatPearls Publishing
- Copyright © 2021, StatPearls Publishing LLC.
- FEDERALREGISTER 2016. Safety and Effectiveness of Consumer Antiseptics; Topical Antimicrobial Drug Products for Over-the-Counter Human Use. *81 FR 61106*, Docket No. FDA-1975-N-0012
- Formerly Part of Docket No. 1975N-0183H, 61106-61130
- FELIS, E., KALKA, J., SOCHACKI, A., KOWALSKA, K., BAJKACZ, S., HARNISZ, M. & KORZENIEWSKA, E. 2020. Antimicrobial pharmaceuticals in the aquatic environment - occurrence and environmental implications. *European Journal of Pharmacology*, 866, 172813.
- FERNANDO, S. S. N., GUNASEKARA, T. & HOLTON, J. 2018a. Antimicrobial Nanoparticles: applications and mechanisms of action. *Sri Lankan Journal of Infectious Diseases*, 8, 2-11.
- FERNANDO, S. S. N., GUNASEKARA, T. & HOLTON, J. 2018b. Antimicrobial Nanoparticles: applications and mechanisms of action. *Sri Lankan Journal of Infectious Diseases*, 8, 2.
- FINK, J. K. 2013. *Hydraulic Fracturing Chemicals and Fluids Technology*.
- GEHRKE, I., GEISER, A. & SOMBORN-SCHULZ, A. 2015. Innovations in nanotechnology for water treatment. *Nanotechnol Sci Appl*, 8, 1-17.
- GEUEKE, B. 2014. Dossier – Biocides and food contact materials. *Food Packaging Forum*, 1-6.
- GILBERT, P. & MCBAIN, A. J. 2003. Potential impact of increased use of biocides in consumer products on prevalence of antibiotic resistance. *Clinical Microbiology Reviews*, 16, 189-+.
- GNANADHAS, D. P., MARATHE, S. A. & CHAKRAVORTTY, D. 2013. Biocides--resistance, cross-resistance mechanisms and assessment. *Expert Opin Investig Drugs*, 22, 191-206.

- GOLD, K., SLAY, B., KNACKSTEDT, M. & GAHARWAR, A. K. 2018. Antimicrobial Activity of Metal and Metal-Oxide Based Nanoparticles. *Advanced Therapeutics*, 1.
- GOUGOULIAS, C., CLARK, J. M. & SHAW, L. J. 2014. The role of soil microbes in the global carbon cycle: tracking the below-ground microbial processing of plant-derived carbon for manipulating carbon dynamics in agricultural systems. *Journal of the science of food and agriculture*, 94, 2362-2371.
- GRANT, D. M. & BOTT, T. R. 2005. Biocide dosing strategies for biofilm control. *Heat Transfer Engineering*, 26, 44-50.
- GREEN, N. W., MCINNIS, D., HERTKORN, N., MAURICE, P. A. & PERDUE, E. M. 2014. Suwannee River Natural Organic Matter: Isolation of the 2R101N Reference Sample by Reverse Osmosis. *Environmental Engineering Science*, 32, 38-44.
- GUARDIOLA, F. A., CUESTA, A., MESEGUER, J. & ESTEBAN, M. A. 2012a. Risks of using antifouling biocides in aquaculture. *International journal of molecular sciences*, 13, 1541-1560.
- GUARDIOLA, F. A., CUESTA, A., MESEGUER, J. & ESTEBAN, M. A. 2012b. Risks of using antifouling biocides in aquaculture. *Int J Mol Sci*, 13, 1541-60.
- GUO, Y., CICHOCKI, N., SCHATTENBERG, F., GEFFERS, R., HARMS, H. & MÜLLER, S. 2019. AgNPs Change Microbial Community Structures of Wastewater. *Frontiers in microbiology*, 9, 3211-3211.
- GUTIERREZ, L., SCHMID, A., ZAOURI, N., GARCES, D. & CROUE, J.-P. 2020. Colloidal stability of capped silver nanoparticles in natural organic matter-containing electrolyte solutions. *NanoImpact*, 19, 100242.
- HEATH, R. J., RUBIN, J. R., HOLLAND, D. R., ZHANG, E., SNOW, M. E. & ROCK, C. O. 1999. Mechanism of triclosan inhibition of bacterial fatty acid synthesis. *J Biol Chem*, 274, 11110-4.
- HEIDLER, J. & HALDEN, R. U. 2009. Fate of organohalogen in US wastewater treatment plants and estimated chemical releases to soils nationwide from biosolids recycling. *J Environ Monit*, 11, 2207-15.
- HERNANDEZ-MORENO, D., BLAZQUEZ, M., ANDREU-SANCHEZ, O., BERMEJO-NOGALES, A. & FERNANDEZ-CRUZ, M. L. 2019. Acute hazard of biocides for the aquatic environmental compartment from a life-cycle perspective. *Sci Total Environ*, 658, 416-423.
- HOU, D., HUANG, Z., ZENG, S., LIU, J., WEI, D., DENG, X., WENG, S., HE, Z. & HE, J. 2017. Environmental Factors Shape Water Microbial Community Structure and Function in Shrimp Cultural Enclosure Ecosystems. *Frontiers in microbiology*, 8, 2359-2359.
- HUNTER, R. J. 1981. Zeta Potential in Colloid Science: Principles and Applications. 10, 219-257.
- HYUNG, H. & KIM, J.-H. 2008. Natural Organic Matter (NOM) Adsorption to Multi-Walled Carbon Nanotubes: Effect of NOM Characteristics and Water Quality Parameters. *Environmental Science & Technology*, 42, 4416-4421.

- J.Y.MAILLARD 2007. Bacterial resistance to biocides in the healthcare environment: should it be of genuine concern. *Journal of Hospital Infection*, 67, 60-72.
- JEFFREY CLOGSTON, A. P. 2010. Zeta Potential Measurement

*Methods in Molecular Biology Characterization of Nanoparticles Intended for Drug Delivery*

- JIANG, J., OBERDÖRSTER, G. & BISWAS, P. 2009. Characterization of size, surface charge, and agglomeration state of nanoparticle dispersions for toxicological studies. *Journal of Nanoparticle Research*, 11, 77-89.
- JOOST, U., JUGANSON, K., VISNAPUU, M., MORTIMER, M., KAHRU, A., NÖMMISTE, E., JOOST, U., KISAND, V. & IVASK, A. 2015. Photocatalytic antibacterial activity of nano-TiO<sub>2</sub> (anatase)-based thin films: Effects on *Escherichia coli* cells and fatty acids. *Journal of Photochemistry and Photobiology B: Biology*, 142, 178-185.
- JORGENSEN, S. L., HANNISDAL, B., LANZÉN, A., BAUMBERGER, T., FLESLAND, K., FONSECA, R., ØVREÅS, L., STEEN, I. H., THORSETH, I. H., PEDERSEN, R. B. & SCHLEPER, C. 2012. Correlating microbial community profiles with geochemical data in highly stratified sediments from the Arctic Mid-Ocean Ridge. *Proceedings of the National Academy of Sciences*, 109, E2846.
- KADIYALA, U., KOTOV, N. A. & VANEPPS, J. S. 2018. Antibacterial Metal Oxide Nanoparticles: Challenges in Interpreting the Literature. *Curr Pharm Des*, 24, 896-903.
- KAHRILAS, G. A., BLOTEVOGEL, J., STEWART, P. S. & BORCH, T. 2015a. Biocides in hydraulic fracturing fluids: a critical review of their usage, mobility, degradation, and toxicity. *Environ Sci Technol*, 49, 16-32.
- KAHRILAS, G. A., BLOTEVOGEL, J., STEWART, P. S. & BORCH, T. 2015b. Biocides in Hydraulic Fracturing Fluids: A Critical Review of Their Usage, Mobility, Degradation, and Toxicity. *Environmental Science & Technology*, 49, 16-32.
- KAMPF, G. 2018. Biocidal Agents Used for Disinfection Can Enhance Antibiotic Resistance in Gram-Negative Species. *Antibiotics (Basel, Switzerland)*, 7, 110.
- KHAN, I., SAEED, K. & KHAN, I. 2019. Nanoparticles: Properties, applications and toxicities. *Arabian Journal of Chemistry*, 12, 908-931.
- KHAN, S., BEATTIE, T. K. & KNAPP, C. W. 2017. The use of minimum selectable concentrations (MSCs) for determining the selection of antimicrobial resistant bacteria. *Ecotoxicology (London, England)*, 26, 283-292.
- KLAINÉ, S. J., ALVAREZ, P. J. J., BATLEY, G. E., FERNANDES, T. F., HANDY, R. D., LYON, D. Y., MAHENDRA, S., MCLAUGHLIN, M. J. & LEAD, J. R. 2008. Nanomaterials in the Environment: Behavior, Fate, Bioavailability, and Effects. *Environmental Toxicology and Chemistry*, 27.
- KRZEMINSKI, P., VOGELSANG, C., MEYN, T., KÖHLER, S. J., POUTANEN, H., DE WIT, H. A. & UHL, W. 2019. Natural organic matter fractions and their removal in full-scale drinking water treatment under cold climate conditions in Nordic capitals. *Journal of Environmental Management*, 241, 427-438.

- KUMARI, J., KUMAR, D., MATHUR, A., NASEER, A., KUMAR, R. R., THANJAVUR CHANDRASEKARAN, P., CHAUDHURI, G., PULIMI, M., RAICHUR, A. M., BABU, S., CHANDRASEKARAN, N., NAGARAJAN, R. & MUKHERJEE, A. 2014. Cytotoxicity of TiO<sub>2</sub> nanoparticles towards freshwater sediment microorganisms at low exposure concentrations. *Environ Res*, 135, 333-45.
- LANGMEAD, B. & SALZBERG, S. L. 2012. Fast gapped-read alignment with Bowtie 2. *Nature Methods*, 9, 357-359.
- LANJE, A. S., SHARMA, S. J., RAMCH & PODE, R. 2010. Synthesis of silver nanoparticles: a safer alternative to conventional antimicrobial and antibacterial agents. *Journal of chemical and pharmaceutical research*, 2.
- LEE, N.-Y., KO, W.-C. & HSUEH, P.-R. 2019. Nanoparticles in the Treatment of Infections Caused by Multidrug-Resistant Organisms. *Frontiers in Pharmacology*, 10.
- LEVY, S. B. 2002a. Active efflux, a common mechanism for biocide and antibiotic resistance. *Journal of Applied Microbiology*, 92, 65s-71s.
- LEVY, S. B. 2002b. Active efflux, a common mechanism for biocide and antibiotic resistance. *J Appl Microbiol* 92, 65s-71s.
- LI, H., HANDSAKER, B., WYSOKER, A., FENNELL, T., RUAN, J., HOMER, N., MARTH, G., ABECASIS, G. & DURBIN, R. 2009. The Sequence Alignment/Map format and SAMtools. *Bioinformatics*, 25, 2078-9.
- LI, Z., SHAKIBA, S., DENG, N., CHEN, J., LOUIE, S. M. & HU, Y. 2020. Natural Organic Matter (NOM) Imparts Molecular-Weight-Dependent Steric Stabilization or Electrostatic Destabilization to Ferrihydrite Nanoparticles. *Environmental Science & Technology*, 54, 6761-6770.
- LIU, Z. H., ZHOU, H. F., LIU, J. F., HUANG, M., YIN, X. D., LIU, Z. S., MAO, Y. F., XIE, W. Y. & LI, D. H. 2018. Evaluation of performance and microbial community successional patterns in an integrated OCO reactor under ZnO nanoparticle stress. *Rsc Advances*, 8, 26928-26933.
- LONDONO, N., DONOVAN, A. R., SHI, H., GEISLER, M. & LIANG, Y. 2017. Impact of TiO<sub>2</sub> and ZnO nanoparticles on an aquatic microbial community: effect at environmentally relevant concentrations. *Nanotoxicology*, 11, 1140-1156.
- LÓPEZ DE DICASTILLO, C., GUERRERO CORREA, M., B. MARTÍNEZ, F., STREIT, C., & JOSÉ GALOTTO, M. 2021. Antimicrobial effect of titanium dioxide nanoparticles. . *Antimicrobial Resistance - A One Health Perspective*. .
- LOVE, M. I., HUBER, W. & ANDERS, S. 2014. Moderated estimation of fold change and dispersion for RNA-seq data with DESeq2. *Genome Biol*, 15, 550.
- LU, H., WANG, J., STOLLER, M., WANG, T., BAO, Y. & HAO, H. 2016. An Overview of Nanomaterials for Water and Wastewater Treatment. *Advances in Materials Science and Engineering*, 2016, 4964828.
- LUO, M., HUANG, Y., ZHU, M., TANG, Y.-N., REN, T., REN, J., WANG, H. & LI, F. 2018. Properties of different natural organic matter influence the adsorption and

- aggregation behavior of TiO<sub>2</sub> nanoparticles. *Journal of Saudi Chemical Society*, 22, 146-154.
- MAIDEN, M. M. & WATERS, C. M. 2020. Triclosan depletes the membrane potential in *Pseudomonas aeruginosa* biofilms inhibiting aminoglycoside induced adaptive resistance. *PLoS Pathog*, 16, e1008529.
- MAILLARD, J. Y. 2002. Bacterial target sites for biocide action. *J Appl Microbiol*, 92 Suppl, 16s-27s.
- MAILLARD, J. Y. 2005. Antimicrobial biocides in the healthcare environment: efficacy, usage, policies, and perceived problems. *Ther Clin Risk Manag*, 1, 307-20.
- MANNAN, M. F. A. K. S. B. 2013. Methods for Analyzing Diversity of Microbial Communities in Natural Environments. *Ceylon Journal of Science* 42(1), 19-33.
- MCDONNELL, G. & RUSSELL, A. D. 1999. Antiseptics and disinfectants: activity, action, and resistance. *Clinical microbiology reviews*, 12, 147-179.
- MCMURDIE, P. J. & HOLMES, S. 2013. phyloseq: an R package for reproducible interactive analysis and graphics of microbiome census data. *PLoS One*, 8, e61217.
- MCSHAN, D., RAY, P. C. & YU, H. 2014. Molecular toxicity mechanism of nanosilver. *Journal of food and drug analysis*, 22, 116-127.
- MD, G. A. H. G. 2007. Efficacy of three commercially available ballast water biocides against vegetative microalgae, dinoflagellate cysts and bacteria. *Harmful Algae* 6(4), 567-584.
- MENDE, S. 2015. Industrial Production of Nanomaterials with Grinding Technologies. *The Nano-Micro Interface*, 629-646.
- MERCHEL PIOVESAN PEREIRA, B. & TAGKOPOULOS, I. 2019. Benzalkonium Chlorides: Uses, Regulatory Status, and Microbial Resistance. *Applied and environmental microbiology*, 85, e00377-19.
- MILLOUR, M., PELLETIER, E. & GAGNÉ, J. P. Interactions Between Silver Nanoparticles and Dissolved Natural Organic Matter Under Estuarine Conditions. *In: XU, J., WU, J. & HE, Y., eds. Functions of Natural Organic Matter in Changing Environment, 2013// 2013 Dordrecht. Springer Netherlands*, 805-809.
- MOËNNE-LOCCOZ, Y., MAVINGUI, P., COMBES, C., NORMAND, P. & STEINBERG, C. 2014. Microorganisms and Biotic Interactions. *Environmental Microbiology: Fundamentals and Applications: Microbial Ecology*, 395-444.
- MOLL, J., KLINGENFUSS, F., WIDMER, F., GOGOS, A., BUCHELI, T. D., HARTMANN, M. & VAN DER HEIJDEN, M. G. A. 2017. Effects of titanium dioxide nanoparticles on soil microbial communities and wheat biomass. *Soil Biology & Biochemistry*, 111, 85-93.
- MOSTAFA M., A.-A., ALMOAMMAR H., ABD-ELSALAM K.A. 2018. Nanoantimicrobials Mechanism of Action. *In: Abd-Elsalam K., Prasad R. (eds) Nanobiotechnology Applications in Plant Protection. Nanotechnology in the Life Sciences. Springer, Cham*.
- MUMFORD, A. C., AKOB, D. M., KLINGES, J. G. & COZZARELLI, I. M. 2018. Common Hydraulic Fracturing Fluid Additives Alter the Structure and Function of Anaerobic Microbial Communities. *Appl Environ Microbiol*, 84, e02729-17.

- MUNITA, J. M. & ARIAS, C. A. 2016. Mechanisms of Antibiotic Resistance. *Microbiol Spectr*, 4.
- MYERS, K. S., YAN, H., ONG, I. M., CHUNG, D., LIANG, K., TRAN, F., KELEŞ, S., LANDICK, R. & KILEY, P. J. 2013. Genome-scale analysis of escherichia coli FNR reveals complex features of transcription factor binding. *PLoS Genet*, 9, e1003565.
- NISAR, P., ALI, N., RAHMAN, L., ALI, M. & SHINWARI, Z. K. 2019. Antimicrobial activities of biologically synthesized metal nanoparticles: an insight into the mechanism of action. *JBIC Journal of Biological Inorganic Chemistry*, 24, 929-941.
- OH, S., TANDUKAR, M., PAVLOSTATHIS, S. G., CHAIN, P. S. G. & KONSTANTINIDIS, K. T. 2013. Microbial community adaptation to quaternary ammonium biocides as revealed by metagenomics. *Environmental Microbiology*, 15, 2850-2864.
- OHSHIMA, H., & MAKINO, K. 2014. Colloid and interface science in pharmaceutical research and development. Amsterdam: Elsevier.
- PADMAVATHY, N. & VIJAYARAGHAVAN, R. 2008. Enhanced bioactivity of ZnO nanoparticles-an antimicrobial study. *Sci Technol Adv Mater*, 9, 035004.
- PAL, S. L., JANA, U., MANNA, P. K., MOHANTA, G. P. & MANAVALAN, R. 2011. Nanoparticle: An overview of preparation and characterization. *J. Appl. Pharm. Sci.*, 1, 228-234.
- PANACEK, A., KVITEK, L., SMEKALOVA, M., VECEROVA, R., KOLAR, M., RODEROVA, M., DYCKA, F., SEBELA, M., PRUCEK, R., TOMANEC, O. & ZBORIL, R. 2018. Bacterial resistance to silver nanoparticles and how to overcome it. *Nat Nanotechnol*, 13, 65-71.
- PARADA, A. E., NEEDHAM, D. M. & FUHRMAN, J. A. 2016. Every base matters: assessing small subunit rRNA primers for marine microbiomes with mock communities, time series and global field samples. *Environ Microbiol*, 18, 1403-14.
- PATERSON, G., ATARIA, J. M., HOQUE, M. E., BURNS, D. C. & METCALFE, C. D. 2011. The toxicity of titanium dioxide nanopowder to early life stages of the Japanese medaka (*Oryzias latipes*). *Chemosphere*, 82, 1002-9.
- PERDUE, E. M. Standard and Reference Samples of Humic Acids, Fulvic Acids, and Natural Organic Matter from the Suwannee River, Georgia: Thirty Years of Isolation and Characterization. In: XU, J., WU, J. & HE, Y., eds. Functions of Natural Organic Matter in Changing Environment, 2013// 2013 Dordrecht. Springer Netherlands, 85-88.
- POOLE, K. 2002. Mechanisms of bacterial biocide and antibiotic resistance. *J Appl Microbiol*, 92 Suppl, 55s-64s.
- PRABHU, S. & POULOSE, E. K. 2012. Silver nanoparticles: mechanism of antimicrobial action, synthesis, medical applications, and toxicity effects. *International Nano Letters*, 2, 32.
- PRESTINACI, F., PEZZOTTI, P. & PANTOSTI, A. 2015. Antimicrobial resistance: a global multifaceted phenomenon. *Pathogens and global health*, 109, 309-318.

- QING, Y. A., CHENG, L., LI, R., LIU, G., ZHANG, Y., TANG, X., WANG, J., LIU, H. & QIN, Y. 2018. Potential antibacterial mechanism of silver nanoparticles and the optimization of orthopedic implants by advanced modification technologies. *International journal of nanomedicine*, 13, 3311-3327.
- QUINLAN, A. R. & HALL, I. M. 2010. BEDTools: a flexible suite of utilities for comparing genomic features. *Bioinformatics*, 26, 841-842.
- RAY, P. C., YU, H. & FU, P. P. 2009. Toxicity and environmental risks of nanomaterials: challenges and future needs. *Journal of environmental science and health. Part C, Environmental carcinogenesis & ecotoxicology reviews*, 27, 1-35.
- REYGAERT, W. C. 2018. An overview of the antimicrobial resistance mechanisms of bacteria. *AIMS microbiology*, 4, 482-501.
- RICHTER, A. P., BROWN, J. S., BHARTI, B., WANG, A., GANGWAL, S., HOUCK, K., COHEN HUBAL, E. A., PAUNOV, V. N., STOYANOV, S. D. & VELEV, O. D. 2015. An environmentally benign antimicrobial nanoparticle based on a silver-infused lignin core. *Nat Nanotechnol*, 10, 817-23.
- RIPOLLES-AVILA, C., MARTINEZ-GARCIA, M., HASCOËT, A.-S. & RODRÍGUEZ-JEREZ, J. J. 2019. Bactericidal efficacy of UV activated TiO<sub>2</sub> nanoparticles against Gram-positive and Gram-negative bacteria on suspension. *CyTA - Journal of Food*, 17, 408-418.
- RUSSELL, A. D. 1999. Bacterial resistance to disinfectants: present knowledge and future problems. *J Hosp Infect*, 43 Suppl, S57-68.
- RUSSELL, A. D. 2003. Biocide use and antibiotic resistance: the relevance of laboratory findings to clinical and environmental situations. *Lancet Infect Dis*, 3, 794-803.
- SHARMA, P., HAYCOCKS, J. R. J., MIDDLEMISS, A. D., KETTLES, R. A., SELLARS, L. E., RICCI, V., PIDDOCK, L. J. V. & GRAINGER, D. C. 2017. The multiple antibiotic resistance operon of enteric bacteria controls DNA repair and outer membrane integrity. *Nature Communications*, 8, 1444.
- SIDDIQUI, A., PINEL, I., PREST, E. I., BUCS, S. S., VAN LOOSDRECHT, M. C. M., KRUIHOF, J. C. & VROUWENVELDER, J. S. 2017a. Application of DBNPA dosage for biofouling control in spiral wound membrane systems. *Desalin Water Treat*, 68, 12-22.
- SIDDIQUI, A., PINEL, I., PREST, E. I., BUCS, S. S., VAN LOOSDRECHT, M. C. M., KRUIHOF, J. C. & VROUWENVELDER, J. S. 2017b. Application of DBNPA dosage for biofouling control in spiral wound membrane systems. *Desalination and Water Treatment*, 68, 12-22.
- SIKDER, M., WANG, J. J., POULIN, B. A., TFAILY, M. M. & BAALOUSHA, M. 2020. Nanoparticle size and natural organic matter composition determine aggregation behavior of polyvinylpyrrolidone coated platinum nanoparticles. *Environmental Science-Nano*, 7, 3318-3332.
- SIMONIN, M. & RICHAUME, A. 2015. Impact of engineered nanoparticles on the activity, abundance, and diversity of soil microbial communities: a review. *Environ Sci Pollut Res Int*, 22, 13710-23.

- SLAVIN, Y. N., ASNIS, J., HÄFELI, U. O. & BACH, H. 2017. Metal nanoparticles: understanding the mechanisms behind antibacterial activity. *Journal of nanobiotechnology*, 15, 65-65.
- SONG, B., CAI, K., SHI, J., XIE, Y. M. & QIN, Q. 2019. Coupling effect of van der Waals, centrifugal, and frictional forces on a GHz rotation–translation nano-converter. *Physical Chemistry Chemical Physics*, 21, 359-368.
- SOTO, S. M. 2013. Role of efflux pumps in the antibiotic resistance of bacteria embedded in a biofilm. *Virulence*, 4, 223-229.
- STANKUS, D. P., LOHSE, S. E., HUTCHISON, J. E. & NASON, J. A. 2011a. Interactions between natural organic matter and gold nanoparticles stabilized with different organic capping agents. *Environ Sci Technol*, 45, 3238-44.
- STANKUS, D. P., LOHSE, S. E., HUTCHISON, J. E. & NASON, J. A. 2011b. Interactions between Natural Organic Matter and Gold Nanoparticles Stabilized with Different Organic Capping Agents. *Environmental Science & Technology*, 45, 3238-3244.
- TADROS, T. 2007. General Principles of Colloid Stability and the Role of Surface Forces. *Colloids and Interface Science Series*, 1.
- TAGHAVI, S. M., MOMENPOUR, M., AZARIAN, M., AHMADIAN, M., SOURI, F., TAGHAVI, S. A., SADEGHAIN, M. & KARCHANI, M. 2013. Effects of Nanoparticles on the Environment and Outdoor Workplaces. *Electronic physician*, 5, 706-712.
- TAKIGAWA, T. & ENDO, Y. 2006. Effects of glutaraldehyde exposure on human health. *J Occup Health*, 48, 75-87.
- TATTAWASART, U., HANN, A. C., MAILLARD, J. Y., FURR, J. R. & RUSSELL, A. D. 2000. Cytological changes in chlorhexidine-resistant isolates of *Pseudomonas stutzeri*. *Journal of Antimicrobial Chemotherapy*, 45, 145-152.
- TECHTMAN, S. M., MAHMOUDI, N., WHITT, K. T., CAMPA, M. F., FORTNEY, J. L., JOYNER, D. C. & HAZEN, T. C. 2017. Comparison of Thaumarchaeotal populations from four deep sea basins. *FEMS Microbiol Ecol*, 93, p. fix128.
- TIWARI, V., MISHRA, N., GADANI, K., SOLANKI, P. S., SHAH, N. A. & TIWARI, M. 2018. Mechanism of Anti-bacterial Activity of Zinc Oxide Nanoparticle Against Carbapenem-Resistant *Acinetobacter baumannii*. *Front Microbiol*, 9, 1218.
- VALLET-REGÍ, M., GONZÁLEZ, B. & IZQUIERDO-BARBA, I. 2019. Nanomaterials as Promising Alternative in the Infection Treatment. *International journal of molecular sciences*, 20, 3806.
- VENTOLA, C. L. 2015. The antibiotic resistance crisis: part 1: causes and threats. *P & T : a peer-reviewed journal for formulary management*, 40, 277-283.
- VIKRAM, A., BOMBERGER, J. M. & BIBBY, K. J. 2015a. Efflux as a Glutaraldehyde Resistance Mechanism in *Pseudomonas fluorescens* and *Pseudomonas aeruginosa* Biofilms. *Antimicrobial Agents and Chemotherapy*, 59, 3433-3440.
- VIKRAM, A., BOMBERGER, J. M. & BIBBY, K. J. 2015b. Efflux as a Glutaraldehyde Resistance Mechanism in *Pseudomonas fluorescens* and *Pseudomonas aeruginosa* Biofilms. 59, 3433-3440.

- VIKRAM, A., BOMBERGER, J. M. & BIBBY, K. J. 2015c. Efflux as a glutaraldehyde resistance mechanism in *Pseudomonas fluorescens* and *Pseudomonas aeruginosa* biofilms. *Antimicrob Agents Chemother*, 59, 3433-40.
- VILA DOMÍNGUEZ, A., AYERBE ALGABA, R., MIRÓ CANTURRI, A., RODRÍGUEZ VILLODRES, Á. & SMANI, Y. 2020. Antibacterial Activity of Colloidal Silver against Gram-Negative and Gram-Positive Bacteria. *Antibiotics (Basel, Switzerland)*, 9, 36.
- WANG, C.-F. & TIAN, Y. 2015. Reproductive endocrine-disrupting effects of triclosan: Population exposure, present evidence and potential mechanisms. *Environmental Pollution*, 206, 195-201.
- WANG, F., GUO, X., CHEN, W., SUN, Y. & FAN, C. 2017a. Effects of triclosan on hormones and reproductive axis in female Yellow River carp (*Cyprinus carpio*): Potential mechanisms underlying estrogen effect. *Toxicol Appl Pharmacol*, 336, 49-54.
- WANG, L., HU, C. & SHAO, L. 2017b. The antimicrobial activity of nanoparticles: present situation and prospects for the future. *International journal of nanomedicine*, 12, 1227-1249.
- WARD, C. S., PAN, J. F., COLMAN, B. P., WANG, Z., GWIN, C. A., WILLIAMS, T. C., ARDIS, A., GUNSCH, C. K. & HUNT, D. E. 2019. Conserved Microbial Toxicity Responses for Acute and Chronic Silver Nanoparticle Treatments in Wetland Mesocosms. *Environ Sci Technol*, 53, 3268-3276.
- WEBBER, M. A. 2002. The importance of efflux pumps in bacterial antibiotic resistance. *Journal of Antimicrobial Chemotherapy*, 51, 9-11.
- WHATMORE, R. 2005. Nanotechnology - should we be worried. *Nanotechnology Perceptions*, 1, 67-77.
- WHO 2014. ANTIMICROBIAL RESISTANCE Global Report on Surveillance.
- WU, J., JIANG, R., LIU, Q. & OUYANG, G. 2021. Impact of different modes of adsorption of natural organic matter on the environmental fate of nanoplastics. *Chemosphere*, 263, 127967.
- YAQOUB, A. A., PARVEEN, T., UMAR, K. & MOHAMAD IBRAHIM, M. N. 2020. Role of Nanomaterials in the Treatment of Wastewater: A Review. *Water*, 12.
- YIN, I. X., ZHANG, J., ZHAO, I. S., MEI, M. L., LI, Q. & CHU, C. H. 2020. The Antibacterial Mechanism of Silver Nanoparticles and Its Application in Dentistry. *International journal of nanomedicine*, 15, 2555-2562.
- ZHANG, Y., CHEN, Y., WESTERHOFF, P., HRISTOVSKI, K. & CRITTENDEN, J. C. 2008. Stability of commercial metal oxide nanoparticles in water. *Water Res*, 42, 2204-12.
- ZHENG, X., CHEN, Y. & WU, R. 2011. Long-term effects of titanium dioxide nanoparticles on nitrogen and phosphorus removal from wastewater and bacterial community shift in activated sludge. *Environ Sci Technol*, 45, 7284-90.
- ZHENG, X., WANG, J., CHEN, Y. & WEI, Y. 2018. Comprehensive analysis of transcriptional and proteomic profiling reveals silver nanoparticles-induced toxicity to bacterial denitrification. *J Hazard Mater*, 344, 291-298.

- ZHU, X., RADOVIC-MORENO, A. F., WU, J., LANGER, R. & SHI, J. 2014. Nanomedicine in the Management of Microbial Infection - Overview and Perspectives. *Nano today*, 9, 478-498.
- ZULARISAM, A. W., ISMAIL, A. F. & SALIM, R. 2006. Behaviours of natural organic matter in membrane filtration for surface water treatment — a review. *Desalination*, 194, 211-231.